



**MASTER OF SCIENCE**  
**IN**  
**ELECTRICAL AND EELCTRONIC ENGINEERING**

**An Approach of Improving the Performance of AC-DC Boost,  
SEPIC and Cuk Converter**

**Khadiza Akter**

**Department of Electrical and Electronic Engineering**

**Islamic University of Technology (IUT)**

**Board Bazar, Gazipur-1704, Bangladesh.**

**September, 2018**

**An Approach of Improving the Performance of AC-DC Boost,  
SEPIC and Cuk Converter**

by

**Khadiza Akter**

**MASTER OF SCIENCE**

**IN**

**ELECTRICAL AND EELCTRONIC ENGINEERING**

**Department of Electrical and Electronic Engineering**

**Islamic University of Technology (IUT)**

**Board Bazar, Gazipur-1704, Bangladesh.**

**September, 2018**

© 2018 Khadiza Akter  
All Rights Reserved

## Certificate of Approval

The thesis entitled "**An Approach of Improving the Performance of AC-DC Boost, SEPIC and Ćuk Converter**" submitted by Khadiza Akter, Student No. 132627 of Academic Year 2013-2014 has been found as satisfactory and accepted as partial fulfillment of the requirement for the Degree of MASTER OF SCIENCE IN ELECTRICAL AND ELECTRONIC ENGINEERING.

### BOARD OF EXAMINERS:

1. -----  
Dr.Md.Ashraful Hoque (Chairman)  
Professor and Head (Supervisor and Ex Officio)  
Department of Electrical and Electronic Engineering  
Islamic University of Technology, Board Bazar, Gazipur-1704

2. -----  
Dr. Golam Sarowar (Member)  
Associate Professor  
Department of Electrical and Electronic Engineering  
Islamic University of Technology, Board Bazar, Gazipur-1704

3. -----  
Dr. Ashik Ahmed (Member)  
Associate Professor  
Department of Electrical and Electronic Engineering  
Islamic University of Technology, Board Bazar, Gazipur-1704

4. -----  
Dr.Md Raju Ahmed Member(External)  
Professor and Head  
Department of Electrical and Electronic Engineering  
Dhaka University of Engineering and Technology, Shimultoly Rd, Gazipur 1707

## **Declaration of Candidate**

It is hereby declared that this thesis report or any part of it has not been submitted elsewhere for the award of any Degree or Diploma.

-----  
Dr. Md. Ashraful Hoque  
Professor & Head  
Department of Electrical and Electronic Engineering  
Islamic University of Technology (IUT)  
Date: 28<sup>th</sup>September, 2018

-----  
Khadiza Akter  
Student No.132627  
Academic Year: 2013-2014

**Dedicated to my adorable daughter**

# Table of Contents

<b>Certificate of Approval</b>	iv
<b>Table of Contents</b>	vii
<b>List of Tables</b>	x
<b>List of Figures</b>	xi
<b>Abstract</b>	xv
<b>Chapter 1 Introduction</b>	1
1.1 Introduction to Power Electronics	1
1.1.1 Modern Power Electronics	2
1.1.2 Power Electronics System	3
1.2 Switch Mode Converter	3
1.2.1 AC-DC Converter	4
1.2.2 DC-AC Converter	5
1.2.3 AC-AC Converter	6
1.2.4 DC-DC Converter	7
1.3 Literature Review	8
1.4 Problem Identification	9
1.5 Thesis Objective	10
1.6 Thesis Organization	10
<b>Chapter 2 AC-DC Converters</b>	11
2.1 Working Principle of Converter	12
2.2 Conventional Circuit Topologies	13
2.2.1 Buck Converter	13
2.2.2 Boost Converter	16
2.2.3 Buck Boost Converter	19

2.2.4	Ćuk Converter	22
2.2.5	SEPIC Converter	25
<b>Chapter 3</b>	<b>Proposed Bridgeless AC-DC Converters</b>	<b>29</b>
3.1	Boost Converter	29
3.1.1	Principle of Operation	29
3.1.2	Open Loop Data Analysis	31
3.1.3	Ideal Voltage Gain Equation	32
3.2	SEPIC Converter	35
3.2.1	Working Principle	35
3.2.2	Open Loop Simulation	37
3.2.3	Ideal Voltage Gain Equation	38
3.3	Ćuk Converter	44
3.3.1	Principle of Operation	44
3.3.2	Open Loop Data Analysis	46
3.3.3	Voltage Gain Expression	47
<b>Chapter 4</b>	<b>Performance Analysis of Proposed Converters</b>	<b>52</b>
4.1	Performance Analysis of Proposed Boost Converter	52
4.1.1	Analysis of Proposed Boost Converter under Duty Cycle Variation	52
4.1.2	Performance Analysis of Proposed Boost Converter under Load Variation	54
4.2	Performance Analysis of Proposed SEPIC Converter	55
4.2.1	Graphical Analysis of Proposed SEPIC Converter under Duty Cycle Variation	56
4.2.2	Performance Analysis of Proposed SEPIC Converter under Load Variation	57
4.3	Performance Analysis of Proposed Ćuk Converter	59
4.3.1	Graphical Analysis of Proposed Ćuk Converter under Duty Cycle Variation	59
4.3.2	Performance Analysis of Proposed Ćuk Converter under Load Variation	60
<b>Chapter 5</b>	<b>Feedback Controller with Proposed Boost Converter</b>	<b>63</b>
5.1	Working Principle of Single Phase PFC	63
5.2	Control of PFC	65



5.3	Designing the Inner Average-Current Control Loop	66
5.4	Designing the Outer Voltage-Control Loop	66
5.5	Simulation with Designed Controller	67
5.6	Discussions	69
<b>Chapter 6</b>	<b>Conclusion and Future Work</b>	<b>70</b>
6.1	Summary and Conclusion	70
6.2	Future Works	71
<b>References</b>		<b>72</b>
<b>List of publications</b>		<b>78</b>

## List of Tables

Table 2.1	Parameter Table for Conventional Buck Converter	14
Table 2.2	Performance Analysis of Conventional Buck Converter under Duty Cycle Variation	15
Table 2.3	Parameter Table for Conventional Boost Converter	17
Table 2.4	Performance Analysis of Conventional Boost Converter with Duty Cycle Variation	18
Table 2.5	Parameter Table for Conventional Buck Boost Converter	20
Table 2.6	Performance Analysis of Conventional Buck Boost Converter with Duty Cycle Variation	21
Table 2.7	Parameter Table for Conventional Ćuk Converter	23
Table 2.8	Performance Analysis of Conventional Ćuk Converter with Duty Cycle Variation	24
Table 2.9	Parameter Table for Conventional SEPIC Converter	26
Table 2.10	Performance Analysis of Conventional SEPIC Converter with Duty Cycle Variation	27
Table 3.1	Parameter Table of Proposed Boost Converter	31
Table 3.2	Performance Analysis of Proposed Boost Converter with Duty Cycle Variation	31
Table 3.3	Comparison between theoretical and simulation result of proposed Boost converter	34
Table 3.4	Parameter Table of Proposed SEPIC Converter	37
Table 3.5	Performance Analysis of Proposed SEPIC Converter with Duty Cycle Variation	37
Table 3.6	Parameter Table of Proposed Ćuk Converter	46
Table 3.7	Performance Analysis of Proposed AC-DC Ćuk Converter	46
Table 4.1	Performance Comparison under Load Variation of Proposed Boost Converter	54
Table 4.2	Performance Comparison under Load Variation of Proposed SEPIC Converter	57
Table 4.3	Performance Comparison under Load Variation of Proposed Ćuk Converter	61
Table 5.1	Parameter Table for Close Loop Controller of Fig. 5.7	67
Table 5.2	Results of the Simulation of the Converter with Feedback Controller	68

## List of Figures

Figure 1.1	Block Diagram of Power Electronics System[4]	2
Figure 2.1	Conventional AC-DC Buck Converter	13
Figure 2.2	Four Modes of Operation of Conventional AC-DC Buck Converter, (a) Mode 1: Conventional Circuit in Positive Half Cycle When S is ON. (b) Mode 2: Conventional Circuit in Positive Half Cycle When S is OFF. (c) Mode 3: Conventional Circuit in Negative Half Cycle When S is ON. (d) Mode 4: Conventional Circuit in Negative Half Cycle When S is OFF.	14
Figure 2.3	Conventional AC-DC Buck Converter with Rectified and Average Output Voltage Label	15
Figure 2.4	Conventional AC-DC Boost Converter	16
Figure 2.5	Four Modes of Operation of Conventional AC-DC Boost Converter, (a) Mode 1: Conventional Circuit in Positive Half Cycle When S is ON. (b) Mode 2: Conventional Circuit in Positive Half Cycle When S is OFF. (c) Mode 3: Conventional Circuit in Negative Half Cycle When S is ON. (d) Mode 4: Conventional Circuit in Negative Half Cycle When S is OFF.	17
Figure 2.6	Conventional AC-DC Boost Converter with Rectified and Average Output Voltage Label.	18
Figure 2.7	Conventional Buck Boost Converter	19
Figure 2.8	Four Modes of Operation of Proposed AC-DC Buck Boost Converter, (a) Mode 1: Conventional Circuit in Positive Half Cycle When S is ON. (b) Mode 2: Conventional Circuit in Positive Half Cycle When S is OFF. (c) Mode 3: Conventional Circuit in Negative Half Cycle When S is ON. (d) Mode 4: Conventional Circuit in Negative Half Cycle When S is OFF.	20
Figure 2.9	Conventional Buck Boost Converter with Rectified and Average Output Voltage Label.	21
Figure 2.10	Conventional Ćuk Converter	22
Figure 2.11	Four Modes of Operation of Conventional AC-DC Ćuk Converter, (a) Mode 1: Conventional Circuit in Positive Half Cycle When S is ON. (b) Mode 2: Conventional Circuit in Positive Half Cycle When S is OFF. (c) Mode 3: Conventional Circuit in Negative Half Cycle When S is ON. (d) Mode 4: Conventional Circuit in Negative Half Cycle When S is OFF.	23
Figure 2.12	Conventional Ćuk Converter with Rectified and Average Output Voltage Label.	24
Figure 2.13	Conventional SEPIC Converter	25
Figure 2.14	Four Modes of Operation of Proposed AC-DC SEPIC Converter, (a) Mode 1: Conventional Circuit in Positive Half Cycle When S is ON.	

	(b) Mode 2: Conventional Circuit in Positive Half Cycle When S is OFF. (c) Mode 3: Conventional Circuit in Negative Half Cycle When S is ON. (d) Mode 4: Conventional Circuit in Negative Half Cycle When S is OFF.	26
Figure 2.15	Conventional SEPIC Converter with Rectified and Average Output Voltage Label	27
Figure 3.1	Proposed Boost Converter	29
Figure 3.2	Four Modes of Operation of Proposed AC-DC Boost Converter, (a) Mode 1: Proposed Circuit in Positive Half Cycle When S is ON. (b) Mode 2: Proposed Circuit in Positive Half Cycle When S is OFF. (c) Mode 3: Proposed Circuit in Negative Half Cycle When S is ON. (d) Mode 4: Proposed Circuit in Negative Half Cycle When S is OFF.	30
Figure 3.3	Proposed Boost Converter with Voltage across the Inductor and Output	32
Figure 3.4	Proposed SEPIC Converter	35
Figure 3.5	Four Modes of Operation of Proposed AC-DC SEPIC Converter, (a) Mode 1: Proposed Circuit in Positive Half Cycle When S is ON. (b) Mode 2: Proposed Circuit in Positive Half Cycle When S is OFF. (c) Mode 3: Proposed Circuit in Negative Half Cycle When S is ON. (d) Mode 4: Proposed Circuit in Negative Half Cycle When S is OFF.	36
Figure 3.3	Input Switched AC-DC SEPIC Converter with Voltage across the components $L_1, L_2, L_3, L_4, C_1, C_2$ and $C_0$	38
Figure 3.7	Proposed Ćuk Converter	44
Figure 3.8	Four Modes of Operation of Proposed AC-DC Ćuk Converter, (a) Mode 1: Proposed Circuit in Positive Half Cycle When S is ON. (b) Mode 2: Proposed Circuit in Positive Half Cycle When S is OFF. (c) Mode 3: Proposed Circuit in Negative Half Cycle When S is ON. (d) Mode 4: Proposed Circuit in Negative Half Cycle When S is OFF.	45
Figure 3.9	Proposed Converters with Voltage Across the Components $L_1, L_2, L_3, L_4, C_1, C_2$ and $C_0$	47
Figure 4.1	Graphical Representation Of Efficiency (a), Power Factor (b), Voltage Gain (c) and Input Current THD (d) for the Proposed AC-DC Boost Converter With Conventional Boost Converter Under Duty Cycle Variation.	52
Figure 4.2	Input Current Waveform of Proposed Boost Converter	53
Figure 4.3	Input Voltage Waveform of Proposed Boost Converter	53
Figure 4.4	Output Voltage Waveform of Proposed Boost Converter	53
Figure 4.5	Graphical Representation of Efficiency (a), Power Factor (b), Voltage Gain (c) and Input Current THD (d) Proposed AC-DC Boost Converter with Conventional Boost Converter under Load Cycle Variation	55
Figure 4.6	Graphical Representation Of Efficiency (a), Power Factor (b), Voltage Gain (c) and Input Current THD (d) for the Proposed AC-DC	

	SEPIC Converter With Conventional SEPIC Converter Under Duty Cycle Variation.	56
Figure 4.7	Input Current Waveform of Proposed SEPIC Converter	57
Figure 4.8	Input Voltage Waveform of Proposed SEPIC Converter	57
Figure 4.9	Output Voltage Waveform of Proposed SEPIC Converter	57
Figure 4.10	Graphical Representation of Efficiency (a), Power Factor (b), Voltage Gain (c) and Input Current THD (d) for the Proposed AC-DC SEPIC Converter with Conventional SEPIC Converter under Load Cycle Variation	58
Figure 4.11	Graphical Representation Of Efficiency (a), Power Factor (b), Voltage Gain (c) and Input Current THD (d) for the Proposed AC-DC Ćuk Converter With Conventional Ćuk Converter Under Duty Cycle Variation.	59
Figure 4.12	Input Current Waveform of Proposed Ćuk Converter	60
Figure 4.13	Input Voltage Waveform of Proposed Ćuk Converter	60
Figure 4.14	Output Voltage Waveform of Proposed Ćuk Converter	60
Figure 4.15	Graphical Representation of Efficiency (a), Power Factor (b), Voltage Gain (c) and Input Current THD (d) for the Proposed AC-DC Ćuk Converter with Conventional Ćuk Converter under Load Cycle Variation	61
Figure 5.1	Proposed Boost Converter with Voltage Across the Components $L_1$ , $L_2$ and $C_o$	63
Figure 5.2	Waveform of PFC Circuit Where Supply Voltage and Supply Current are in the Same Phase [4]	64
Figure 5.3	DC Transformer Model of Proposed AC-DC Boost Converter	64
Figure 5.4	Block Diagram of PFC	65
Figure 5.5	PFC Current Loop	66
Figure 5.6	PFC Voltage Loop	67
Figure 5.7	Proposed AC-DC Boost Converter with PFC Controller	68
Figure 5.8	Input Voltage-Current and Output Voltage Waveforms of the PFC Controlled Converter of Fig. 5.7	69

## **Acknowledgement**

First, I offer gratitude to the Almighty ALLAH Subhanahu Wa Ta'la for giving me the capability to do this work with good health.

I am very much grateful to my research supervisor, Professor Dr. Md. Ashraful Hoque for his support and guidance throughout the course of this work. He has created a research environment for which I was able to explore many ideas without constraint. I have gained a wealth of knowledge and experience in science and engineering through his direction that is beyond value to my future endeavors.

Dr. Golam Sarowar, Associate Professor of Electrical and Electronic Engineering department of Islamic University of Technology (IUT) deserves special mention for his outstanding and generous helps in various aspects of this research.

Besides doing a job and having a child the journey was not easy for me to complete my thesis work unless I got continuous support from my family. I am thankful to my family members specially my mother, for her understanding and continuous support throughout my entire academic life. I would also like to acknowledge the support from some of my friends who have been a constant source of inspiration all along this work.

## Abstract

A new topology of single-phase AC-DC converter using Boost, SEPIC and Ćuk converter with low input current THD and high input power factor are proposed. Instead of using a bridge rectifier with two diodes and two switches, or using a single phase rectifier followed by AC-DC converter, the input is chopped at high frequency during positive and negative cycles by a single switch to get step-up AC-DC conversion. Total Harmonic Distortion (THD) of the input current of the proposed circuit with small input current filter is low. Input power factor and the efficiency of conversion of the circuit are high. Feedback control strategy for PFC is used with proposed converters to improve the input power factor and to keep the input current THD within prescribed IEEE limits. In this research work a new family of bridgeless Single phase AC-D CSEPIC Boost and Ćuk Converter with improved efficiency, power factor than conventional converter is proposed. Conventional AC-DC converter suffers from demerits like usage of rectifier bridge, high diode loss in bridge, low efficiency, low power factor, high THD in input current. Proposed converter reduces harmonic contamination in power lines; improve transmission efficiency along with power factor correction. Because of the high frequency switching, the power factor of the circuit is inherently corrected and it requires a small filter to make the input current near sinusoidal with limited THD. The significant improvement in THD makes the circuit a suitable choice in applications needing AC-DC conversion with power conditioning. The circuit of Boost, SEPIC and Ćuk exhibits such better performances than conventional AC-DC Boost, SEPIC and Ćuk converter with variable loads at constant frequency switching with no additional control circuits. Closed loop technique applied to the bridgeless proposed converters to make the results more precise. Addition of feedback controller reduced input current THD significantly at input AC mains along with power factor correction (near unity power factor). The efficiency of the circuit is also satisfactory. Analysis and simulation results of the circuit are obtained by using PSIM 9.11 environment. The main advantages of these new AC-DC converters are its superior power quality over conventional AC-DC converters.

# Chapter 1 Introduction

## 1.1 Introduction to Power Electronics

Because of the persistent progressions in Power Electronic technology, the AC-DC Converters are broadly utilized as a part of numerous power appliances. Prior, an AC-DC Converter utilized a substantial electrolytic capacitor after a diode-bridge rectifier to get a smooth DC voltage which is additionally filtered by a DC-DC Converter working at high-frequency to acquire a steady DC output voltage. Such AC-DC Converter introduces highly distorted input current resulting in serious current harmonics and low power factor. With the goals of improving the power factor, an additional power conversion stage, Power-Factor-Correction (PFC) is included in the AC-DC Converter [1]. Traditionally used active PFC circuits and conventional SMPS AC-DC converters comprise of front-end full bridge rectifier followed by high frequency DC-DC converters which suffers from low efficiency because of high voltage and current stresses acting on switching devices and other circuit parameters. The introduction of resonant converters along with the conventional step-up and step-down converters provide a very sensible solution for the above mentioned problem. Normally two controllers are essential to perform the operation which causes increased cost and requires more processing time. Gradually, the golden age of power electronics was ushered in by inventions of many sophisticated power semiconductor devices, microprocessor, digital signal processors (DSPs), field-programmable gate arrays (FPGAs), application-specific integrated circuit (ASIC) chips, advanced converter topologies, PWM techniques, and advanced control techniques. The reduction of cost and size, along with performance improvement, started proliferation of power electronics applications everywhere, that is, industrial, commercial, residential, transportation, aerospace, and military systems [3]. In modern systems most of the conversions are performed with semiconductor switching devices such as diodes, thyristor and transistors. An AC-DC converter is the most commonly used power electronics devices found in many consumer electronics device (e.g. television, computer, battery chargers etc). Power electronics devices are characterized being either a short circuit or an open circuit, as the switching capability combined with efficiency and performance makes power electronics research a fast growing area in electrical engineering. At the same time it is desirable because of relatively small power loss in the



device. An AC-DC converter enables integrated circuits to operate from a 50/60 Hz AC line voltage by converting the AC signal to a DC signal of the suitable voltage.

### 1.1.1 Modern Power Electronics

Power electronics is very important in modern high-efficiency energy processing systems, such as high voltage DC(HVDC), static VAR compensator (SVC), flexible ac transmission system (FACTS) for active and reactive power flow control, uninterruptible power supply (UPS), and industrial process control with variable-frequency drives for improving productivity and quality of products in modern automated factories [3]. Power electronics deals with the conversion and control of electrical energy with the help of power semiconductor devices that operate in a switching mode and therefore, efficiency of power electronic apparatus may approach higher [3]. In most power electronics systems, this conversion is accomplished with two functional modules called the control stage and the power stage. Figure 1.1 shows the topology for a single source and single load converter application that includes a power processor (the power stage) and a controller (the control stage). The converter, handles the power transfer from the input to output, or vice versa, and is constituted of power semiconductor devices acting as switches, plus passive devices (inductor and capacitor). The controller is responsible for operating the switches according to specific algorithms monitoring physical quantities (usually voltages and currents) measured at the system input and or output.

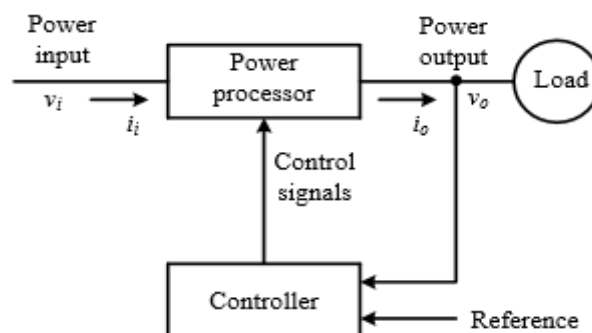


Figure 1.1 Block Diagram of Power Electronics System[4].

### **1.1.2 Power Electronics System**

Power electronics is an interdisciplinary subject within electrical engineering. A power electronic system consists of power electronic switching devices, linear circuit elements, digital circuits, microprocessors, electromagnetic devices, DSPs, filters, controllers, sensors, etc.

There are lots of applications in power electronic systems such as: Residential, commercial, transportation, industrial pump, utility system, aerospace, telecommunication etc [4]-[5]. One simple example is chopper-controlled dc motor or inverter-controlled ac motor drive in subway transportation, replacing the traditional rheostatic-controlled dc motor drives, which are still used in many parts of the world today. According to the estimate by the Electric Power Research Institute (EPRI), the major portion of the grid energy is used in pumps, fans, and compressor drives. The majority of these are used in the industrial environment for fluid flow control. In these applications, the traditional method of flow control is done by variable throttle or damper opening, where an induction motor running at constant speed is coupled to the fan. This method causes a lot of energy waste by the fluid vortex. If these applications use variable-frequency motor speed control with fully open throttle, energy can be saved up to 30%.

## **1.2 Switch Mode Converter**

A switched-mode power supply (SMPS) is an electronic power supply that incorporates a switching regulator to convert electrical power efficiently. Like other power supplies, an SMPS transfers power from a DC or an AC source (often mains power) to DC loads, such as a personal computer, while converting voltage and current characteristics. Unlike a linear power supply, the pass transistor of a switching-mode supply continually switches between low dissipation, full-on and full-off states, and spends very little time in the high dissipation transitions, which minimizes wasted energy. Ideally, a switched-mode power supply dissipates no power [6]. Voltage regulation is achieved by varying the ratio of on-to-off time. In contrast, a linear power supply regulates the output voltage by continually dissipating power in the pass transistor [6]. This higher power conversion efficiency is an important advantage of a switched mode power supply. Switched-mode power supplies may also be substantially smaller and lighter than a linear supply due to the smaller transformer size and weight.

Switching regulators are used as replacements for linear regulators when higher efficiency, smaller size or lighter weight is required. They are, however, more complicated; their switching currents can cause electrical noise problems if not carefully suppressed, and simple designs may have a poor power factor.

If a diode-and-capacitor combination is placed in parallel to the switch, the peak voltage can be stored in the capacitor, and the capacitor can be used as a DC source with an output voltage greater than the DC voltage driving the circuit. This Boost converter acts like a step-up transformer for DC signals. A Buck–Boost converter works in a similar manner, but yields an output voltage which is opposite in polarity to the input voltage. Other Buck circuits exist to boost the average output current with a reduction of voltage.

In a SMPS, the output current flow depends on the input power signal, the storage elements and circuit topologies used, and also on the pattern used (e.g., pulse-width modulation with an adjustable duty cycle) to drive the switching elements. The spectral density of these switching waveforms has energy concentrated at relatively high frequencies. As such, switching transients and ripple introduced onto the output waveforms can be filtered with a small LC filter.

Based on the form (frequency) on the two sides, power converters can be divided into the following broad categories:

- AC-DC converters
- DC-AC converters
- AC-AC converters
- DC- DC converters

### **1.2.1 AC-DC Converter**

Electric power is transported on wires either as a direct current (DC) flowing in one direction at a non-oscillating constant voltage, or as an alternating current (AC) flowing backwards and forwards due to an oscillating voltage. AC is the dominant method of transporting power because it offers several advantages over DC, including lower distribution costs and simple way of converting between voltage levels, invention of the transformer is really deserve thanks. AC power that is sent at high voltage over long distances and then converted down to a lower voltage is a more efficient and safer source of power in homes. Depending on the location, high voltage can range from 4kV (kilo-volts) up to 765kV. As a reminder, AC

mains in homes range from 110V to 250V, depending on which part of the world you live in. In Bangladesh the typical AC main line is 220V.

Converters steer an alternating current, as its voltage also alternates, into reactive impedance elements, such as inductors (L) and capacitors (C), where it is stored and integrated. This process separates the power associated with the positive and negative potentials. Filters are used to smooth out the energy stored, resulting in creation of a DC source for other circuits. This circuit can take many forms but always comprises of the same essential elements, and may have one or more stages of conversion [7]-[12]. A Flyback converter differs from a forward converter in that its operation depends upon energy stored in the air gap of the transformer in the circuit. Apart from this difference, they can utilize the same essential blocks [13].

### **1.2.2 DC-AC Converter**

DC-AC converters are known as inverters. A power inverter, or inverter, is an electronic device or circuitry that changes direct current (DC) to alternating current (AC). The input voltage, output voltage, frequency, and overall power handling depend on the design of the specific device or circuitry. The inverter does not produce any power; the power is provided by the DC source.

A power inverter can be entirely electronic or may be a combination of mechanical effects (such as a rotary apparatus) and electronic circuitry. Static inverters do not use moving parts in the conversion process. A typical power inverter device or circuit requires a relatively stable DC power source capable of supplying enough current for the intended power demands of the system. The input voltage depends on the design and purpose of the inverter. Examples include:

- 12V DC, for smaller consumer and commercial inverters that typically run from a rechargeable 12 V lead acid battery or automotive electrical outlet
- 24V, 36V and 48V DC, which are common standards for home energy systems.
- (200-400)V DC, when power is from photovoltaic solar panels.
- (300-450)V DC, when power is from electric vehicle battery packs in vehicle-to-grid systems.

- Hundreds of thousands of volts, where the inverter is part of a high-voltage direct current power transmission system.

### 1.2.3 AC-AC Converter

A solid-state AC-AC converter converts an AC waveform to another AC waveform, where the output voltage and frequency can be set arbitrarily. An AC-AC converter with approximately sinusoidal input currents and bidirectional power flow can be realized by coupling a pulse-width modulation (PWM) rectifier and a PWM inverter to the DC-link. The DC-link quantity is then impressed by an energy storage element that is common to both stages, which is a capacitor, C for the voltage DC-link or an inductor, L for the current DC-link. The PWM rectifier is controlled in a way that a sinusoidal AC line current is drawn, which is in phase or anti-phase (for energy feedback) with the corresponding AC line phase voltage.

Due to the DC-link storage element, there is the advantage that both converter stages are to a large extent decoupled for control purposes. Furthermore, a constant, AC line independent input quantity exists for the PWM inverter stage, which results in high utilization of the converter's power capability. On the other hand, the DC-link energy storage element has a relatively large physical volume, and when electrolytic capacitors are used, in the case of a voltage DC-link, there is potentially a reduced system lifetime [15].

A cyclo converter constructs an output, variable-frequency, approximately sinusoid waveform by switching segments of the input waveform to the output; there is no intermediate DC link. With switching elements such as SCRs, the output frequency must be lower than the input. Very large cyclo converters (on the order of 10MW) are manufactured for compressor and wind-tunnel drives, or for variable-speed applications such as cement kilns [16]. In order to achieve higher power density and reliability, it makes sense to consider Matrix Converters that achieve three-phase AC-AC conversion without any intermediate energy storage element.

Matrix converters are often seen as a future concept for variable speed drives technology, but despite intensive research over the decades they have until now only achieved low industrial penetration [17]. However, citing recent availability of low-cost, high performance semiconductors, one larger drive manufacturer has over past few years been actively promoting matrix converters.

#### 1.2.4 DC-DC Converter

DC-DC converters are known as choppers. They convert a fixed-voltage dc source into a variable –voltage dc source. DC-DC converters can be considered as dc equivalent to an auto transformer with a continuously variable turns ratio. Like a transformer, it could be used to step-up or step-down a dc source. DC-DC converters are used in portable electronic devices such as cellular phones and laptop computers, which are supplied with power from batteries primarily. Such electronic devices often contain several sub-circuits, each with its own voltage level requirement different from that supplied by the battery or an external supply (sometimes higher or lower than the supply voltage). Additionally, the battery voltage declines as its stored energy is drained. Switched DC-DC converters offer a method to increase voltage from a partially lowered battery voltage thereby saving space instead of using multiple batteries to accomplish the same thing.

Most DC-DC converter circuits also regulate the output voltage. Some exceptions include high-efficiency LED power sources, which are a kind of DC-DC converter that regulates the current through the LEDs, and simple charge pumps which double or triple the output voltage.

DC-DC converters developed to maximize the energy harvest for photovoltaic systems and for wind turbines are called power optimizers [18]-[23].

Transformers used for voltage conversion at mains frequencies of 50–60 Hz must be large and heavy for powers exceeding a few watts. This makes them expensive, and they are subject to energy losses in their windings and due to eddy currents in their cores. DC-DC techniques that use transformers or inductors work at much higher frequencies, requiring only smaller, lighter, and cheaper wound components. Consequently these techniques are used even where a mains transformer could be used; for example, for domestic electronic appliances it is preferable to rectify mains voltage to DC, uses switch-mode techniques to high-frequency AC at the desired voltage, then, usually, rectify to DC. The entire complex circuit is cheaper and more efficient than a simple mains transformer circuit of the same output.

### 1.3 Literature Review

The thesis work concentrates on the development of input switched AC-DC step-up converters to provide high voltage gain, high efficiency, low input current THD and improved power factor (0.99) at small duty cycle. However, different circuit topologies of both conventional and proposed AC-DC step-up converters have been studied from the beginning of the thesis work. It has been found that various isolated and non-isolated converter topologies have been developed to provide a high step-up conversion. SMPS (Switched Mode Power Supply) converters are very important in this aspect due to ease of application and scope of improvement. Conventional single-phase AC-DC converter using full wave rectifiers in bridge configuration suffer from problems of distorted input current and low input power factor. Various methods have been proposed to resolve these problems. One method is to use input filter but the value of filter inductor and capacitor required in such solution are too large which cannot be implemented practically. THD improvement is possible by changing circuit parameters but it will not give us the desired value of power factor. Different topologies have been made to develop the PFC converters [24]–[28]. As a matter of fact, the PFC circuits are becoming a crucial topic on single-phase power supplies as more stringent power quality regulations and strict limits on the Total Harmonic Distortion (THD) of input current are imposed [29]. The preferable type of PFC is active PFC since it makes the load behave like a pure resistor, leading to near-unity load power factor and producing negligible harmonics in the input line current [30]–[32]. Most of the presented bridgeless topologies so far implement a boost-type circuit configuration because of its low cost and its high performance in terms of efficiency, power factor, and simpler in design. These features have led power supply companies to start looking for bridgeless PFC circuit topologies. Bridgeless PFC boost rectifier implementations that have received the most attention is presented along with their performance comparison with the conventional PFC boost rectifier. On the other hand, the bridgeless boost rectifier has the same major practical drawbacks as the conventional boost converter. Most active PFC circuits as well as switched-mode power supplies in the market today made by bridge rectifier, followed by a high-frequency DC-DC converter such as a Boost, a Buck–Boost, a Ćuk, a Single-Ended Primary Inductance Converter (SEPIC), and a Flyback converter [33]–[34]. Using of rectifier is suitable for a low-to-medium power range. As the power level increases, the high conduction loss caused by the high forward voltage drop of the diode bridge begins to degrade the overall system efficiency, and the heat generated within the bridge rectifier may damage the

individual diodes. Hence, it becomes necessary to utilize a bridge rectifier with higher current-controlling capability or heat-absorbing characteristics. To improve the power supply efficiency, a good number of bridgeless high performance PFC circuit designs have been proposed [35]-[53]. Single phase AC-DC converter is a SMPS converter which converts an AC signal to a high level DC signal. Conventional AC-DC converters suffers from disadvantages like usage of bridge rectifier, high diode loss in bridge, low efficiency, low power factor, high THD in input current. To improve transmission efficiency, power factor and to reduce harmonic contamination in power lines, many topologies have been proposed earlier for the improvement of these drawbacks [54]-[59].

As the power level increases, the conduction loss caused by the forward voltage drop of the diode bridge begins to deteriorate the overall efficiency, and the heat generated within the bridge rectifier may destroy the individual diode. Actually, these bridgeless PFC circuit combines the operation of bridge rectifier and DC-DC converter into a single circuit. All these proposed configurations differ in their topology, and they have some drawbacks. Sometimes the AC-DC converter is claimed as bridgeless, but it suffers from increased number of diodes leading to more power losses in diodes and less efficiency [60]-[62]. In most of the conventional converters only works on very small voltage, and shows very little efficiency and low power factor at typical supply voltage and load. Traditional rectifier circuits suffer from low efficiency at typical supply voltage and at low output power. It also shows low power factor at small load and at low output power. To remove all these drawbacks it requires designing an improved AC-DC converter with high power quality than the conventional AC-DC converters.

#### **1.4 Problem Identification**

The study of step-up AC-DC converters to provide a high voltage gain at a small duty cycle has been crucial for different applications. Several AC-DC step-up converters have been introduced in the literature review to address this point. It is observed that the conventional converters involving transformer suffer from leakage inductance causing large voltage spike across the switches, diode bridge loss, and low power factor. Moreover, the size and cost of these converters is high because of transformer, multi-stage DC-AC-DC conversion and isolated sensors and controllers. Like the isolated converters, coupled type non-isolated converters also suffer from leakage inductance of the coupled inductor. On the other hand,



non-coupled type non-isolated converters are free from these disadvantages. Conventional AC-DC converters suffer from lots of demerits which causes poor power quality. So many topologies have been designed to improve the overall performance. All these configurations differ in their topology, but all are aiming to have more & more possible improvement.

## 1.5 Thesis Objective

The main objective of this thesis is to develop a new topology of input switched bridgeless AC-DC converters. However, more particularly, the objectives include:

- To make possible improvements in performance in contrary to conventional AC-DC converters.
- To reduce the diode losses and increase efficiency.
- To improve the input current THD in comparison to the conventional converters.

## 1.6 Thesis Organization

This thesis focuses on the study of a new topology of AC-DC step-up converters for possible applications in renewable energy systems with an attempt to reduce THD and to increase the power factor with higher efficiency.

- In Chapter 2, different types of existing widely used AC-DC converters are discussed. The methods of how to analyze AC-DC converters are presented in details.
- In Chapter 3, topological derivation of proposed AC-DC converters is discussed. Then, the operations of three proposed converters are analyzed in detail with ideal voltage gain.
- In Chapter 4, performance of proposed converters is analyzed. A theoretical comparison between the proposed converters is made in tabular form. Then, simulation results are provided to measure the effectiveness of the theoretical expressions of the proposed converters derived in Chapter 3.
- In Chapter 5 analysis of the Proposed Boost Circuit with feedback controller is given.
- Chapter 6 contains the conclusion of the thesis, where the brief summary of the results is given with some recommendations for future works.

## Chapter 2 AC-DC Converters

AC-DC converters consist of a transformer following the input filtering, which then passes onto a rectifier to produce DC. In this case, rectification occurs after the transformer because transformers do not pass DC. However, many AC-DC converters use more sophisticated, multi-stage conversion topologies as illustrated in figure 2.1 due to advantages of smaller transformer requirements and lower noise referred back to the mains power supply.

Rectifiers are implemented using semiconductor devices that conditionally conduct current in one direction only, like diodes. More sophisticated semiconductor rectifiers include thyristors. Silicon controlled rectifiers (SCR) and triode for alternating current (TRIAC) are analogous to a relay in that a small amount of voltage can control the flow of a larger voltage and current. The way these work is, they only conduct when a controlling ‘gate’ is triggered by an input signal. By switching the device on and off at the right time as the AC waveform flows – current is steered to create a DC separation. There are many circuits for doing this, with signals tapped off the AC waveform used as control signals that set the phase quadrants thyristors are on or off. This is commutation, and can be either natural (in the case of a simple diode) or forced, as in the case of devices that are more sophisticated.

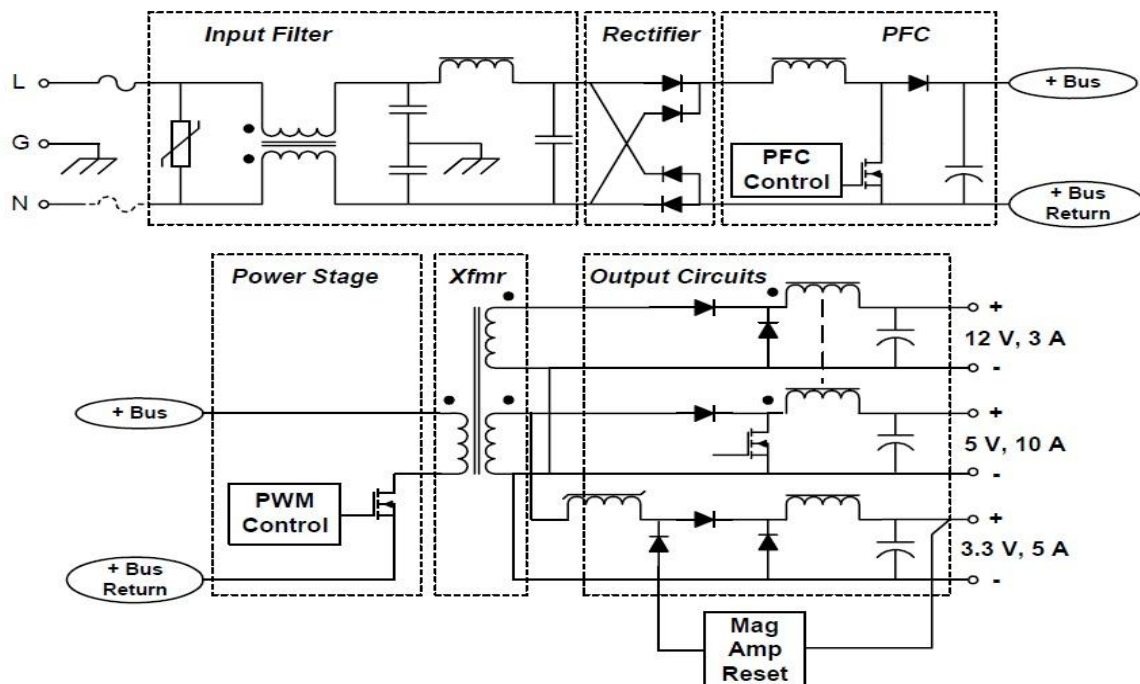


Figure 2.1 Power Stage of AC-DC Converter [14].

High efficiency power supplies can use active devices like MOSFETs as switches in such circuits. The reason for using topologies that are more complex is usually for efficiency improvement, to lower noise or to act as a power control. Diodes have an intrinsic voltage drop across them when they conduct. This causes power to be dissipated in them, but other active elements may have much lower drop and therefore lower power loss. SCR and TRIAC circuits are particularly common in low cost power control circuits like the light dimmer example below – used to directly steer and control current delivered to the load as the input mains alternates. Note that these implementations are not galvanic when they do not have a transformer in the circuit – only useful in circuits that are appropriate like direct mains connected light control. They are also used in high power industrial and military power supplies where simplicity and robustness is essential.

## **2.1 Working Principle of Converter**

The output voltage coming from full-wave full bridge rectifier is unregulated. That means output voltage cannot be controlled. The output of rectifier is fed into a converter for regulation. There are four different types of converter available. A brief study of the kinds is presented below.

Before proceeding further the following assumptions are made: that all the elements in the circuit are considered ideal, i.e. the inductor and capacitor absorbs no energy, the average voltage drop across the inductor and the average capacitor current is zero, the net change in inductor current and the net change in the capacitor voltage at the end of a commutation cycle is zero and the circuit is operating in steady state.

There are four basic types of converter, the Buck, the Boost, the Buck-Boost and the Ćuk and the SEPIC. All these converters have some basic common feature. All these converters use an energy storing element to transfer energy from the source to the load. They all use electronic switches like MOSFET, transistors, etc to control the power flow.

All these converters have two modes of conduction 1) continuous mode and 2) discontinuous mode. In the continuous mode the current through the inductors of the converters are never zero and thus the inductor never discharges totally whereas in discontinuous mode the inductor current falls back to zero showing total discharge of inductor energy.

## 2.2 Conventional Circuit Topologies

### 2.2.1 Buck Converter

The Buck converter is used to step down an input voltage from a higher potential to a lower potential. Buck converter steps down voltage (while stepping up current) from its input to the load. The input and output power ideally remain the same. It is a class of switched-mode power supply (SMPS) typically containing at least two semiconductors and at least one energy storage element, a capacitor, inductor, or the two in combination. The circuit usually consists of an inductor to store energy and a switch to control the power flow. To reduce voltage ripple, filters made of capacitors are normally added to such a converter's output and input.

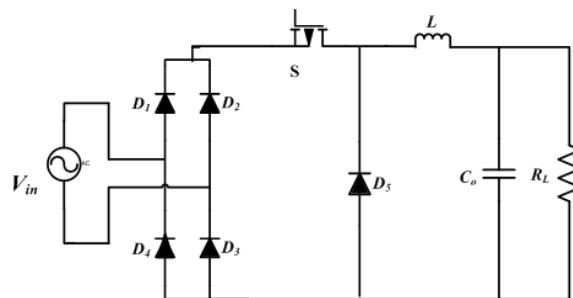


Figure 2.1 Conventional AC-DC Buck Converter.

#### 2.2.1.1 Principle of Operation

The four working stages of the conventional converter is illustrated in Figure 2.2, where Figure 2.2 (a) and (b) are for switch ON and OFF condition during positive supply cycle and Figure 2.2 (c) and (d) are for switch ON and OFF during negative cycle. When the switch is ON the diode  $D_5$  is reverse biased, current flows through the inductor to the load. During the ON period inductor stores energy from the input current whereas During OFF period source isolate from the rest of the circuit, the diode  $D_5$  becomes forward biased as the inductor changes polarity and the inductor discharges to provide energy to the load.

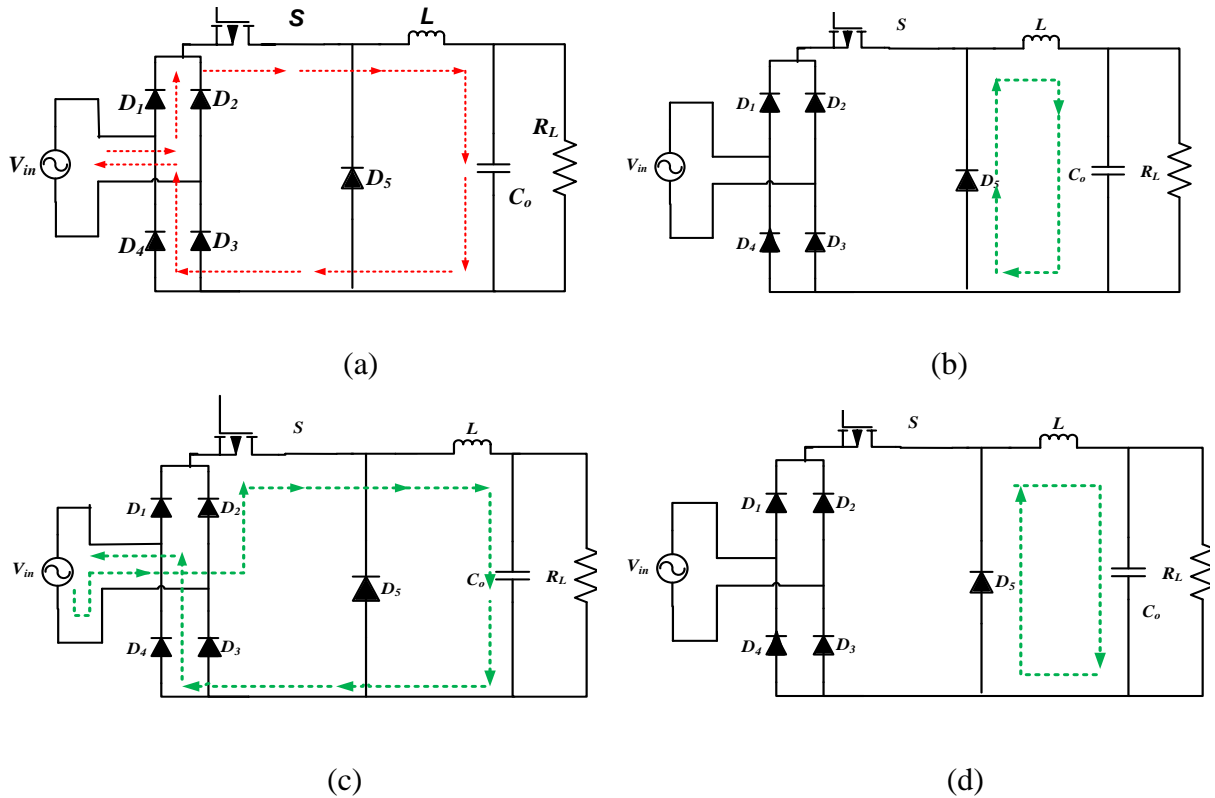


Figure 2.2 Four Modes of Operation of Conventional AC-DC Buck Converter, (a) Mode 1: Conventional Circuit in Positive Half Cycle When S is ON. (b) Mode 2: Conventional Circuit in Positive Half Cycle When S is OFF. (c) Mode 3: Conventional Circuit in Negative Half Cycle When S is ON. (d) Mode 4: Conventional Circuit in Negative Half Cycle When S is OFF.

### 2.2.1.2 Open Loop Data Analysis

The simulation of the conventional Buck converter has been performed using software simulation and the results obtained are presented in Table 2.2. Here MOSFET has considered as the switching device. The value of different circuit components are given in Table 2.1.

Table 2.1 Parameter Table for Conventional Buck Converter

Parameters	Value
Input voltage ( $V_i$ )	220V
Switching Frequency (S)	5kHz
Inductor (L)	2.5mH
Output Capacitor( $C_o$ )	220 $\mu$ F
Load Resistor ( $R_L$ )	10 $\Omega$

Table 2.2 Performance Analysis of Conventional Buck Converter under Duty Cycle Variation

Duty Cycle	Efficiency (%)	Power Factor	THD	Voltage Gain
0.1	99	0.3	3.19	0.1
0.2	99	0.4	2.28	0.2
0.3	99	0.5	1.84	0.21
0.4	99	0.53	1.58	0.4
0.5	99	0.6	1.23	0.5
0.6	99	0.6	1.24	0.6
0.7	99	0.61	1.24	0.7
0.8	99	0.6	1.29	0.8
0.9	99	0.57	1.37	0.9

### 2.2.1.3 Voltage Gain Expression

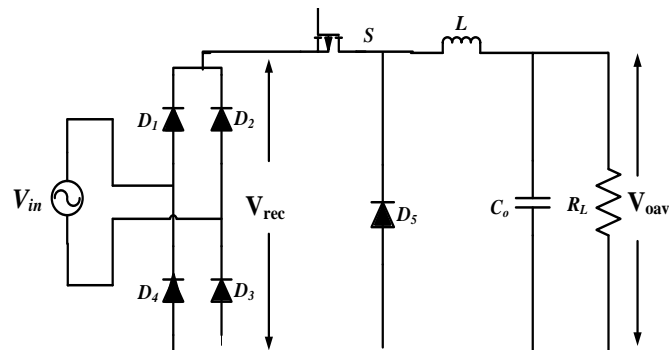


Figure 2.3 Conventional AC-DC Buck Converter with Rectified and Average Output Voltage Label.

The rectified average voltage after the conventional bridge is,

$$V_{orectave} = \frac{V_{inmax}}{\pi} \int_0^{\pi} \sin \theta d\theta = \frac{2V_{inmax}}{\pi}$$

For DC-DC Buck converter

$$V_{oav} = DV_{rec} \tag{2.1}$$

Where,  $D = \text{Duty Cycle} = \frac{T_{on}}{T}$ ,  $1-D = \frac{T_{off}}{T}$  and  $T = \text{Switching frequency}$ .

Therefore, the output voltage from equation (2.1) can be written as

$$V_{oav} = D \frac{2V_{inmax}}{\pi} \quad (2.2)$$

### 2.2.2 Boost Converter

The Boost converter is used to step a voltage up from a lower value to higher value. The circuit uses an inductor to store and transfer energy to the load from the input. An inductor always tends to resist changes in current. When being charged, it acts as a load and absorbs energy; when being discharged it acts as an energy source. The voltage it produces during the discharge phase is proportional to the rate of change of current, and not to the original charging voltage, thus allowing different input and output voltages.

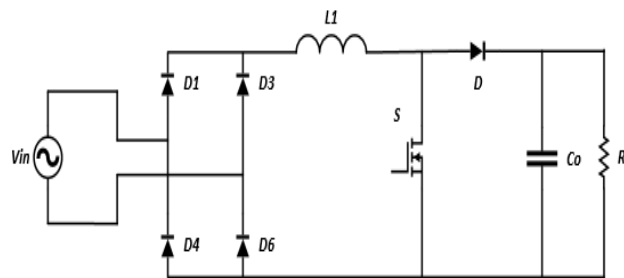


Figure 2.4 Conventional AC-DC Boost Converter.

#### 2.2.2.1 Principle of Operation

The four working stages of the conventional Boost converter is illustrated in Figure 2.5, where Figure 2.5 (a) and (b) are for switch ON and OFF condition during positive supply cycle and Figure 2.5 (c) and (d) are for switch ON and OFF during negative cycle. When the switch is ON during positive half cycle the Boost inductor charges from the source through the short circuit of the source. As the switch turns OFF, the source and the inductor voltage forward biases the output diode and charges the output capacitor. Same phenomenon takes place during the negative half cycle as the output of the diode rectifier has same polarity.

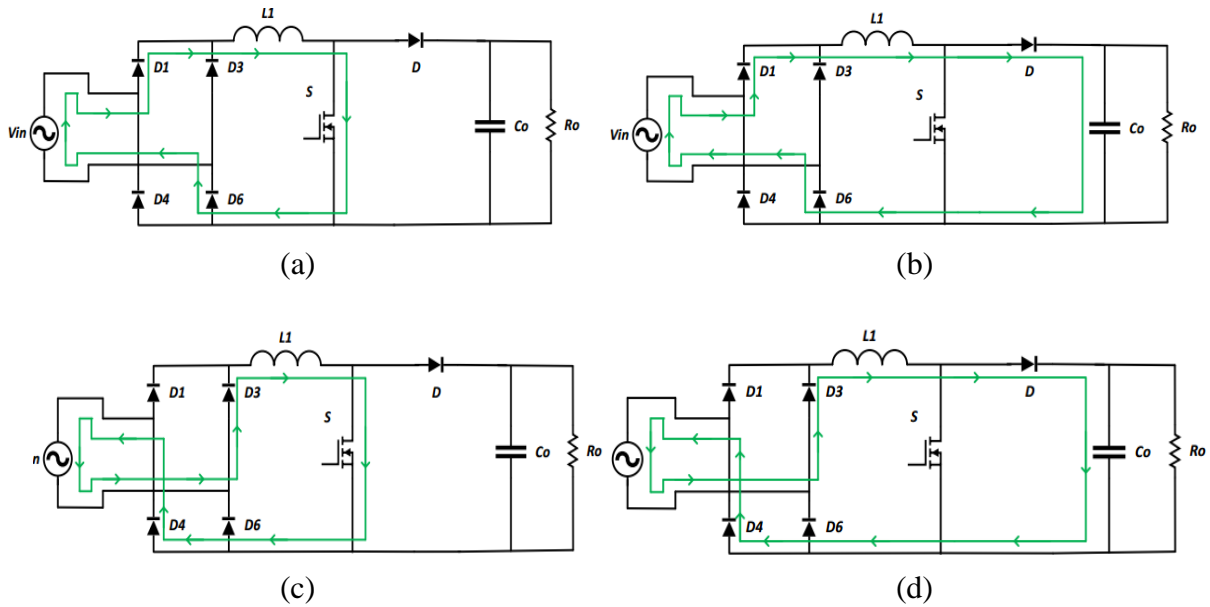


Figure 2.5 Four Modes of Operation of Conventional AC-DC Boost Converter, (a) Mode 1: Conventional Circuit in Positive Half Cycle When S is ON. (b) Mode 2: Conventional Circuit in Positive Half Cycle When S is OFF. (c) Mode 3: Conventional Circuit in Negative Half Cycle When S is ON. (d) Mode 4: Conventional Circuit in Negative Half Cycle When S is OFF.

### 2.2.2.2 Open Loop Data Analysis

The simulation of the circuit of the conventional AC-DC Boost converter is shown in Fig. 2.4 with the parameter of Table 2.3 the results of the simulation are given in Table 2.4.

Table 2.3 Parameter Table for Conventional Boost Converter

Parameters	Value
Input voltage ( $V_{in}$ )	220V
Switching Frequency ( $F_s$ )	5kHz
Inductor (L)	1.5mH
Output Capacitor( $C_o$ )	220 $\mu$ F
Load Resistor ( $R_l$ )	100 $\Omega$



Table 2.4 Performance Analysis of Conventional Boost Converter with Duty Cycle Variation

Duty Cycle	Efficiency (%)	Power Factor	THD	Voltage Gain
0.1	98	100	0.67	1.53
0.2	98	88	0.72	1.72
0.3	98	77	0.75	1.92
0.4	97	69	0.77	2.26
0.5	97	64	0.79	2.6
0.6	97	59	0.59	3.2
0.7	97	52	0.79	4.1
0.8	97	41	0.77	5.52
0.9	97	48	0.79	9.0

### 2.2.2.3 Voltage Gain Expression

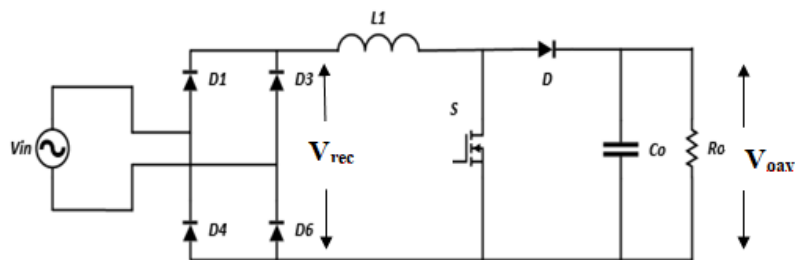


Figure 2.6 Conventional AC-DC Boost Converter with Rectified and Average Output Voltage Label.

The rectified average voltage after the conventional bridge is,

$$V_{orectave} = \frac{V_{in\max}}{\pi} \int_0^{\pi} \sin \theta d\theta = \frac{2V_{in\max}}{\pi}$$

For DC-DC Boost Converter

$$V_{oav} = \frac{V_{orec}}{1-D} \quad (2.3)$$

Where,  $D = \text{Duty Cycle} = \frac{T_{on}}{T}$ ,  $1-D = \frac{T_{off}}{T}$  and  $T = \text{Switching frequency}$

Therefore, the output voltage from equation (2.3) can be written as

$$V_{oav} = \frac{2V_{inmax}}{\pi(1-D)} \quad (2.4)$$

### 2.2.3 Buck Boost Converter

The Buck-Boost is a converter that can be regulated to give an output voltage that is higher or lower than the input voltage. During normal operation of the Buck-Boost power stage, the switch is repeatedly turned on and off. This switching action gives rise to a train of pulses at the junction of the switch, diode and the inductor.

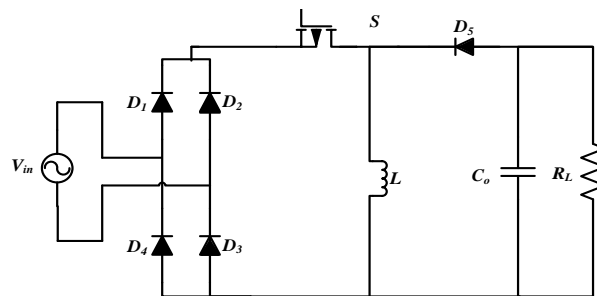


Figure 2.7 Conventional Buck Boost Converter.

**A Buck Followed by a Boost Converter:** The output is in the same polarity of the input and can be regulated to be higher or lower than the input. Such a non-inverting Buck-Boost converter may use a single inductor that is used as both the Buck inductor and the Boost inductor.

**The Inverting Topology:** The output is negative in polarity. The duty cycle again determines the output voltage.

#### 2.2.3.1 Principle of Operation

The four working stages of the conventional Buck Boost converter is illustrated in Fig. 2.8, where Figure 2.8 (a) and (b) are for switch ON and OFF condition during positive half cycle of supply and Figure 2.8 (c) and (d) are for switch ON and OFF during negative half cycle. When the switch is ON during positive half cycle the Buck Boost inductor charges from the source through switch. As the switch turns OFF, the source and the inductor voltage forward

biases the diode  $D_5$  and charges the output capacitor. Same phenomenon takes place during the negative supply cycle as the output of the diode rectifier has same polarity.

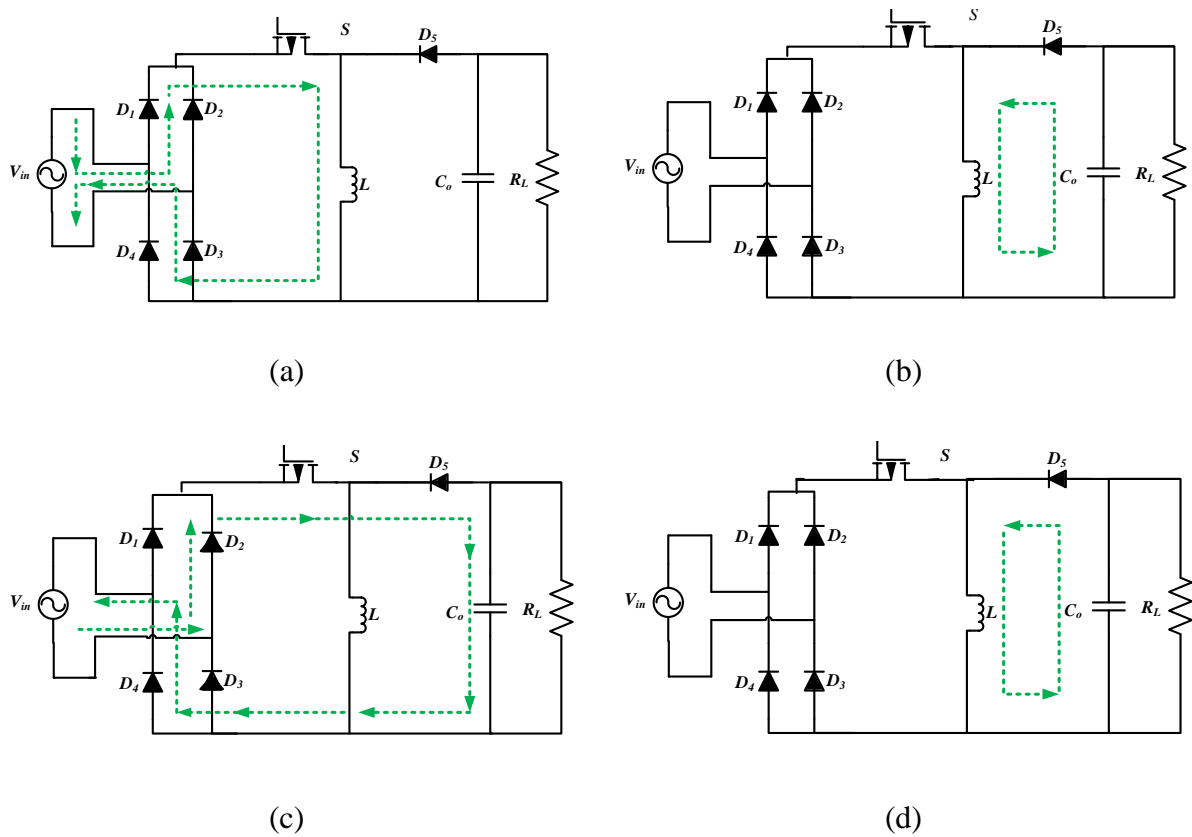


Figure 2.8 Four Modes of Operation of Proposed AC-DC Buck Boost Converter, (a) Mode 1: Conventional Circuit in Positive Half Cycle When S is ON. (b) Mode 2: Conventional Circuit in Positive Half Cycle When S is OFF. (c) Mode 3: Conventional Circuit in Negative Half Cycle When S is ON. (d) Mode 4: Conventional Circuit in Negative Half Cycle When S is OFF.

### 2.2.3.2 Open Loop Data Analysis

The conventional Buck Boost converter as shown in Fig. 2.7 with the parameters of Table 2.5 has been simulated and the results of the simulation are given in Table 2.6.

Table 2.5 Parameter Table for Conventional Buck Boost Converter

Parameters	Value
Input voltage ( $V_{in}$ )	220V
Switching Frequency ( $F_s$ )	8kHz
Inductor (L)	2.2mH
Output Capacitor ( $C_o$ )	220 $\mu$ F
Load Resistor ( $R_L$ )	100 $\Omega$

Table 2.6 Performance Analysis of Conventional Buck Boost Converter with Duty Cycle Variation

Duty Cycle	Efficiency (%)	Power Factor	THD	Voltage Gain
0.1	87	0.16	0.16	0.15
0.2	95	0.71	0.48	0.34
0.3	96	0.64	0.72	0.50
0.4	97	0.67	0.74	0.86
0.5	97	0.53	0.79	1.23
0.6	97	0.39	0.77	1.69
0.7	97	0.25	0.70	2.17
0.8	96	0.09	0.50	2.50
0.9	92	0.02	0.16	1.50

### 2.2.3.3 Voltage Gain Expression

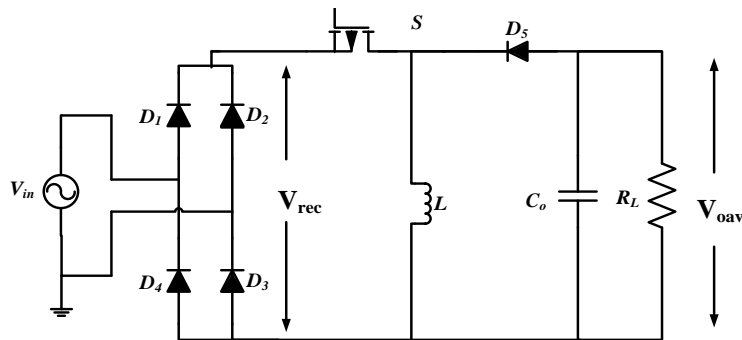


Figure 2.9 Conventional Buck Boost Converter with Rectified and Average Output Voltage Label.

The rectified voltage after the conventional bridge is,

$$V_{orectave} = \frac{V_{inmax}}{\pi} \int_0^{\pi} \sin \theta d\theta = \frac{2V_{inmax}}{\pi}$$

For DC-DC Ćuk Converter

$$V_{oav} = -D \frac{V_{rec}}{1-D} \quad (2.5)$$

Where,  $D = \text{Duty Cycle} = \frac{T_{on}}{T}$ ,  $1-D = \frac{T_{off}}{T}$  and  $T = \text{Switching frequency}$

Therefore, the output voltage from equation (2.5) can be written as

$$V_{oav} = -D \frac{2V_{inmax}}{\pi(1-D)} \quad (2.6)$$

## 2.2.4 Ćuk Converter

Like the Buck-Boost circuit it delivers an inverted output. Virtually all of the output current passes through  $C_1$ , and as ripple current. So  $C_1$  is usually a large electrolytic with a high ripple current rating and low ESR (equivalent series resistance), to minimize losses. The main difference between the Ćuk and the other converters is that the Ćuk used a capacitor as the energy storing element.

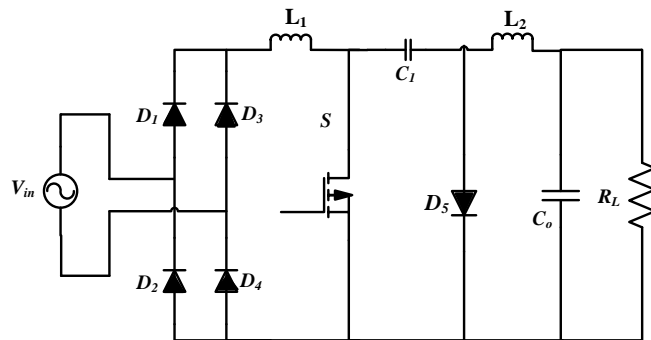


Figure 2.10 : Conventional Ćuk Converter.

### 2.2.4.1 Working Principle

The four working stages of the conventional Ćuk converter is illustrated in Figure 2.11, where Figure 2.11 (a) and (b) are for switch ON and OFF condition during positive supply cycle and Figure 2.11 (c) and (d) are for switch ON and OFF during negative cycle. When the switch is ON during positive half cycle the Ćuk inductor charges from the source through the short circuit of the source. Current continue to flow following two paths as mention in the Figure 2.11 As the switch turns OFF, the source and the inductor voltage forward biases the output diode and charges the output capacitor. Same phenomenon takes place during the negative supply cycle.

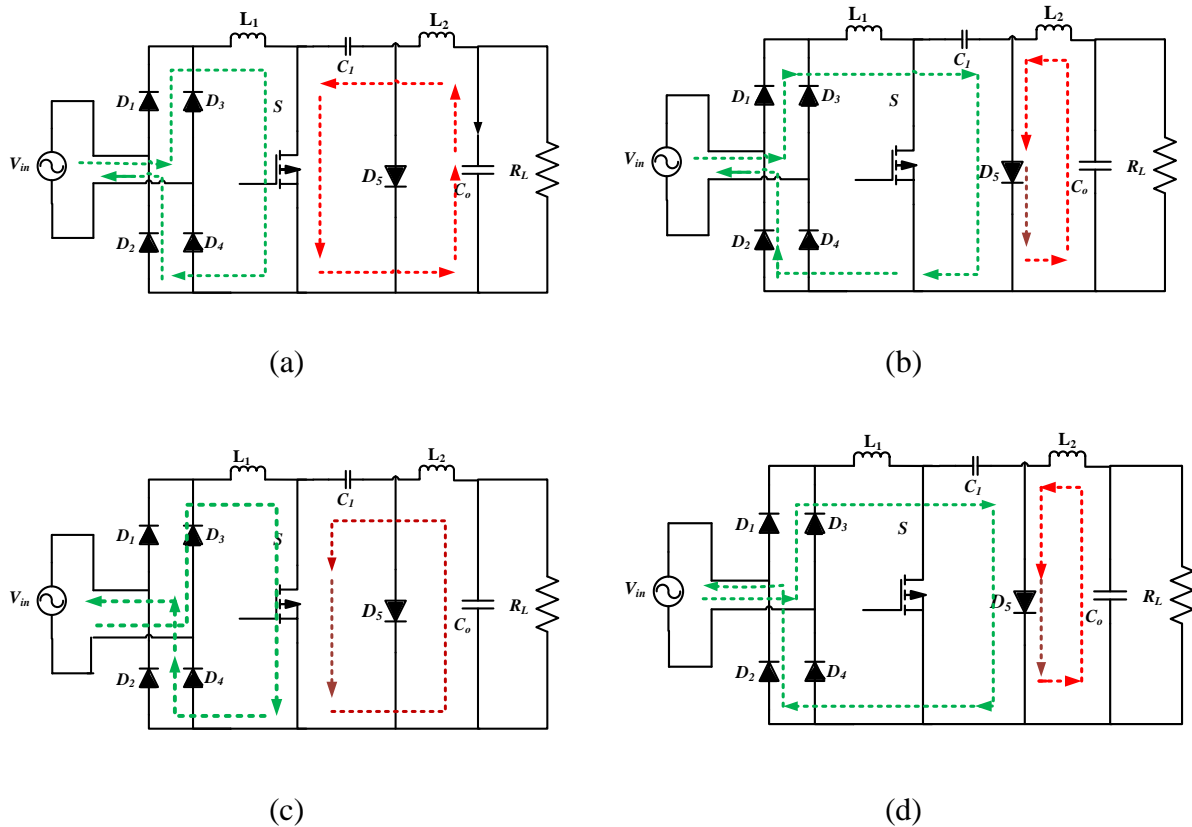


Figure 2.11 Four Modes of Operation of Conventional AC-DC Ćuk Converter, (a) Mode 1: Conventional Circuit in Positive Half Cycle When S is ON. (b) Mode 2: Conventional Circuit in Positive Half Cycle When S is OFF. (c) Mode 3: Conventional Circuit in Negative Half Cycle When S is ON. (d) Mode 4: Conventional Circuit in Negative Half Cycle When S is OFF.

### 2.2.4.2 Open Loop Simulation

The conventional Ćuk converter as shown in Fig. 2.10 with the parameters of Table 2.7 has been simulated and the results of the simulation are given in Table 2.8.

Table 2.7 Parameter Table for Conventional Ćuk Converter

Parameters	Value
Input voltage ( $V_{in}$ )	220V
Switching Frequency ( $F_s$ )	5kHz
Inductor ( $L_1$ )	2.5mH
Inductor ( $L_2$ )	1.5mH
Output Capacitor ( $C_o$ )	220 $\mu$ F
Load Resistor ( $R_L$ )	100 $\Omega$

Table 2.8 Performance Analysis of Conventional Ćuk Converter with Duty Cycle Variation

Duty Cycle	Efficiency (%)	THD	Power Factor	Voltage Gain
0.1	91	2.30	0.39	0.23
0.2	93	1.58	0.52	0.44
0.3	93	1.25	0.62	0.64
0.4	93	1.00	0.70	0.85
0.5	93	0.80	0.80	1.00
0.6	93	0.65	0.83	1.31
0.7	93	0.47	0.89	1.90
0.8	93	0.33	0.93	3.23
0.9	93	0.37	0.92	7.32

### 2.2.4.3 Ideal Voltage Gain Expression

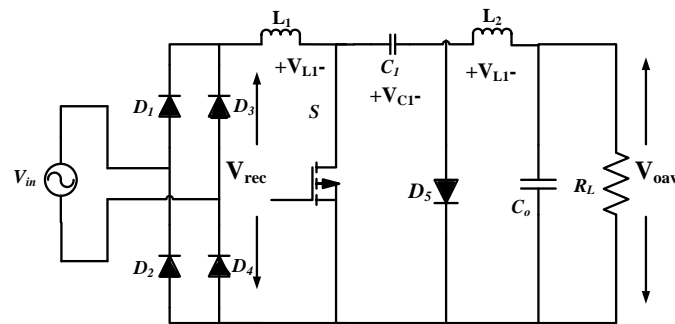


Figure 2.12 : Conventional Ćuk Converter with Rectified and Average Output Voltage Label.

The rectified average voltage after the conventional bridge is,

$$V_{orectave} = \frac{V_{in\max}}{\pi} \int_0^{\pi} \sin \theta d\theta = \frac{2V_{in\max}}{\pi}$$

For DC-DC Ćuk Converter

$$V_{oav} = -D \frac{V_{rec}}{1-D} \quad (2.7)$$

Where,  $D = \text{Duty Cycle} = \frac{T_{on}}{T}$ ,  $1-D = \frac{T_{off}}{T}$  and  $T = \text{Switching frequency}$

Therefore the output voltage can be written as

$$V_{oav} = -D \frac{2V_{in,max}}{\pi(1-D)} \quad (2.8)$$

### 2.2.5 SEPIC Converter

The Single-Ended Primary-Inductor Converter (SEPIC) is a type of AC-DC converter allowing the electrical potential (voltage) at its output to be greater than, less than, or equal to that at its input. The output of the SEPIC is controlled by the duty cycle of the control transistor.

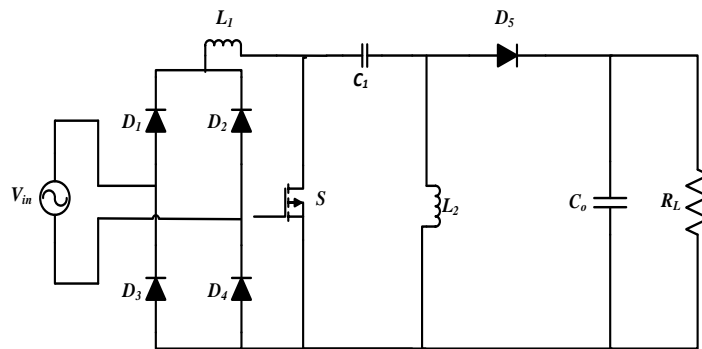


Figure 2.13 : Conventional SEPIC Converter.

#### 2.2.5.1 Principle of Operation

The four working stages of the conventional converter is illustrated in Figure 2.14, where Figure 2.14 (a) and (b) are for switch ON and OFF condition during positive supply cycle and Figure 2.14 (c) and (d) are for switch ON and OFF during negative cycle. During positive half signal of the input voltage current flows in two paths. The SEPIC inductor charges from the source through the short path of the switch as given in the figure 2.14(a). As the switch turns OFF, the source and the inductor voltage forward biases the diode  $D_5$  and charges the output capacitor. For the negative half cycle of the input same thing repeat again.



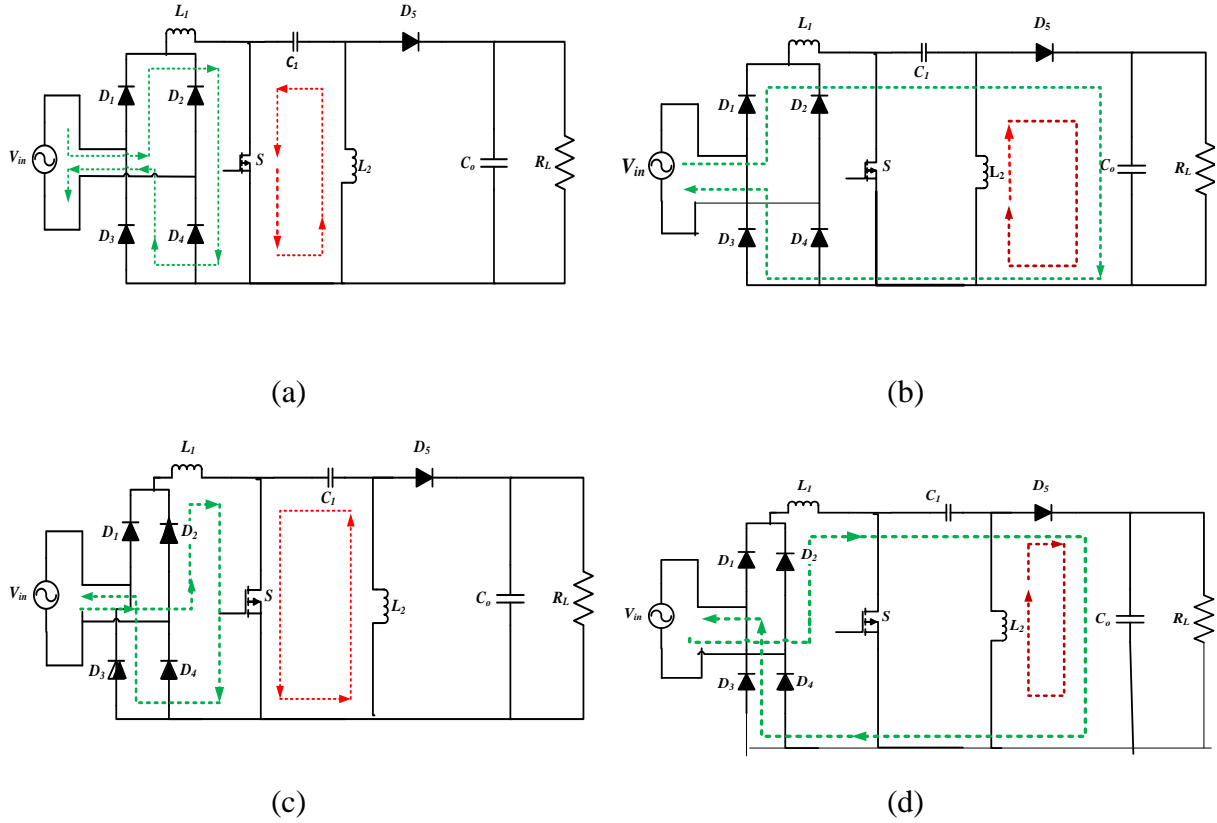


Figure 2.14 Four Modes of Operation of Proposed AC-DC SEPIC Converter, (a) Mode 1: Conventional Circuit in Positive Half Cycle When S is ON. (b) Mode 2: Conventional Circuit in Positive Half Cycle When S is OFF. (c) Mode 3: Conventional Circuit in Negative Half Cycle When S is ON. (d) Mode 4: Conventional Circuit in Negative Half Cycle When S is OFF.

### 2.2.5.2 Open Loop Simulation

The conventional SEPIC converter as shown in Fig. 2.13 with the parameters of Table 2.9 has been simulated and the results of the simulation are given in Table 2.10.

Table 2.9 Parameter Table for Conventional SEPIC Converter

Parameters	Value
Input voltage ( $V_{in}$ )	220V
Switching Frequency ( $F_s$ )	5kHz
Inductor (L)	1.5mH
Capacitor (C)	0.8 $\mu$ F
Output Capacitor ( $C_o$ )	220 $\mu$ F
Load Resistor ( $R_L$ )	100 $\Omega$

Table 2.10 Performance Analysis of Conventional SEPIC Converter with Duty Cycle Variation

Duty Cycle	Efficiency (%)	THD	Power Factor	Voltage Gain
0.1	075	1.00	0.50	0.20
0.2	90	0.98	0.65	0.40
0.3	94	0.81	0.77	0.70
0.4	95	0.56	0.86	0.90
0.5	96	0.41	0.90	1.41
0.6	95	0.43	0.90	2.00
0.7	94	0.38	0.90	2.90
0.8	91	0.30	0.89	4.30
0.9	80	0.43	0.87	7.27

### 2.2.5.3 Ideal Voltage Gain Expression

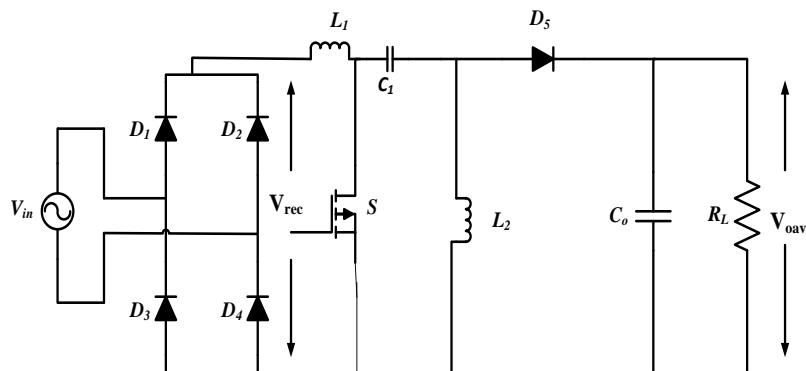


Figure 2.15 : Conventional SEPIC Converter with Rectified and Average Output Voltage Label.

The rectified average voltage after the conventional bridge is,

$$V_{orectave} = \frac{V_{inmax}}{\pi} \int_0^{\pi} \sin \theta d\theta = \frac{2V_{inmax}}{\pi}$$

For DC-DC Ćuk Converter

$$V_{oav} = D \frac{V_{orec}}{1-D} \quad (2.9)$$

Where,  $D = \text{Duty Cycle} = \frac{T_{on}}{T}$ ,  $1 - D = \frac{T_{off}}{T}$  and  $T = \text{Switching frequency}$

Therefore the output voltage can be written as

$$V_{oav} = D \frac{2V_{inmax}}{\pi(1-D)} \quad (2.10)$$

# Chapter 3 Proposed Bridgeless AC-DC Converters

## 3.1 Boost Converter

Bridgeless AC-DC Boost Converter is used to convert the alternating voltage to direct voltage without using bridges. In normal boost converter only the variable DC voltage is converted to required DC voltage, but here AC is directly converted to DC. In the proposed Boost converter the high frequency switching can be done at the input side of the converter. The converter works as high frequency chopper. The near sinusoidal chopped high frequency current is improved easily by the Boost inductor. The converter is shown in Figure 3.1. During the positive half cycle as the switch turns ON the input inductor is charged by the input voltage and when the switch is OFF the output capacitor is charged by the input voltage.

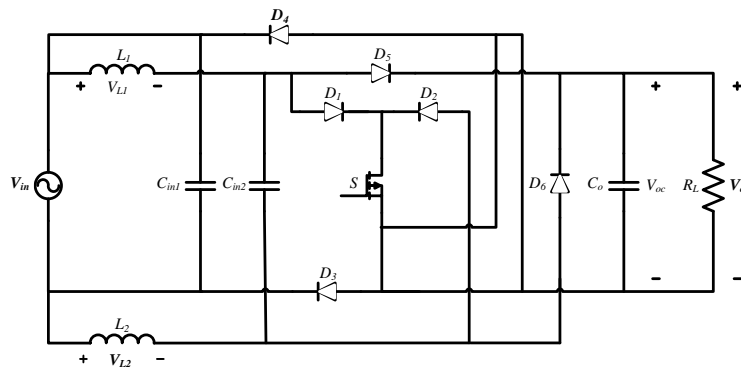


Figure 3.1 Proposed Boost Converter.

### 3.1.1 Principle of Operation

The four working stages of the proposed converter is illustrated in Figure 3.2, where Figure 3.2 (a) and (b) are for switch ON and OFF condition during positive supply cycle and Figure 3.2 (c) and (d) are for switch ON and OFF during negative cycle. The proposed converter is operating like conventional converter. During the positive half cycle of the input when switch is ON the Boost inductor get charged. When switch is OFF, the source and the inductor voltage forward biases the output diode and charges the output capacitor. For the negative half cycle of the input signal same phenomenon takes as the output of the diode rectifier has same polarity.

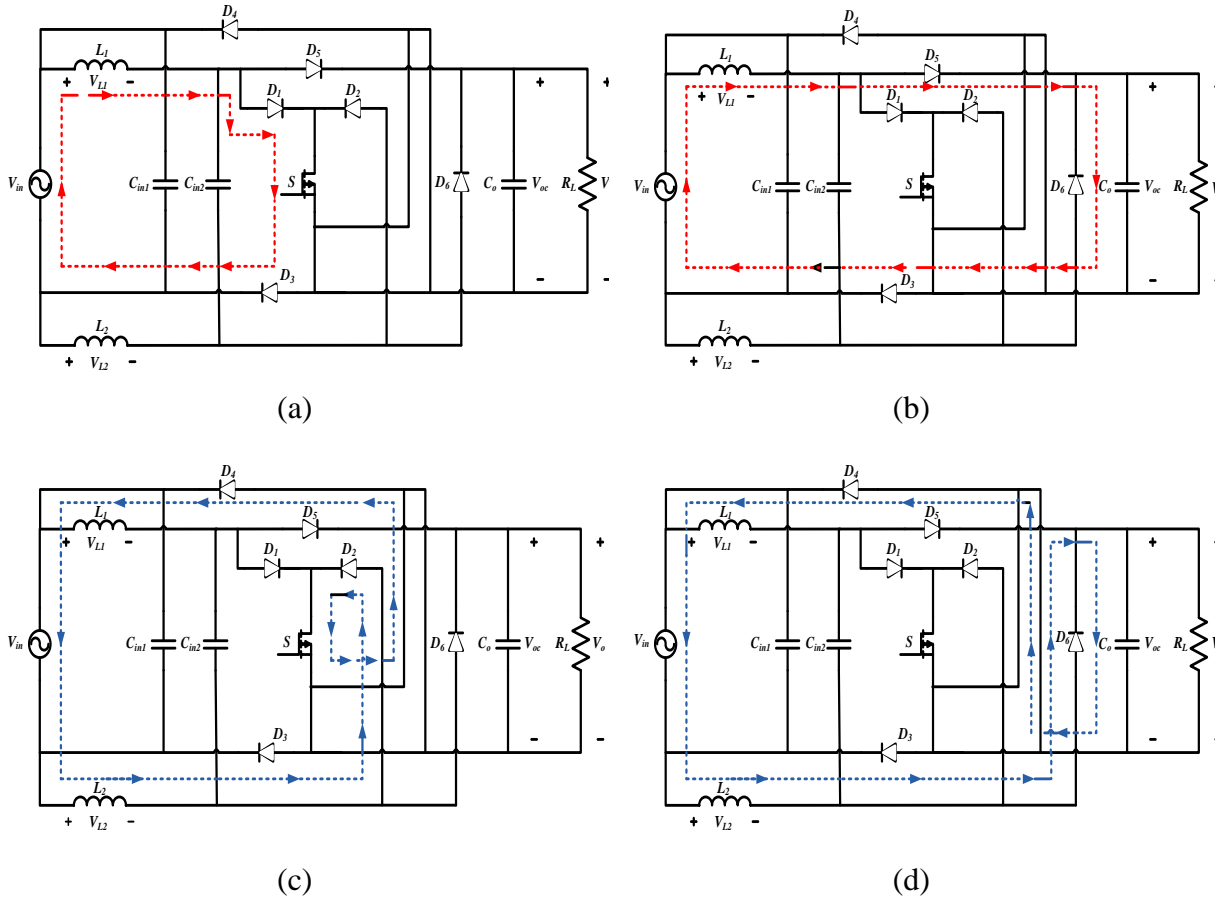


Figure 3.2 Four Modes of Operation of Proposed AC-DC Boost Converter, (a) Mode 1: Proposed Circuit in Positive Half Cycle When S is ON. (b) Mode 2: Proposed Circuit in Positive Half Cycle When S is OFF. (c) Mode 3: Proposed Circuit in Negative Half Cycle When S is ON. (d) Mode 4: Proposed Circuit in Negative Half Cycle When S2 is OFF.

State 1. During the positive cycle of the input signal when the switch S is turned ON, the diode  $D_2, D_4, D_5$  and  $D_6$  are OFF. Current flows through  $L_1, D_1$  switch S and  $D_3$  as shown in Fig. 3.2(a).

State 2. In the positive cycle of the input signal when the switch S is OFF, the diode  $D_5$  is forward biased. The input capacitors are disconnected, but current continues to flow through  $L_1, D_5$  output capacitor  $C_o$  and  $D_3$  as shown in Fig. 3.2(b).

State 3. Similar to State 1 operation, during the negative cycle of the input signal when the switch S is turned ON, the diode  $D_1, D_3, D_5$  and  $D_6$  are OFF. Current flows through  $L_2$  and  $D_4$ , as shown in Fig. 3.2(c).

State 4. In the negative cycle of the input signal when the switch S is turned OFF the diode  $D_6$  become conductive, current flowing through the inductor  $L_2$ , as shown in Fig. 3.2(d).

### 3.1.2 Open Loop Data Analysis

The simulation of the circuit of Fig. 3.1 with no feedback for PFC and input current THD improvement is carried out with the parameters of Table 3.1. The results of the simulation are given in Table 3.2.

Table 3.1 Parameter Table of Proposed Boost Converter

Parameters	Value
Input voltage ( $V_{in}$ )	220V
Switching Frequency ( $F_s$ )	5kHz
Inductor ( $L_1, L_2$ )	1.5mH
Capacitor ( $C_{in1}, C_{in2}$ )	4.5 $\mu$ F
Output Capacitor ( $C_o$ )	220 $\mu$ F
Load Resistor ( $R_L$ )	100 $\Omega$

Table 3.2 Performance Analysis of Proposed Boost Converter with Duty Cycle Variation

Duty Cycle	Proposed				Conventional			
	Efficiency (%)	THD	Power Factor	Voltage Gain	Efficiency (%)	THD	Power Factor	Voltage Gain
0.1	98	0.92	0.7	1.5	98	1.00	0.67	1.53
0.2	98	0.62	0.8	1.72	98	0.88	0.72	1.72
0.3	98	0.47	0.84	1.98	98	0.77	0.75	1.92
0.4	98	0.38	0.87	2.31	97	0.69	0.77	2.26
0.5	98	0.36	.88	2.71	97	0.64	0.79	2.6
0.6	98	0.37	0.87	3.34	97	0.59	0.59	3.2
0.7	98	0.40	0.85	4.2	97	0.52	0.79	4.1
0.8	98	0.37	0.82	5.6	97	0.41	0.77	5.52
0.9	97	0.32	0.74	8.2	97	0.48	0.79	9.0

### 3.1.3 Ideal Voltage Gain Equation

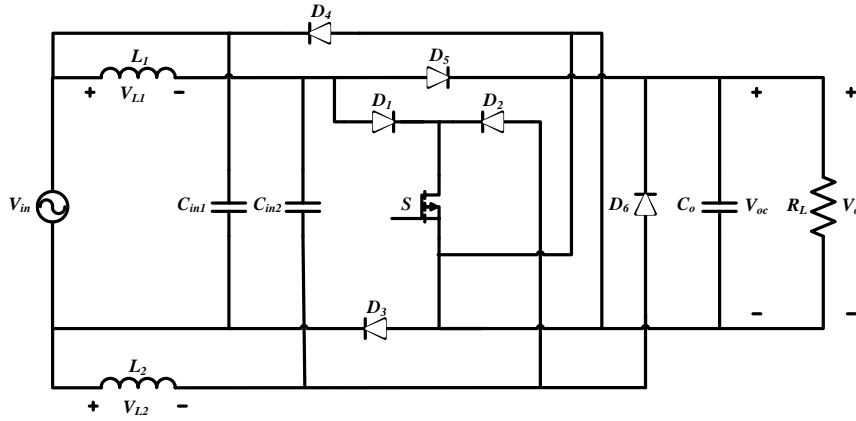


Figure 3.3 Proposed Boost Converter with Voltage across the Inductor and Output Capacitor.

From Fig. 3.3,

When Switch is ON,

$$v_{L1} = v_{in}$$

When switch is OFF,

$$v_{L1} = v_{in} - v_{oc}$$

Volt –sec balance over one switching cycle will not be equal to zero since the input is sinusoidal. Volt –Sec balance for on switching cycle is therefore

$$\int_{t_i}^{t_i+T_{sw}} v_{L1} dt = \int_{t_i}^{t_i+DT_{sw}} v_{in} dt + \int_{t_i+DT_{sw}}^{t_i+T_{sw}} (v_{in} - v_{oc}) dt$$

The volt –sec balance over a line frequency period will be zero. For full supply cycle of N switching per period

$$\sum_{n=1}^N \int_{t_i}^{t_i+T_{sw}} v_{L1} dt = \sum_{n=1}^N \int_{t_i}^{t_i+DT_{sw}} v_{in} dt + \sum_{n=1}^N \int_{t_i+DT_{sw}}^{t_i+T_{sw}} (v_{in} - v_{oc}) dt \quad (3.1)$$

Where

$$v_{oc} = V_{o\max} \sin(\omega t - \theta_{oc})$$

$$v_{in} = V_{in\max} \sin(\omega t - \theta_{in})$$

From Equation (3.1),

$$\begin{aligned} \sum_{n=1}^N \int_{t_i}^{t_i+DT_{sw}} v_{in} dt &= -\sum_{n=1}^N \int_{t_i+DT_{sw}}^{t_i+T_{sw}} (v_{in} - v_{oc}) dt \\ \Rightarrow \sum_{n=1}^N \int_{t_i+DT_{sw}}^{t_i+T_{sw}} (V_{in\max} \sin(\omega t - \theta_{in})) dt &= -\sum_{n=1}^N \int_{t_i+DT_{sw}}^{t_i+T_{sw}} [V_{in\max} \sin(\omega t - \theta_{in}) dt \\ &\quad - V_{o\max} \sin(\omega t - \theta_{oc})] dt \\ \Rightarrow \sum_{n=1}^N \left[ -\frac{V_{in\max}}{\omega} \cos(\omega t - \theta_{in}) \right]_{t_i}^{t_i+DT_{sw}} &= \sum_{n=1}^N \left[ -\frac{V_{in\max}}{\omega} \cos(\omega t - \theta_{in}) \right]_{t_i+DT_{sw}}^{t_i+T_{sw}} \\ &\quad - \sum_{n=1}^N \left[ -\frac{V_{o\max}}{\omega} \cos(\omega t - \theta_{oc}) \right]_{t_i+DT_{sw}}^{t_i+T_{sw}} \end{aligned}$$

Using identity  $\cos A - \cos B = 2 \sin \frac{A+B}{2} \sin \frac{A-B}{2}$ ,

$$\begin{aligned} \Rightarrow \sum_{n=1}^N \frac{V_{in\max}}{\omega} \left[ 2 \sin \frac{\omega t_i - \theta_{in} + \omega t_i + \omega DT_{sw} - \theta_{in}}{2} \sin \frac{\omega t_i - \theta_{in} - \omega t_i - \omega DT_{sw} + \theta_{in}}{2} \right] \\ = \sum_{n=1}^N \frac{V_{o\max}}{\omega} \left[ 2 \sin \frac{\omega t_i - \omega DT_{sw} - \theta_{oc} + \omega t_i + \omega T_{sw} - \theta_{oc}}{2} \right. \\ \left. \times \sin \frac{\omega t_i + \omega T_{sw} - \theta_{oc} - \omega t_i - \omega DT_{sw} + \theta_{oc}}{2} \right] \\ \Rightarrow \sum_{n=1}^N \frac{V_{in\max}}{\omega} \left[ \sin \left( \omega t_i - \theta_{in} + \frac{\omega T_{sw}}{2} \right) \sin \frac{\omega T_{sw}}{2} \right] = \sum_{n=1}^N \frac{V_{o\max}}{\omega} \left[ \sin \left( \omega t_i - \theta_{in} + \frac{(1+D)\omega T_{sw}}{2} \right) \right. \\ \left. \times \sin \frac{(1-D)\omega T_{sw}}{2} \right] \\ \Rightarrow \frac{\sin \frac{\omega T_{sw}}{2}}{\sin \frac{(1+D)\omega T_{sw}}{2}} \times \sum_{n=1}^N V_{o\max} \left[ \sin \left( \omega t_i - \theta_{in} + \frac{\omega T_{sw}}{2} \right) \right] = \sum_{n=1}^N V_{o\max} \left[ \sin \left( \omega t_i - \theta_{in} + \frac{(1+D)\omega T_{sw}}{2} \right) \right] \\ \Rightarrow \frac{\sin \frac{\omega T_{sw}}{2}}{\frac{\omega T_{sw}}{2}} \times \sum_{n=1}^N V_{o\max} \left[ \sin \left( \omega t_i - \theta_{in} + \frac{\omega T_{sw}}{2} \right) \right] = \\ \frac{\sin \frac{(1-D)\omega T_{sw}}{2}}{\frac{(1-D)\omega T_{sw}}{2}} \times (1-D) \sum_{n=1}^N V_{o\max} \left[ \sin \left( \omega t_i - \theta_{in} + \frac{(1+D)\omega T_{sw}}{2} \right) \right] \end{aligned}$$



Using identities,  $\lim_{\theta \rightarrow 0} \frac{\sin \theta}{\theta} = 1$  and

i.  $\frac{\omega T_{sw}}{2} \rightarrow 0$  as  $T_{sw} \rightarrow 0$

ii.  $\frac{(1+D)\omega T_{sw}}{2} \rightarrow 0$  as  $T_{sw} \rightarrow 0$

$$\Rightarrow \frac{1}{(1-D)} \times \sum_{n=1}^N V_{o\max} \left[ \sin(\omega t_i - \theta_{in}) \right] = \sum_{n=1}^N V_{in\max} \left[ \sin(\omega t_i - \theta_o) \right]$$

$$\Rightarrow \sum_{n=1}^N V_{o\max} \left[ \sin(\omega t_i - \theta_o) \right] = \frac{1}{(1-D)} \times \sum_{n=1}^N V_{in\max} \left[ \sin(\omega t_i - \theta_{in}) \right]$$

Thus the average voltage can be found as,

$$V_{oav} = \frac{1}{\pi} \int_0^{\pi} V_{o\max} \sin \theta d\theta$$

$$\Rightarrow V_{OAV} = \frac{1}{\pi} \int_0^{\pi} \frac{V_{in\max}}{1-D} \sin \theta d\theta$$

$$\Rightarrow V_{OAV} = \frac{V_{in\max}}{\pi(1-D)} \int_0^{\pi} \sin \theta d\theta$$

$$\Rightarrow V_{OAV} = \frac{V_{in\max}}{\pi(1-D)} \left[ -\cos \theta \right]_0^{\pi}$$

$$\Rightarrow V_{OAV} = \frac{2V_{in\max}}{\pi(1-D)} \tag{3.2}$$

Table 3.3 Comparison between theoretical and simulation result of proposed Boost converter

Duty Cycle	V <sub>oav</sub> (Theoretical)	V <sub>oav</sub> (Simulation)
0.1	18V	24V
0.2	20V	29V
0.3	23V	34V
0.4	27V	40V
0.5	32V	47V
0.6	40V	56V
0.7	53V	73V
0.8	80V	99V
0.9	159V	114V

Comparison has been made between theoretical simulation values by taking 25V the peak value of the output voltage. From the comparison table it has been found that there is a deviation between simulation and theoretical value. Theoretical value of the output voltages have been calculated by considering ideal behavior of the components but simulation values show the non ideal characteristics of the components.

### 3.2 SEPIC Converter

Basic SEPIC topology based on single phase AC-DC converter that can rectify both positive and negative half cycle of the input individually. A SEPIC is essentially a boost converter followed by a buck-boost converter, therefore it is similar to a traditional buck-boost converter, but has advantages of having non-inverted output (the output has the same voltage polarity as the input).

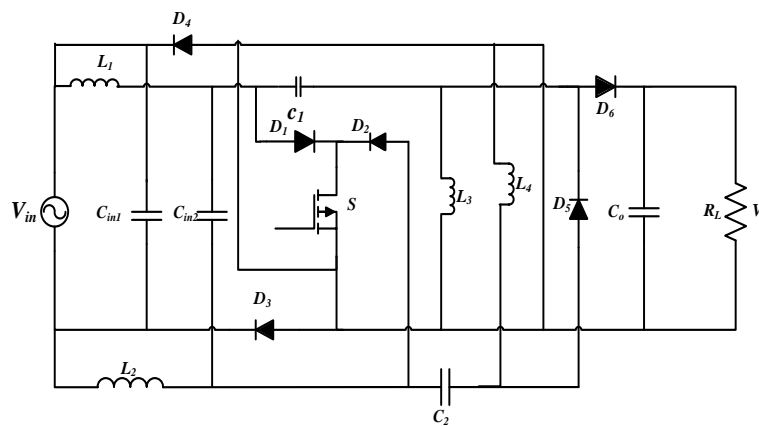


Figure 3.4 Proposed SEPIC Converter.

#### 3.2.1 Working Principle

The four working stages of the proposed SEPIC converter is illustrated in Figure 3.5, where Figure 3.5 (a) and (b) are for switch ON and OFF condition during positive supply cycle and Figure 3.5 (c) and (d) are for switch ON and OFF during negative cycle. The proposed converter is operating like conventional SEPIC converter. Detail operation of proposed SEPIC converter along with circuit diagram is given below.

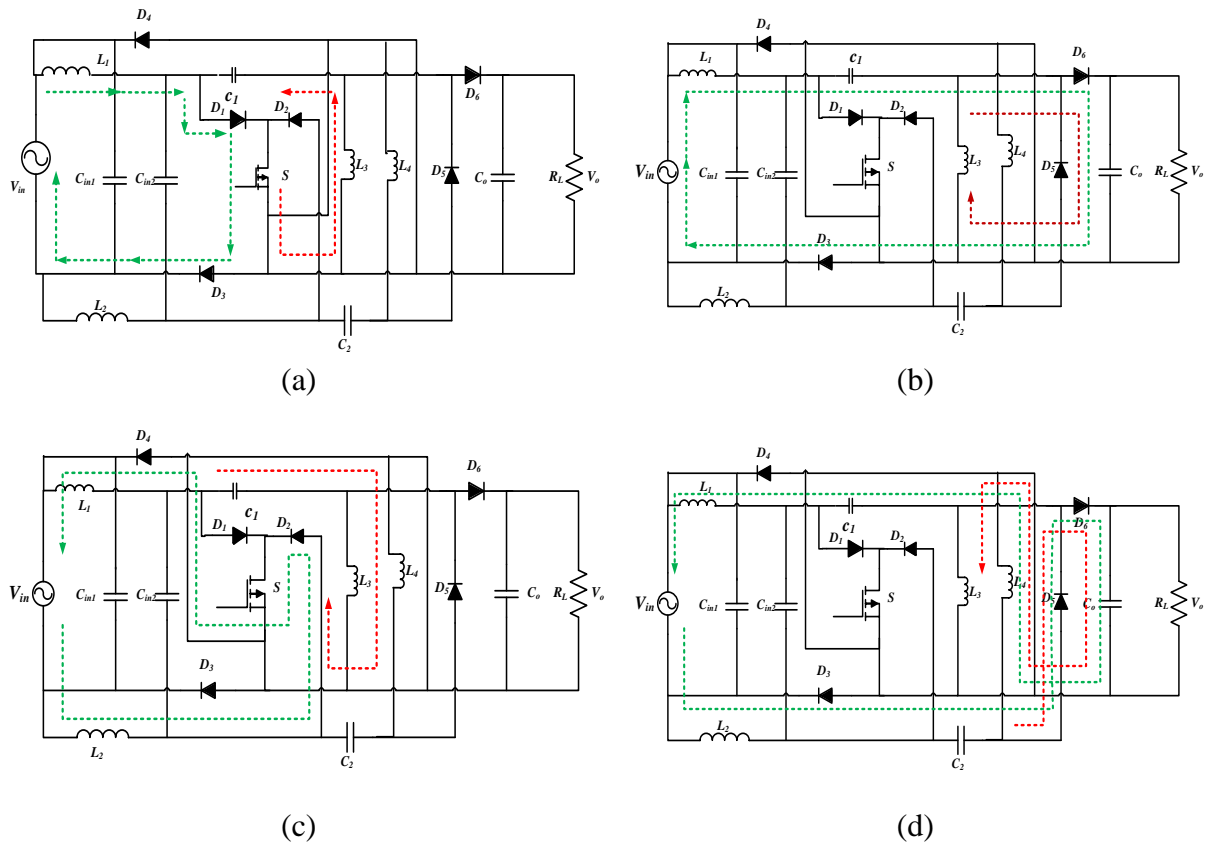


Figure 3.5: Four Modes of Operation of Proposed AC-DC SEPIC Converter, (a) Mode 1: Proposed Circuit in Positive Half Cycle When S is ON. (b) Mode 2: Proposed Circuit in Positive Half Cycle When S is OFF. (c) Mode 3: Proposed Circuit in Negative Half Cycle When S is ON. (d) Mode 4: Proposed Circuit in Negative Half Cycle When S is OFF.

State 1. During the positive cycle of the input signal when the switch S is turned ON, current flows in two paths, as shown in Fig. 3.5(a) the first is from the input, inductor  $L_1$ , through the switch S, in the second path capacitor  $C_1$  and inductor  $L_3$  will get charged.

State 2. In the positive cycle of the input signal when the switch S is OFF, the diode  $D_6$  is forward biased. The input capacitors are disconnected, but the current continues to flow through the inductors in two paths, as shown in Fig. 3.5(b). The first is from the input inductor  $L_1$  through the load, and back to the output inductor through the diode  $D_6$ . The second path is from the inductor  $L_3$  and the diode  $D_6$ .

State 3. Similar to State 1 operation, during the negative cycle of the input signal when the switch S is turned ON, the diodes  $D_5$  and  $D_6$  are reverse biased. Current flows in two paths, as shown in Fig. 3.5(c).

State 4. In the negative cycle of the input signal when the switch S is turned OFF and the diodes  $D_4, D_5$  and  $D_6$  are forward biased and current continues to flow in two paths shown in Fig 3.5(d).

During both positive and negative cycle of the supply, the energy transferred to the load is unidirectional, thus AC-DC conversion is achieved.

### 3.2.2 Open Loop Simulation

Table 3.4 Parameter Table of Proposed SEPIC Converter

Parameters	Value
Input voltage ( $V_{in}$ )	220V
Switching Frequency ( $F_s$ )	8kHz
Inductor ( $L_1, L_2$ )	2.5 mH
Capacitor ( $C_1, C_2$ )	0.8 $\mu$ F
Capacitor ( $C_{in1}, C_{in2}$ )	5.5 $\mu$ F
Output Capacitor ( $C_o$ )	220 $\mu$ F
Load Resistor ( $R_L$ )	100 $\Omega$

Table 3.5 Performance Analysis of Proposed SEPIC Converter with Duty Cycle Variation

Duty Cycle	Proposed Circuit				Conventional Circuit			
	Efficiency (%)	THD	Power Factor	V Gain	Efficiency (%)	THD	Power Factor	V Gain
0.1	89	0.31	0.35	0.3	75	1.00	0.5	0.2
0.2	95	0.48	0.71	0.6	90	0.98	0.65	0.4
0.3	96	0.39	0.88	1.01	94	0.81	0.77	0.7
0.4	97	0.28	0.94	1.41	95	0.56	0.86	0.9
0.5	97	0.20	0.97	1.81	96	0.41	0.9	1.41
0.6	98	0.16	0.98	2.28	95	0.43	0.9	2.00
0.7	97	0.31	0.94	3.3	94	0.38	0.9	2.9
0.8	97	0.31	0.86	4.9	91	0.30	0.89	4.3
0.9	92	0.33	0.74	6.9	80	0.43	0.87	7.27

### 3.2.3 Ideal Voltage Gain Equation

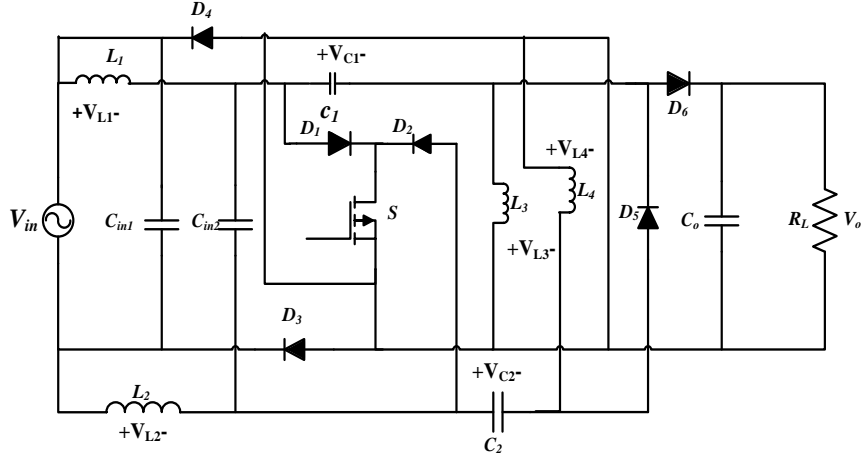


Figure 3.6 Input Switched AC-DC SEPIC Converter with Voltage across the components  $L_1$ ,  $L_2$ ,  $L_3$ ,  $L_4$ ,  $C_1$ ,  $C_2$  and  $R_L$ .

At the input stage:

When switch is ON,

$$v_{L1} = v_{in}$$

When switch is OFF,

$$v_{L1} = v_{in} - v_{c1} - v_o$$

Volt-sec balance over one switching cycle will not be equal to zero since the input is sinusoidal. Volt-sec balance for one switching cycle is therefore

$$\int_{t_i}^{t_i+T_{sw}} v_{L1} dt = \int_{t_i}^{t_i+DT_{sw}} v_{in} dt + \int_{t_i+DT_{sw}}^{t_i+T_{sw}} (v_{in} - v_{c1} - v_o) dt$$

Where,

$$v_{oc} = v_{o1}$$

The volt-sec balance over a line frequency period will be zero. For full supply cycle of  $N$  switching per period,

$$\sum_{n=1}^N \int_{t_i}^{t_i+T_{sw}} v_{L1} dt = \sum_{n=1}^N \int_{t_i}^{t_i+DT_{sw}} v_{in} dt + \sum_{n=1}^N \int_{t_i+DT_{sw}}^{t_i+T_{sw}} (v_{in} - v_{c1} - v_o) dt \quad (3.3)$$

Suppose,

$$v_{in} = V_{inmax} \sin(\omega t - \theta_{in})$$

$$v_{c1} = V_{c1max} \sin(\omega t - \theta_{c1})$$

$$v_o = V_{omax} \sin(\omega t - \theta_o)$$

From (3.3),

$$\begin{aligned} \Rightarrow \sum_{n=1}^N \int_{t_i}^{t_i+DT_{sw}} v_{in} dt &= -\sum_{n=1}^N \int_{t_i+DT_{sw}}^{t_i+T_{sw}} (v_{in} - v_{c1} - v_o) dt \\ \Rightarrow \sum_{n=1}^N \int_{t_i}^{t_i+DT_{sw}} V_{in\max} \sin(\omega t - \theta_{in}) dt &= -\sum_{n=1}^N \int_{t_i+DT_{sw}}^{t_i+T_{sw}} [V_{in\max} \sin(\omega t - \theta_{in}) \\ &\quad - V_{c\max} \sin(\omega t - \theta_c) - V_{o\max} \sin(\omega t - \theta_o)] dt \end{aligned}$$

After Integration,

$$\begin{aligned} \Rightarrow \sum_{n=1}^N \left[ -\frac{V_{in\max}}{\omega} \cos(\omega t - \theta_{in}) \right]_{t_i}^{t_i+DT_{sw}} &= \sum_{n=1}^N \left[ -\frac{V_{in\max}}{\omega} \cos(\omega t - \theta_{in}) \right]_{t_i+DT_{sw}}^{t_i+T_{sw}} \\ &\quad - \sum_{n=1}^N \left[ -\frac{V_{c\max}}{\omega} \cos(\omega t - \theta_c) \right]_{t_i+DT_{sw}}^{t_i+T_{sw}} - \sum_{n=1}^N \left[ -\frac{V_{o\max}}{\omega} \cos(\omega t - \theta_o) \right]_{t_i+DT_{sw}}^{t_i+T_{sw}} \\ \Rightarrow -\sum_{n=1}^N \left[ \frac{V_{in\max}}{\omega} \cos(\omega t_i + \omega DT_{sw} - \theta_{in}) \right] &+ \sum_{n=1}^N \left[ -\frac{V_{in\max}}{\omega} \cos(\omega t_i - \theta_{in}) \right] = \sum_{n=1}^N \left[ \frac{V_{in\max}}{\omega} \cos(\omega t_i + \omega T_{sw} - \theta_{in}) \right] - \sum_{n=1}^N \left[ -\frac{V_{in\max}}{\omega} \cos(\omega t_i + \omega DT_{sw} - \theta_{in}) \right] \\ &\quad - \sum_{n=1}^N \left[ \frac{V_{c\max}}{\omega} \cos(\omega t_i + \omega T_{sw} - \theta_c) \right] + \sum_{n=1}^N \left[ \frac{V_{c\max}}{\omega} \cos(\omega t_i + \omega DT_{sw} - \theta_c) \right] \\ &\quad - \sum_{n=1}^N \left[ \frac{V_{o\max}}{\omega} \cos(\omega t_i + \omega T_{sw} - \theta_o) \right] + \sum_{n=1}^N \left[ \frac{V_{o\max}}{\omega} \cos(\omega t_i + \omega DT_{sw} - \theta_o) \right] \\ \Rightarrow \sum_{n=1}^N \left[ \frac{V_{in\max}}{\omega} \cos(\omega t_i - \theta_{in}) \right] &- \sum_{n=1}^N \left[ \frac{V_{in\max}}{\omega} \cos(\omega t_i + \omega T_{sw} - \theta_{in}) \right] = \\ \sum_{n=1}^N \left[ \frac{V_{c\max}}{\omega} \cos(\omega t_i + \omega DT_{sw} - \theta_c) \right] &- \sum_{n=1}^N \left[ \frac{V_{c\max}}{\omega} \cos(\omega t_i + \omega T_{sw} - \theta_c) \right] \\ + \sum_{n=1}^N \left[ \frac{V_{o\max}}{\omega} \cos(\omega t_i + \omega DT_{sw} - \theta_o) \right] &- \sum_{n=1}^N \left[ \frac{V_{o\max}}{\omega} \cos(\omega t_i + \omega T_{sw} - \theta_o) \right] \\ \Rightarrow \sum_{n=1}^N \frac{V_{in\max}}{\omega} [\cos(\omega t_i - \theta_{in}) - \cos(\omega t_i + \omega T_{sw} - \theta_{in})] &= \sum_{n=1}^N \frac{V_{c1\max}}{\omega} [\cos(\omega t_i + \omega DT_{sw} - \theta_c) - \cos(\omega t_i + \omega T_{sw} - \theta_c)] \\ &\quad + \sum_{n=1}^N \frac{V_{o\max}}{\omega} [\cos(\omega t_i + \omega DT_{sw} - \theta_o) - \cos(\omega t_i + \omega T_{sw} - \theta_o)] \end{aligned}$$

Using Identity,  $\cos A - \cos B = 2 \sin \frac{A+B}{2} \sin \frac{B-A}{2}$

$$\sum_{n=1}^N \frac{V_{in\max}}{\omega} \left[ 2 \sin \frac{\omega t_i - \theta_{in} + \omega t_i + \omega T_{sw} - \theta_{in}}{2} \sin \frac{\omega t_i + \omega T_{sw} - \theta_{in} + \omega t_i + \theta_{in}}{2} \right] =$$

Or,

$$\sum_{n=1}^N \frac{V_{c\max}}{\omega} \left[ \frac{2 \sin \frac{\omega t_i + \omega DT_{sw} - \theta_c + \omega t_i + \omega T_{sw} - \theta_{c1}}{2}}{\sin \frac{\omega t_i + \omega T_{sw} - \theta_c - \omega t_i - \omega DT_{sw} + \theta_{c1}}{2}} \right]$$

$$\sum_{n=1}^N \frac{V_{o\max}}{\omega} \left[ \frac{2 \sin \frac{\omega t_i + \omega DT_{sw} - \theta_o + \omega t_i + \omega T_{sw} - \theta_o}{2}}{\sin \frac{\omega t_i + \omega T_{sw} - \theta_o - \omega t_i - \omega DT_{sw} + \theta_o}{2}} \right]$$

$$\sum_{n=1}^N V_{in\max} \left[ \sin \left( \omega t_i - \theta_{in} + \frac{\omega T_{sw}}{2} \right) \sin \frac{\omega T_{sw}}{2} \right] =$$

Or,

$$\sum_{n=1}^N V_{c\max} \left[ \sin \left( \omega t_i - \theta_{c1} + \frac{(1+D)\omega T_{sw}}{2} \right) \sin \frac{(1-D)\omega T_{sw}}{2} \right]$$

$$+ \sum_{n=1}^N V_{o\max} \left[ \sin \left( \omega t_i - \theta_o + \frac{(1+D)\omega T_{sw}}{2} \right) \sin \frac{(1-D)\omega T_{sw}}{2} \right]$$

$$\frac{\sin \frac{\omega T_{sw}}{2}}{\sin \frac{(1-D)\omega T_{sw}}{2}} \times V_{in\max} \sum_{n=1}^N \left[ \sin \left( \omega t_i - \theta_{in} + \frac{\omega T_{sw}}{2} \right) \right] =$$

Or,

$$V_{c\max} \sum_{n=1}^N \left[ \sin \left( \omega t_i - \theta_{c1} + \frac{(1+D)\omega T_{sw}}{2} \right) \right]$$

$$+ V_{o\max} \sum_{n=1}^N \left[ \sin \left( \omega t_i - \theta_o + \frac{(1+D)\omega T_{sw}}{2} \right) \right]$$

Using identities,  $\lim_{\theta \rightarrow 0} \frac{\sin \theta}{\theta} = 1$  and i.  $\frac{\omega T_{sw}}{2} \rightarrow 0$  as  $T_{sw} \rightarrow 0$  ii.  $\frac{(1+D)\omega T_{sw}}{2} \rightarrow 0$  as  $T_{sw} \rightarrow 0$

$$\frac{\omega T_{sw}}{2}$$

Or,

$$\frac{(1-D)\omega T_{sw}}{2} \times V_{in\max} \sum_{n=1}^N [\sin(\omega t_i - \theta_{in})] =$$

$$V_{c\max} \sum_{n=1}^N [\sin(\omega t_i - \theta_{c1})] + V_{o\max} \sum_{n=1}^N [\sin(\omega t_i - \theta_o)]$$

Or,

$$\frac{1}{(1-D)} \times V_{in\max} \sum_{n=1}^N [\sin(\omega t_i - \theta_{in})] =$$

$$V_{c\max} \sum_{n=1}^N [\sin(\omega t_i - \theta_{c1})] + V_{o\max} \sum_{n=1}^N [\sin(\omega t_i - \theta_o)]$$

$$\begin{aligned} & V_{c \max} \sum_{n=1}^N [\sin(\omega t_i - \theta_{c1})] + V_{o \max} \sum_{n=1}^N [\sin(\omega t_i - \theta_o)] = \\ \text{Or,} \quad & \frac{1}{(1-D)} \times V_{in \max} \sum_{n=1}^N [\sin(\omega t_i - \theta_{in})] \end{aligned} \quad (3.4)$$

At the output stage:

When switch is ON,

$$v_{L3} = -v_{c1}$$

When switch is OFF,

$$v_{L3} = v_o$$

Volt-sec balance over one switching cycle will not be equal to zero since the input is sinusoidal. Volt-sec balance for one switching cycle is therefore

$$\int_{t_i}^{t_i+T_{sw}} v_{L2} dt = \int_{t_i}^{t_i+DT_{sw}} -v_{c1} dt + \int_{t_i+DT_{sw}}^{t_i+T_{sw}} v_{oc} dt$$

Where,

$$V_{oc} = V_o$$

The volt-sec balance over a line frequency period will be zero. For full supply cycle of N switching per period,

$$\sum_{n=1}^N \int_{t_i}^{t_i+T_{sw}} v_{L2} dt = \sum_{n=1}^N \int_{t_i}^{t_i+DT_{sw}} -v_c dt + \sum_{n=1}^N \int_{t_i+DT_{sw}}^{t_i+T_{sw}} v_{oc} dt \quad (3.5)$$

Suppose,

$$v_c = V_{c1 \max} \sin(\omega t - \theta_{c1})$$

$$v_{oc} = V_{o \max} \sin(\omega t - \theta_o)$$

From (3.5),

$$\begin{aligned} \sum_{n=1}^N \int_{t_i}^{t_i+DT_{sw}} v_c dt &= \sum_{n=1}^N \int_{t_i+DT_{sw}}^{t_i+T_{sw}} v_{oc} dt \\ \sum_{n=1}^N \int_{t_i}^{t_i+DT_{sw}} V_{c \max} \sin(\omega t - \theta_{in}) dt &= \sum_{n=1}^N \int_{t_i+DT_{sw}}^{t_i+T_{sw}} V_{o \max} \sin(\omega t - \theta_o) dt \end{aligned}$$



After Integration,

$$\sum_{n=1}^N \left[ -\frac{V_{c\max}}{\omega} \cos(\omega t - \theta_c) \right]_{t_i}^{t_i+DT_{sw}} = \sum_{n=1}^N \left[ -\frac{V_{o\max}}{\omega} \cos(\omega t - \theta_o) \right]_{t_i+DT_{sw}}^{t_i+T_{sw}}$$

$$\begin{aligned} \text{Or,} \quad & V_{c\max} \sum_{n=1}^N [\cos(\omega t_i + \omega DT_{sw} - \theta_c) - \cos(\omega t_i - \theta_c)] \\ & = V_{o\max} \sum_{n=1}^N [\cos(\omega t_i + \omega T_{sw} - \theta_o) - \cos(\omega t_i + \omega DT_{sw} - \theta_o)] \end{aligned}$$

Using identity,  $\cos A - \cos B = 2 \sin \frac{A+B}{2} \sin \frac{B-A}{2}$

$$V_{c\max} \sum_{n=1}^N \left[ 2 \sin \frac{\omega t_i + \omega DT_{sw} - \theta_c + \omega t_i - \theta_c}{2} \sin \frac{\omega t_i - \theta_c - \omega t_i - \omega DT_{sw} + \theta_c}{2} \right] =$$

$$\text{Or,} \quad V_{o\max} \sum_{n=1}^N \left[ \frac{2 \sin \frac{\omega t_i + \omega T_{sw} - \theta_o + \omega t_i + \omega DT_{sw} - \theta_o}{2}}{\sin \frac{\omega t_i + \omega DT_{sw} - \theta_o - \omega t_i - \omega T_{sw} + \theta_o}{2}} \right]$$

$$\text{Or,} \quad V_{c\max} \sum_{n=1}^N \left[ \sin \left( \omega t_i - \theta_c + \frac{\omega T_{sw}}{2} \right) \sin \frac{-\omega DT_{sw}}{2} \right] =$$

$$V_{o\max} \sum_{n=1}^N \left[ \sin \left( \omega t_i - \theta_o + \frac{(1+D)\omega T_{sw}}{2} \right) \sin \frac{(D-1)\omega T_{sw}}{2} \right]$$

$$\text{Or,} \quad \frac{\sin \frac{\omega DT_{sw}}{2}}{\sin \frac{(1-D)\omega T_{sw}}{2}} \times \sum_{n=1}^N V_{c\max} \left[ \sin \left( \omega t_i - \theta_c + \frac{\omega T_{sw}}{2} \right) \right] =$$

$$\sum_{n=1}^N V_{o\max} \left[ \sin \left( \omega t_i - \theta_o + \frac{(1+D)\omega T_{sw}}{2} \right) \right]$$

Using identities,  $\lim_{\theta \rightarrow 0} \frac{\sin \theta}{\theta} = 1$  and i.  $\frac{\omega T_{sw}}{2} \rightarrow 0$  as  $T_{sw} \rightarrow 0$  ii.  $\frac{(1+D)\omega T_{sw}}{2} \rightarrow 0$  as  $T_{sw} \rightarrow 0$

$$\text{Or,} \quad \frac{\frac{\omega DT_{sw}}{2}}{\frac{2}{(1-D)\omega T_{sw}}} \times \sum_{n=1}^N V_{c\max} [\sin(\omega t_i - \theta_c)] = \sum_{n=1}^N V_{o\max} [\sin(\omega t_i - \theta_o)]$$

$$\text{Or, } \sum_{n=1}^N V_{c\max} [\sin(\omega t_i - \theta_c)] = \frac{(1-D)}{D} \times \sum_{n=1}^N V_{o\max} [\sin(\omega t_i - \theta_o)] \quad (3.6)$$

Equating equation (3.4) and (3.6)

$$\text{Or, } \frac{(1-D)}{D} \times \sum_{n=1}^N V_{o\max} [\sin(\omega t_i - \theta_o)] + V_{o\max} \sum_{n=1}^N [\sin(\omega t_i - \theta_o)] = \frac{1}{(1-D)} \times V_{in\max} \sum_{n=1}^N [\sin(\omega t_i - \theta_{in})]$$

$$\text{Or, } \frac{(1-D+D)}{D} \times \sum_{n=1}^N V_{o\max} [\sin(\omega t_i - \theta_o)] = \frac{1}{(1-D)} \times V_{in\max} \sum_{n=1}^N [\sin(\omega t_i - \theta_{in})]$$

$$\text{Or, } \frac{1}{D} \times \sum_{n=1}^N V_{o\max} [\sin(\omega t_i - \theta_o)] = \frac{1}{(1-D)} \times V_{in\max} \sum_{n=1}^N [\sin(\omega t_i - \theta_{in})]$$

$$\text{Or, } \sum_{n=1}^N V_{o\max} [\sin(\omega t_i - \theta_o)] = \frac{D}{(1-D)} \times V_{in\max} \sum_{n=1}^N [\sin(\omega t_i - \theta_{in})]$$

Therefore the average output voltage can be derived as,

$$V_{O_{AV}} = \frac{1}{\pi} \int_0^{\pi} V_{o\max} \sin \theta d\theta$$

$$\Rightarrow V_{O_{AV}} = \frac{1}{\pi} \int_0^{\pi} \frac{D}{1-D} V_{in\max} \sin \theta d\theta$$

$$\Rightarrow V_{O_{AV}} = \frac{DV_{in\max}}{\pi(1-D)} \int_0^{\pi} \sin \theta d\theta$$

$$\Rightarrow V_{O_{AV}} = \frac{DV_{in\max}}{\pi(1-D)} [-\cos \theta]_0^{\pi}$$

$$\Rightarrow V_{O_{AV}} = \frac{2DV_{in\max}}{\pi(1-D)} \quad (3.7)$$

### 3.3 Ćuk Converter

The AC-DC Ćuk converter has an output voltage magnitude that is either greater than or less than the input voltage magnitude. Similar to the Buck–Boost converter with inverting topology, the output voltage of non-isolated Ćuk is typically also inverting, and can be lower or higher than the input. It uses a capacitor as its main energy-storage component, unlike most other types of converters which use an inductor.

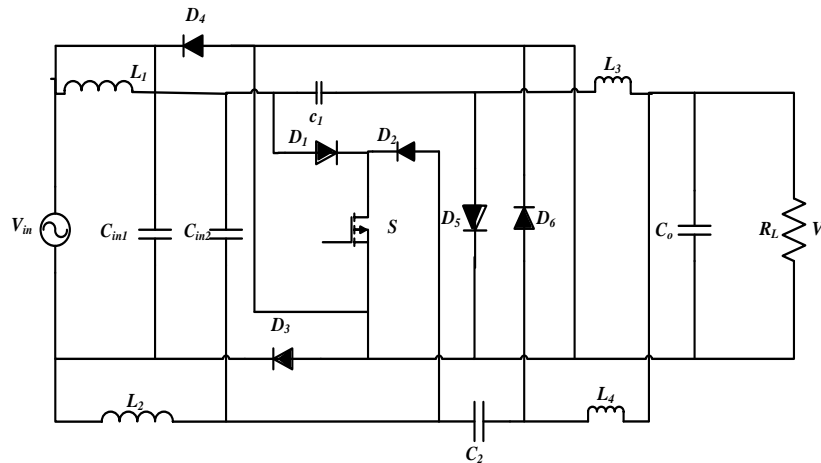


Figure 3.7 Proposed Ćuk Converter.

#### 3.3.1 Principle of Operation

The four working stages of the proposed Ćuk converter is illustrated in Figure 3.8, where Figure 3.8 (a) and (b) are for switch ON and OFF condition during positive supply cycle and Figure 3.8 (c) and (d) are for switch ON and OFF during negative cycle. The proposed converter is operating like conventional Ćuk converter. Detail operation of proposed Ćuk converter along with circuit diagram is given below.

State 1. During the positive cycle of the input signal when the switch S is turned on, current flows in two paths, as shown in Fig. 3.8(a). The first is from the input, inductor  $L_1$ , through the switch S, in the second path capacitor  $C_1$  and inductor  $L_3$  and output capacitor  $C_o$  get charged.

State 2. In the positive cycle of the input signal when the switch S is OFF, the diode  $D_6$  is forward biased. The input capacitors are disconnected, but current continues to flow through the inductors in two paths, as shown in Fig. 3.8(b).

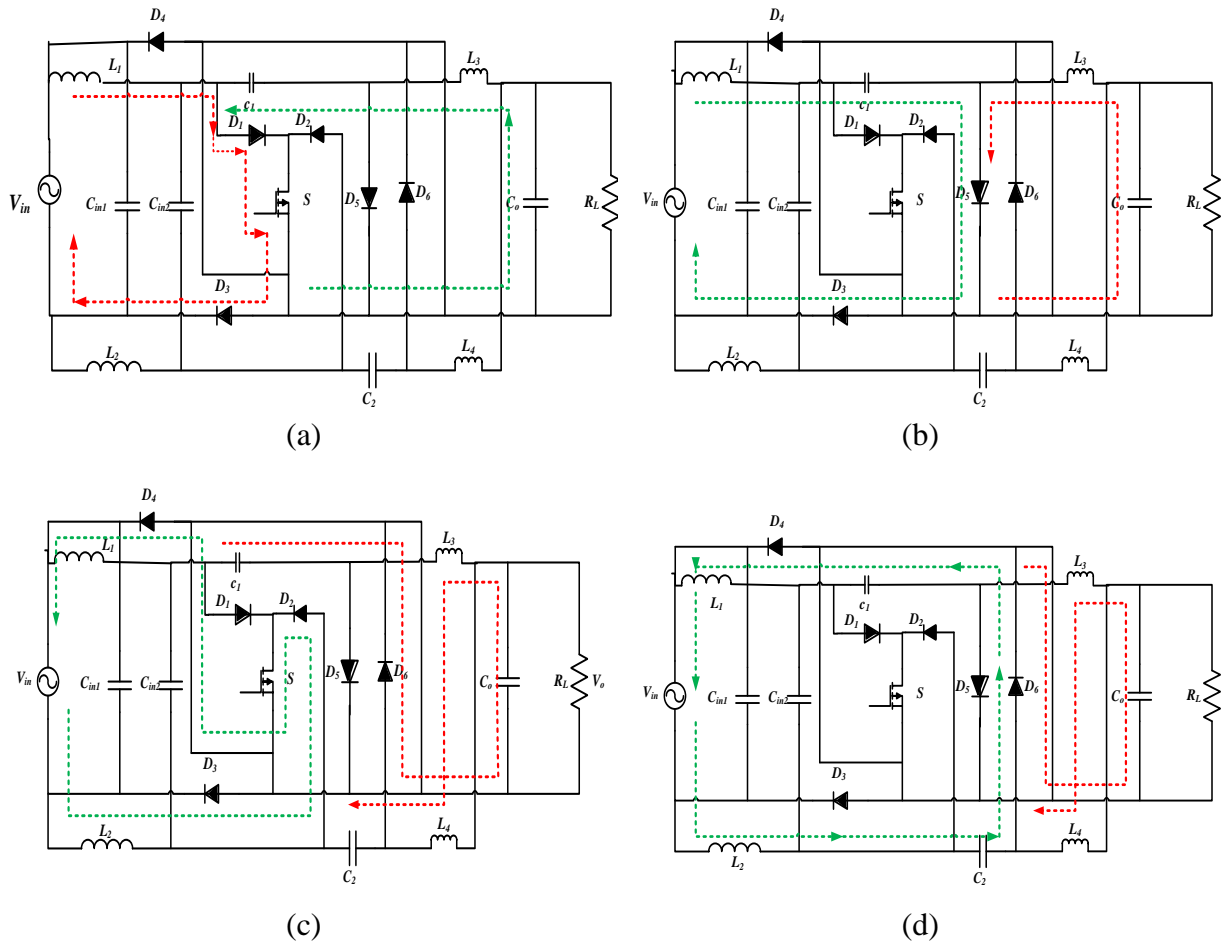


Figure 3.8 : Four Modes of Operation of Proposed AC-DC Ćuk Converter, (a) Mode 1: Proposed Circuit in Positive Half Cycle When S is ON. (b) Mode 2: Proposed Circuit in Positive Half Cycle When S is OFF. (c) Mode 3: Proposed Circuit in Negative Half Cycle When S is ON. (d) Mode 4: Proposed Circuit in Negative Half Cycle When S is OFF.

State 3. Similar to State 1, during the negative cycle of the input signal when the switch S is turned ON, the diode  $D_5$  and  $D_6$  is reverse biased. Current flows in two paths, as shown in Fig. 3.8(c).

State 4. In the negative cycle of the input signal when the switch S is turned OFF and the diode  $D_5$  and  $D_6$  is forward biased and current continue to flow in two paths shown in Fig. 3.8(d).

During both positive and negative cycle of the supply, the energy transferred to the load is unidirectional, thus AC-DC conversion is achieved.

### 3.3.2 Open Loop Data Analysis

Table 3.6 Parameter Table of Proposed Ćuk Converter

Parameters	Value
Input voltage ( $V_i$ )	220V
Switching Frequency ( $F_s$ )	8kHz
Inductor ( $L_1, L_2$ )	2.5mH
Capacitor ( $C_1$ )	1 $\mu$ F
Inductor ( $L_3, L_4$ )	1.5m
Capacitor ( $C_2$ )	1 $\mu$ F
Capacitor ( $C_{in1}$ )	4.5 $\mu$ F
Capacitor ( $C_{in2}$ )	4.5 $\mu$ F
Output Capacitor ( $C_o$ )	220 $\mu$ F
Load Resistor ( $R_L$ )	100 $\Omega$

Table 3.7 Performance Analysis of Proposed AC-DC Ćuk Converter

Duty Cycle	Proposed Circuit				Conventional Circuit			
	Efficiency (%)	THD	Power Factor	Voltage Gain	Efficiency (%)	THD	Power Factor	Voltage Gain
0.1	93	0.44	0.55	0.43	94	2.30	0.39	0.23
0.2	99	0.38	0.87	0.88	94	1.58	0.52	0.44
0.3	98	0.34	0.96	1.40	95	1.25	0.62	0.64
0.4	99	0.26	0.98	2.07	95	1.00	0.70	0.85
0.5	98	0.19	0.99	2.81	96	0.80	0.80	1.00
0.6	99	0.15	0.98	3.51	96	0.65	0.83	1.31
0.7	97	0.24	0.97	4.37	96	0.47	0.89	1.90
0.8	98	0.27	0.93	5.41	95	0.33	0.93	3.23
0.9	91	0.33	0.81	7.41	95	0.37	0.92	7.32

### 3.3.3 Voltage Gain Expression

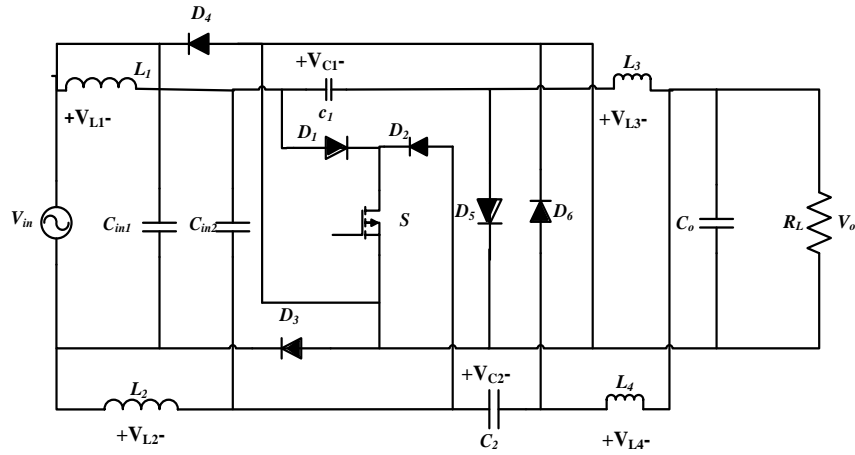


Figure 3.9 : Proposed Converters with Voltage across the Components  $L_1, L_2, L_3, L_4, C_1, C_2$  and  $C_o$

At the input stage:

When switch is ON,

$$v_{L1} = v_{in}$$

When switch is OFF,

$$v_{L1} = v_{in} - v_{c1}$$

Volt-sec balance over one switching cycle will not be equal to zero since the input is sinusoidal. Volt-sec balance for one switching cycle is therefore

$$\int_{t_i}^{t_i+T_{sw}} v_{L1} dt = \int_{t_i}^{t_i+DT_{sw}} v_{in} dt + \int_{t_i+DT_{sw}}^{t_i+T_{sw}} (v_{in} - v_{c1}) dt$$

The volt-sec balance over a line frequency period will be zero. For full supply cycle of  $N$  switching per period,

$$\sum_{n=1}^N \int_{t_i}^{t_i+T_{sw}} v_{L1} dt = \sum_{n=1}^N \int_{t_i}^{t_i+DT_{sw}} v_{in} dt + \sum_{n=1}^N \int_{t_i+DT_{sw}}^{t_i+T_{sw}} (v_{in} - v_{c1}) dt \quad (3.8)$$

Suppose,

$$v_{in} = V_{in\max} \sin(\omega t - \theta_{in})$$

$$v_{c1} = V_{c1\max} \sin(\omega t - \theta_{c1})$$

From Equation (3.8),

$$\begin{aligned} &\Rightarrow \sum_{n=1}^N \int_{t_i}^{t_i+DT_{sw}} v_{in} dt = - \sum_{n=1}^N \int_{t_i+DT_{sw}}^{t_i+T_{sw}} (v_{in} - v_{c1}) dt \\ &\Rightarrow \sum_{n=1}^N \int_{t_i}^{t_i+DT_{sw}} V_{in\max} \sin(\omega t - \theta_{in}) dt = - \sum_{n=1}^N \int_{t_i+DT_{sw}}^{t_i+T_{sw}} [V_{in\max} \sin(\omega t - \theta_{in}) - V_{c1\max} \sin(\omega t - \theta_{c1})] dt \end{aligned}$$

After Integration,

$$\begin{aligned} &\Rightarrow \sum_{n=1}^N \left[ -\frac{V_{in\max}}{\omega} \cos(\omega t - \theta_{in}) \right]_{t_i}^{t_i+DT_{sw}} = + \sum_{n=1}^N \left[ -\frac{V_{in\max}}{\omega} \cos(\omega t - \theta_{in}) \right]_{t_i+DT_{sw}}^{t_i+T_{sw}} - \sum_{n=1}^N \left[ -\frac{V_{c1\max}}{\omega} \cos(\omega t - \theta_{c1}) \right]_{t_i+DT_{sw}}^{t_i+T_{sw}} \\ &\Rightarrow - \sum_{n=1}^N \left[ \frac{V_{in\max}}{\omega} \cos(\omega t_i + \omega DT_{sw} - \theta_{in}) \right] + \sum_{n=1}^N \left[ -\frac{V_{in\max}}{\omega} \cos(\omega t_i - \theta_{in}) \right] \\ &\quad = \sum_{n=1}^N \left[ \frac{V_{in\max}}{\omega} \cos(\omega t_i + \omega T_{sw} - \theta_{in}) \right] - \sum_{n=1}^N \left[ -\frac{V_{in\max}}{\omega} \cos(\omega t_i + \omega DT_{sw} - \theta_{in}) \right] \\ &\quad - \sum_{n=1}^N \left[ \frac{V_{c1\max}}{\omega} \cos(\omega t_i + \omega T_{sw} - \theta_{c1}) \right] + \sum_{n=1}^N \left[ \frac{V_{c1\max}}{\omega} \cos(\omega t_i + \omega DT_{sw} - \theta_{c1}) \right] \\ &\Rightarrow \sum_{n=1}^N \left[ \frac{V_{in\max}}{\omega} \cos(\omega t_i - \theta_{in}) \right] - \sum_{n=1}^N \left[ \frac{V_{in\max}}{\omega} \cos(\omega t_i + \omega T_{sw} - \theta_{in}) \right] = \sum_{n=1}^N \left[ \frac{V_{c1\max}}{\omega} \cos(\omega t_i + \omega DT_{sw} - \theta_{c1}) \right] \\ &\quad + \sum_{n=1}^N \left[ \frac{V_{c1\max}}{\omega} \cos(\omega t_i + \omega T_{sw} - \theta_{c1}) \right] \\ &\Rightarrow \sum_{n=1}^N \frac{V_{in\max}}{\omega} [\cos(\omega t_i - \theta_{in}) - \cos(\omega t_i + \omega T_{sw} - \theta_{in})] = \sum_{n=1}^N \frac{V_{c1\max}}{\omega} [\cos(\omega t_i + \omega DT_{sw} - \theta_{c1}) - \cos(\omega t_i + \omega T_{sw} - \theta_{c1})] \end{aligned}$$

Using identity,  $\cos A - \cos B = 2 \sin \frac{A+B}{2} \sin \frac{B-A}{2}$

$$\begin{aligned} &\Rightarrow \sum_{n=1}^N \frac{V_{in\max}}{\omega} \left[ 2 \sin \frac{\omega t_i - \theta_{in} + \omega t_i + \omega T_{sw} - \theta_{in}}{2} \sin \frac{\omega t_i + \omega T_{sw} - \theta_{in} + \omega t_i + \theta_{in}}{2} \right] = \\ &\quad \sum_{n=1}^N \frac{V_{c1\max}}{\omega} \left[ 2 \sin \frac{\omega t_i + \omega DT_{sw} - \theta_{c1} + \omega t_i + \omega T_{sw} - \theta_{c1}}{2} \sin \frac{\omega t_i + \omega T_{sw} - \theta_{c1} - \omega t_i - \omega DT_{sw} + \theta_{c1}}{2} \right] \\ &\Rightarrow \sum_{n=1}^N V_{in\max} \left[ \sin \left( \omega t_i - \theta_{in} + \frac{\omega T_{sw}}{2} \right) \sin \frac{\omega T_{sw}}{2} \right] = \sum_{n=1}^N V_{c1\max} \left[ \sin \left( \omega t_i - \theta_{c1} + \frac{(1+D)\omega T_{sw}}{2} \right) \sin \frac{(1-D)\omega T_{sw}}{2} \right] \\ &\Rightarrow \frac{\sin \frac{\omega T_{sw}}{2}}{\sin \frac{(1-D)\omega T_{sw}}{2}} \times V_{in\max} \sum_{n=1}^N \left[ \sin \left( \omega t_i - \theta_{in} + \frac{\omega T_{sw}}{2} \right) \right] = V_{c1\max} \sum_{n=1}^N \left[ \sin \left( \omega t_i - \theta_{c1} + \frac{(1+D)\omega T_{sw}}{2} \right) \right] \end{aligned}$$

Using identities,  $\lim_{\theta \rightarrow 0} \frac{\sin \theta}{\theta} = 1$  and i.  $\frac{\omega T_{sw}}{2} \rightarrow 0$  as  $T_{sw} \rightarrow 0$  ii.  $\frac{(1+D)\omega T_{sw}}{2} \rightarrow 0$  as  $T_{sw} \rightarrow 0$ ,

$$\Rightarrow \frac{1}{(1-D)} \times V_{inmax} \sum_{n=1}^N [\sin(\omega t_i - \theta_{in})] = V_{c1max} \sum_{n=1}^N [\sin(\omega t_i - \theta_{c1})]$$

$$\Rightarrow V_{c1max} \sum_{n=1}^N [\sin(\omega t_i - \theta_{c1})] = \frac{1}{(1-D)} \times V_{inmax} \sum_{n=1}^N [\sin(\omega t_i - \theta_{in})] \quad (3.9)$$

At the output stage:

When switch is ON,

$$v_{L3} = v_{c1} + v_{oc}$$

When switch is OFF,

$$v_{L3} = v_{oc}$$

Volt-sec balance over one switching cycle will not be equal to zero since the input is sinusoidal. Volt-sec balance for one switching cycle is therefore

$$\int_{t_i}^{t_i+T_{sw}} v_{L3} dt = \int_{t_i}^{t_i+DT_{sw}} (v_{oc} + v_{c1}) dt + \int_{t_i+DT_{sw}}^{t_i+T_{sw}} v_{oc} dt$$

The volt-sec balance over a line frequency period will be zero. For full supply cycle of N switching per period,

$$\begin{aligned} \sum_{n=1}^N \int_{t_i}^{t_i+T_{sw}} v_{L3} dt &= \sum_{n=1}^N \int_{t_i}^{t_i+DT_{sw}} (v_{c1} + v_{oc}) dt + \sum_{n=1}^N \int_{t_i+DT_{sw}}^{t_i+T_{sw}} v_{oc} dt \\ \sum_{n=1}^N \int_{t_i}^{t_i+DT_{sw}} (v_{c1} + v_{oc}) dt &= - \sum_{n=1}^N \int_{t_i+DT_{sw}}^{t_i+T_{sw}} v_{oc} dt \end{aligned} \quad (3.10)$$

Suppose,

$$v_{c1} = V_{c1max} \sin(\omega t - \theta_{c1})$$

$$v_{oc} = V_{o\max} \sin(\omega t - \theta_o)$$

From Equation (3.9),

$$\sum_{n=1}^N \int_{t_i}^{t_i+DT_{sw}} [V_{c1max} \sin(\omega t - \theta_{c1}) + V_{o\max} \sin(\omega t - \theta_o)] dt = - \sum_{n=1}^N \int_{t_i+DT_{sw}}^{t_i+T_{sw}} V_{o\max} \sin(\omega t - \theta_o) dt$$

After Integration,





$$\begin{aligned}
&\Rightarrow \frac{1}{D} \times \sum_{n=1}^N V_{o\max} \sin(\omega t_i - \theta_o) = - \sum_{n=1}^N V_{c_1\max} \sin(\omega t_i - \theta_{c_1}) \\
&\Rightarrow \sum_{n=1}^N V_{c_1\max} \sin(\omega t_i - \theta_{c_1}) = - \frac{1}{D} \sum_{n=1}^N V_{o\max} \sin(\omega t_i - \theta_o)
\end{aligned} \tag{3.11}$$

Equating equation (3.9) and (3.11),

$$\begin{aligned}
&\Rightarrow - \frac{1}{D} \sum_{n=1}^N V_{o\max} \sin(\omega t_i - \theta_o) = \frac{1}{(1-D)} \times V_{in\max} \sum_{n=1}^N [\sin(\omega t_i - \theta_{in})] \\
&\Rightarrow \sum_{n=1}^N V_{o\max} \sin(\omega t_i - \theta_o) = - \frac{D}{(1-D)} \times V_{in\max} \sum_{n=1}^N [\sin(\omega t_i - \theta_{in})]
\end{aligned}$$

Therefore the average output voltage can be derived as,

$$\begin{aligned}
V_{O_{AV}} &= \frac{1}{\pi} \int_0^\pi V_{o\max} \sin \theta d\theta \\
\Rightarrow V_{O_{AV}} &= - \frac{1}{\pi} \int_0^\pi \frac{D}{(1-D)} V_{in\max} \sin \theta d\theta \\
\Rightarrow V_{O_{AV}} &= - \frac{D V_{in\max}}{\pi(1-D)} \int_0^\pi \sin \theta d\theta \\
\Rightarrow V_{O_{AV}} &= - \frac{D V_{in\max}}{\pi(1-D)} [-\cos \theta]_0^\pi \\
\Rightarrow V_{O_{AV}} &= - \frac{2D V_{in\max}}{\pi(1-D)}
\end{aligned} \tag{3.12}$$

# Chapter 4 Performance Analysis of Proposed Converters

## 4.1 Performance Analysis of Proposed Boost Converter

### 4.1.1 Analysis of Proposed Boost Converter under Duty Cycle Variation

The performance analysis of the proposed circuits from Table 3.2 in terms of efficiency (%) is presented by the bar diagram as illustrated in Fig. 4.1(a).

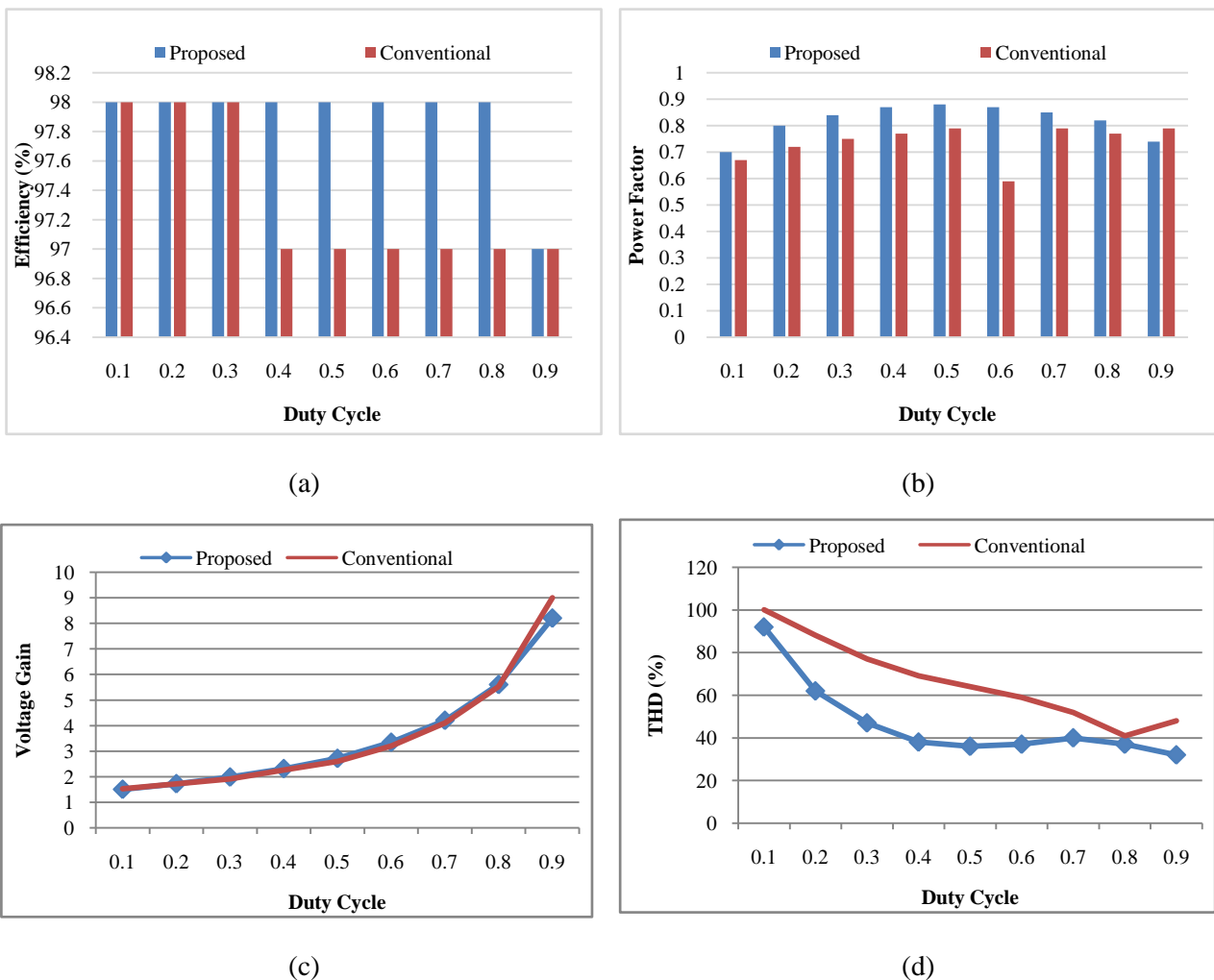


Figure 4.1 Graphical Representation Of Efficiency (a), Power Factor (b), Voltage Gain (c) and Input Current THD (d) for the Proposed AC-DC Boost Converter With Conventional Boost Converter Under Duty Cycle Variation.

The proposed circuit shows good performance offering more than 96% efficiency throughout the range of duty cycle. From the line chart in Fig. 4.1(d) percentage Total Harmonic Distortion (THD) of input current demonstrates better performance in case of the proposed scheme over the conventional one. All through the operation of the proposed circuit the THD (%) has found to be less than 30%. The proposed converter represents higher voltage gain than the conventional circuit under the variation of duty cycle as illustrated in the line chart presented in Fig. 4.1(c). Input power factor comparison as shown in the overlaying bar diagram in Fig.4.1 (b) indicates that the proposed scheme is competitive providing near unity power factor during duty cycle variations except 90% of the duty cycle where performance of both schemes are not good due the enhancement mode operation of the MOSFET switch.

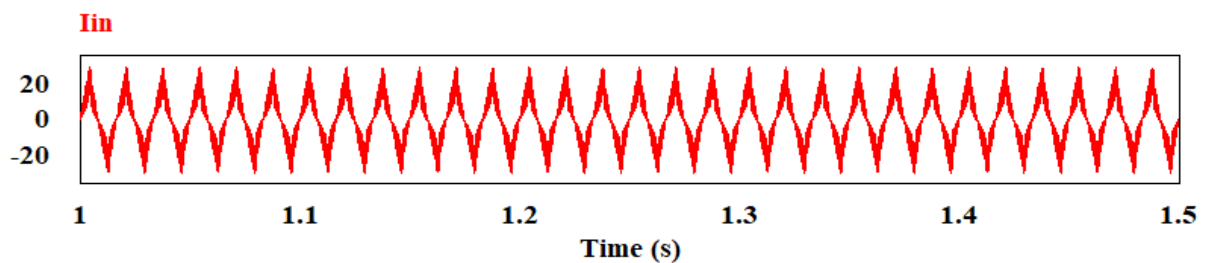


Figure 4.2 Input Current Waveform of Proposed Boost Converter.

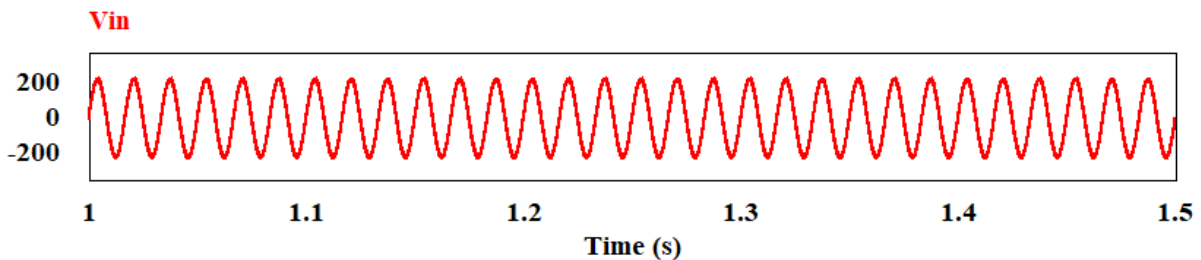


Figure 4.3 Input Voltage Waveform of Proposed Boost Converter.

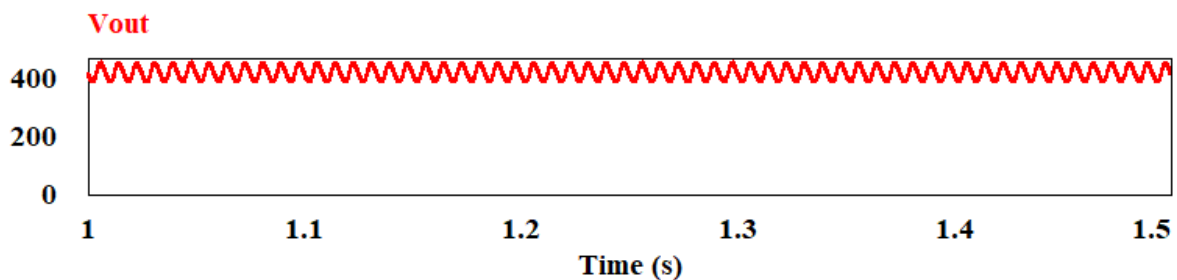


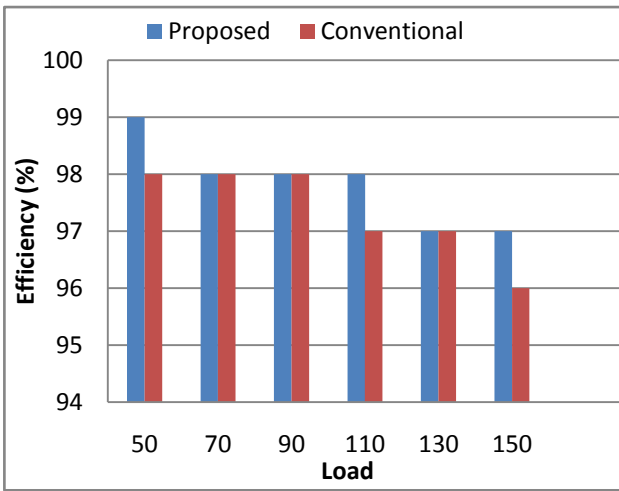
Figure 4.4 Output Voltage Waveform of Proposed Boost Converter.

#### 4.1.2 Performance Analysis of Proposed Boost Converter under Load Variation

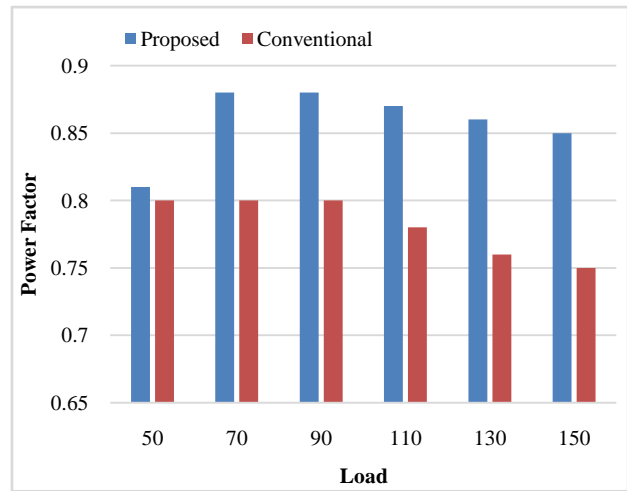
In Table 4.1 the circuit performance under load variation is justified for both conventional and proposed converter for the switching frequency 5 KHz and 50% of duty cycle. Fig.4.1 graphically shows the performance of conventional to proposed Boost converter with respect to efficiency, input current THD and power factor for duty cycle variation. Fig.4.5 shows the performance for load variation of the proposed circuit and the conventional one. It is evident from the table that the circuit performance of the proposed converter shows better performance than the conventional converter under load variation with respect to the measured parameters.

Table 4.1 Performance Comparison under Load Variation of Proposed Boost Converter

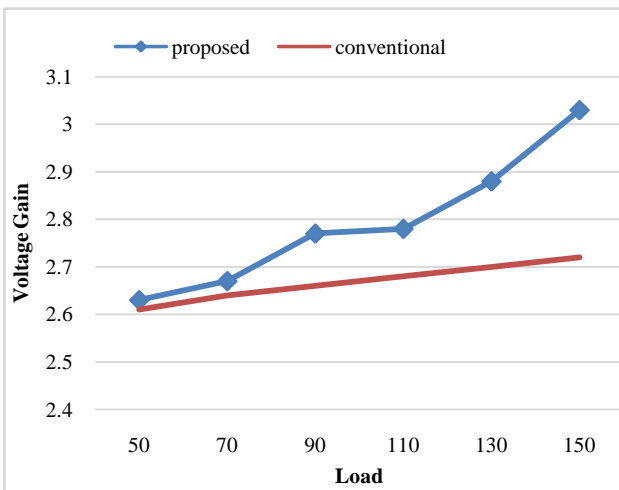
Load	Proposed Circuit				Conventional Circuit			
	Efficiency (%)	THD (%)	Power Factor	Voltage Gain	Efficiency (%)	THD (%)	Power Factor	Voltage Gain
50	99	49	0.81	2.63	98	62	0.80	2.61
70	98	44	0.88	2.67	98	64	0.80	2.64
90	98	38	0.88	2.77	98	64	0.80	2.66
110	98	34	0.87	2.78	97	64	0.78	2.68
130	97	35	0.86	2.88	97	63	0.76	2.70
150	97	36	0.85	3.03	96	63	0.75	2.72



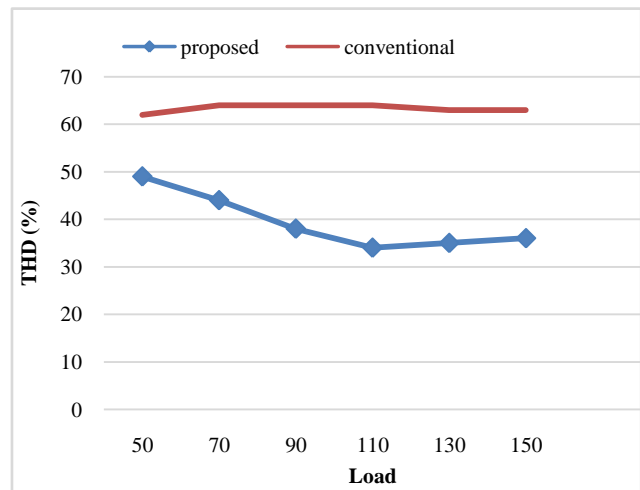
(a)



(b)



(c)



(d)

Figure 4.5 Graphical Representation of Efficiency (a), Power Factor (b), Voltage Gain(c) and Input Current THD (d) Proposed AC-DC Boost Converter with Conventional Boost Converter under Load Cycle Variation

## 4.2 Performance Analysis of Proposed SEPIC Converter

### 4.2.1 Graphical Analysis of Proposed SEPIC Converter under Duty Cycle Variation

The performance analysis of the circuit from Table 3.4 in terms of efficiency (%) is presented by the bar diagram as illustrated in Fig. 4.6(a). The proposed circuit shows good performance offering more than 90% efficiency throughout the range of duty cycle. The line chart in Fig. 4.6(d) shows percent Total harmonic distortion (THD) of input current demonstrates better

performance in case of the proposed scheme over the conventional one. Throughout the complete operation of the proposed circuit the

THD (%) was found to be less than 20%. The proposed Boost converter presents higher voltage gain than the conventional circuit all over the duty cycle as illustrated in the line chart presented in Fig. 4.6(c). Input power factor comparison as shown in the overlaying bar diagram in Fig. 4.6(b).

Indicates that the proposed scheme is competitive providing near unity power factor during duty cycle variations except at  $D = 0.9$  where performance of both schemes is not good.

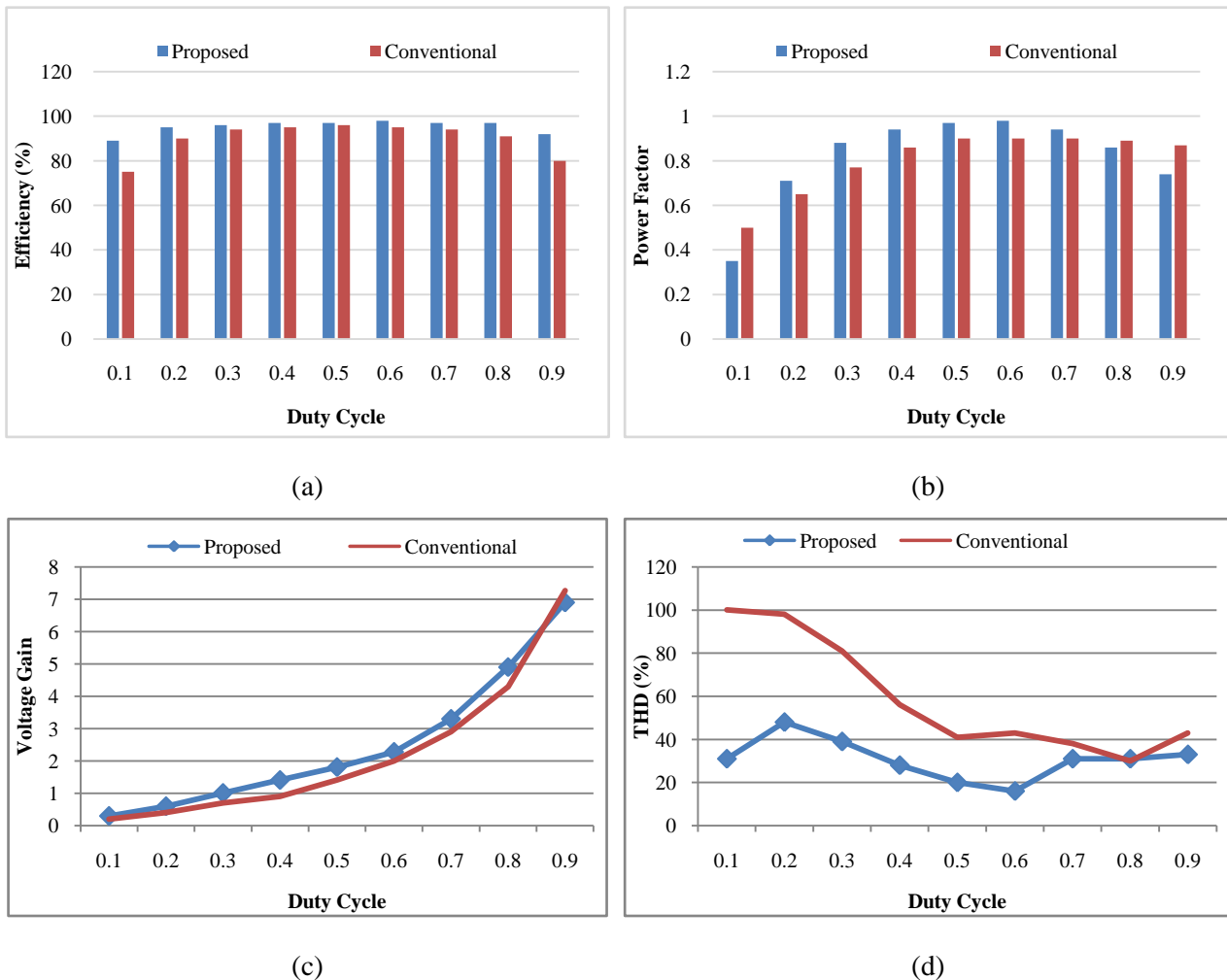


Figure 4.6 Graphical Representation Of Efficiency (a), Power Factor (b), Voltage Gain (c) and Input Current THD (d) for the Proposed AC-DC SEPIC Converter With Conventional SEPIC Converter Under Duty Cycle Variation.

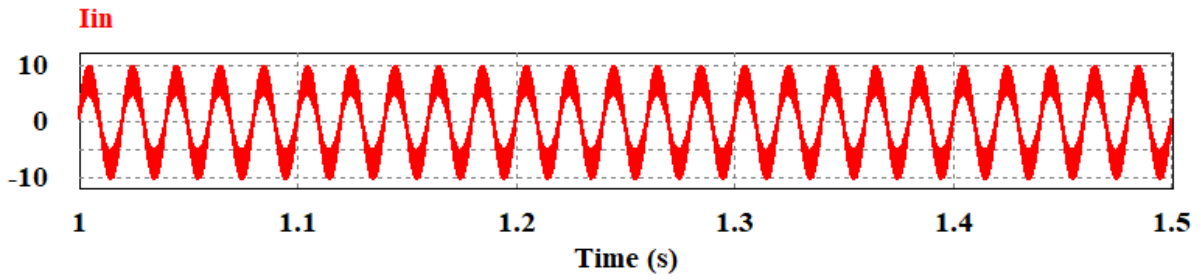


Figure 4.7 Input Current Waveform of Proposed SEPIC Converter.

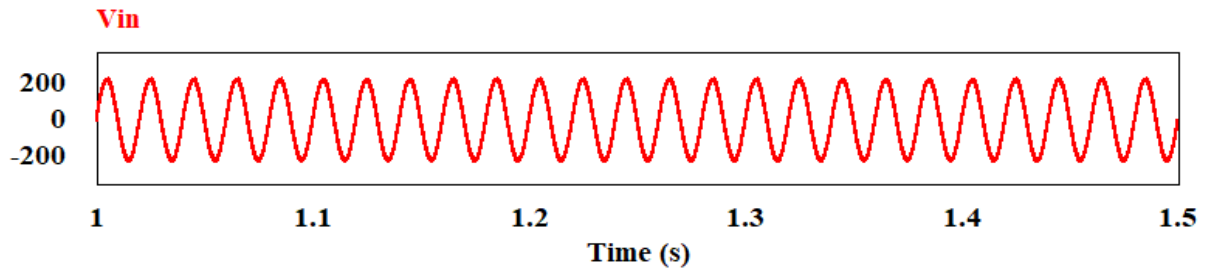


Figure 4.8 Input Voltage Waveform of Proposed SEPIC Converter.

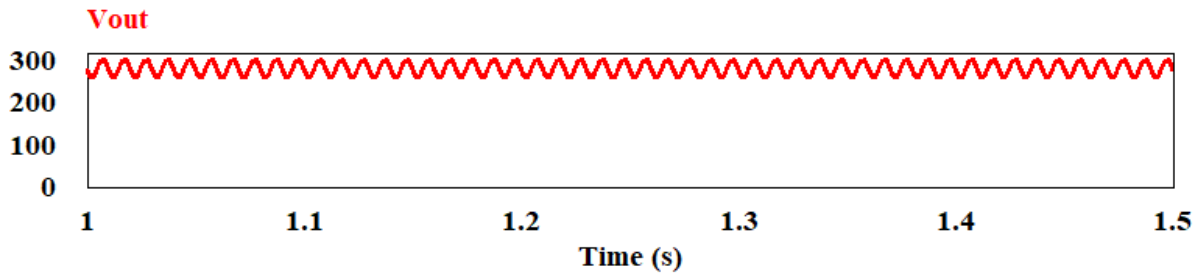


Figure 4.9 Output Voltage Waveform of Proposed SEPIC Converter.

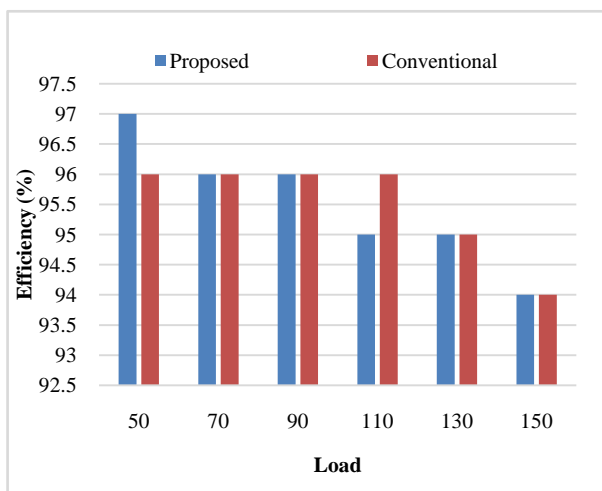
#### 4.2.2 Performance Analysis of Proposed SEPIC Converter under Load Variation

Table 4.2 Performance Comparison under Load Variation of Proposed SEPIC Converter

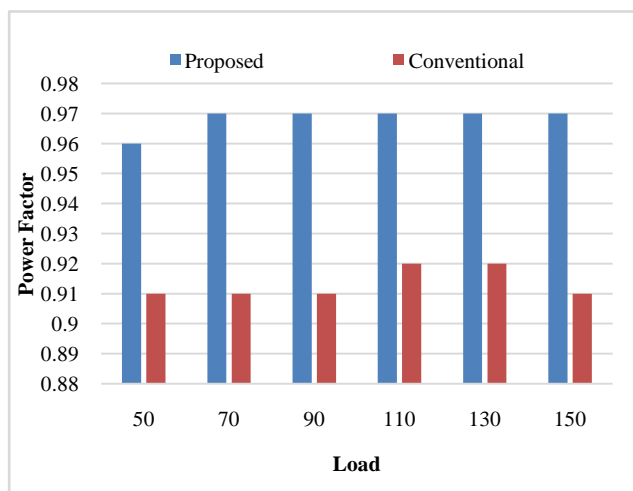
Load	Proposed Circuit				Conventional Circuit			
	Efficiency (%)	THD (%)	Power Factor	Voltage Gain	Efficiency (%)	THD (%)	Power Factor	Voltage Gain
50	97	27	0.96	1.43	96	41	0.91	1.25
70	96	20	0.97	1.53	96	47	0.91	1.37
90	96	20	0.97	1.72	96	43	0.91	1.40
110	95	21	0.97	1.90	96	40	0.92	1.42
130	95	21	0.97	2.05	95	41	0.92	1.42
150	94	21	0.97	2.20	94	42	0.91	1.54



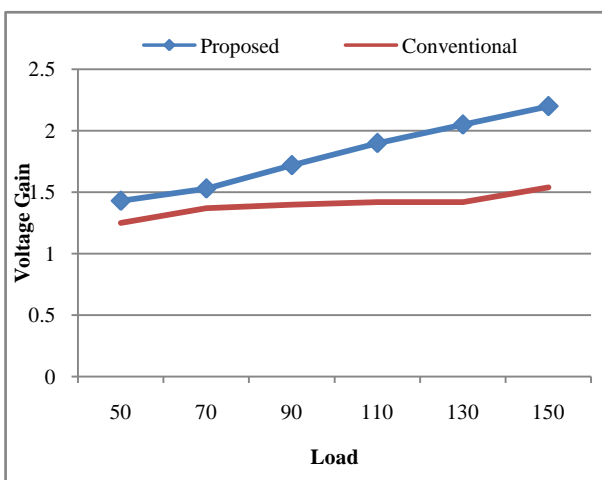
In Table 4.2 the circuit performance under load variation is justified for both conventional and proposed converter for the switching frequency 5 KHz and duty cycle of 0.5.



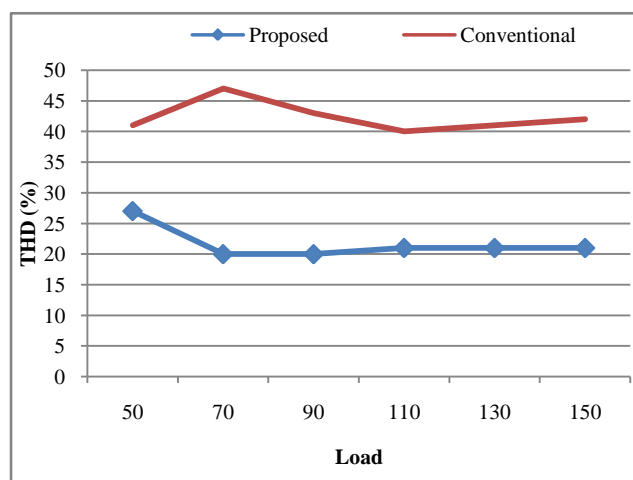
(a)



(b)



(c)



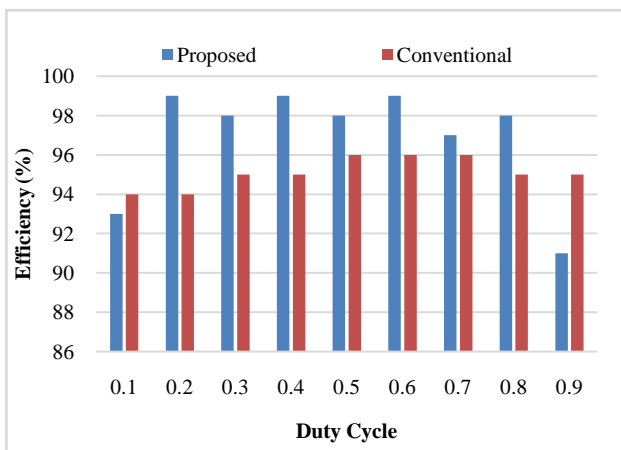
(d)

Figure 4.10 Graphical Representation of Efficiency (a), Power Factor (b), Voltage Gain (c) and Input Current THD (d) for the Proposed AC-DCSEPIC Converter with Conventional SEPIC Converter under Load Cycle Variation.

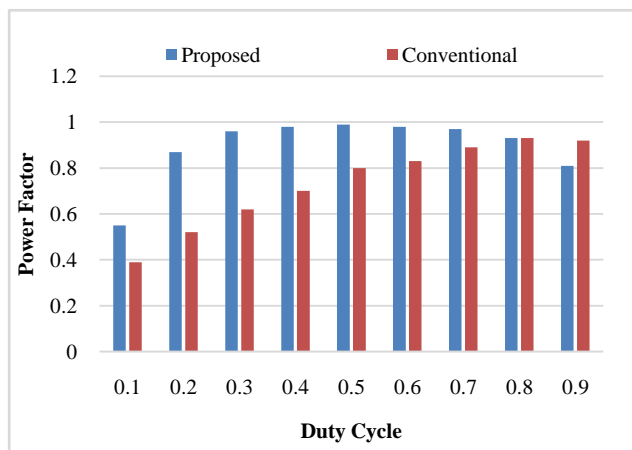
### 4.3 Performance Analysis of Proposed Ćuk Converter

#### 4.3.1 Graphical Analysis of Proposed Ćuk Converter under Duty Cycle Variation

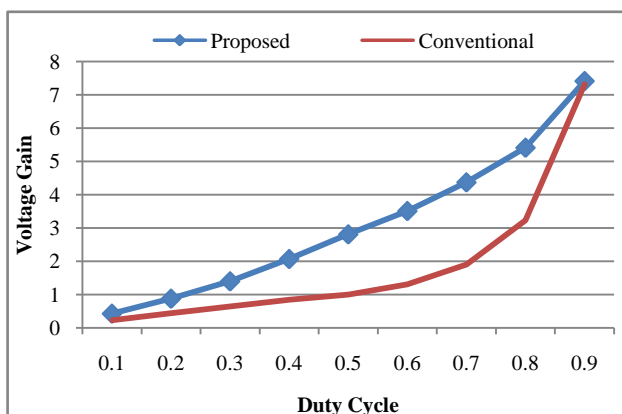
The performance of the circuits in terms of efficiency (%) is presented by the bar diagram as illustrated in Fig. 4.11(b). The proposed circuit shows better performance offering more than 95% efficiency throughout the range of duty cycle. From the line chart in Fig. 4.11(d) showing percent Total harmonic distortion (THD) of input current demonstrates better performance in case of the proposed scheme over the conventional one.



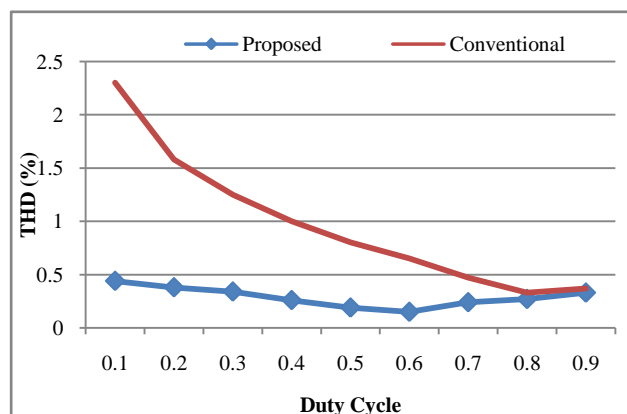
(a)



(b)



(c)



(d)

Figure 4.11 Graphical Representation Of Efficiency (a), Power Factor (b), Voltage Gain (c) and Input Current THD (d) for the Proposed AC-DC Ćuk Converter With Conventional Ćuk Converter Under Duty Cycle Variation.

All through the operation of the proposed circuit the THD (%) was found to be less than 10%. The proposed converter presents higher voltage gain than the conventional circuit all over the duty cycle as illustrated in the line chart presented in Fig. 4.11(c). Input power factor comparison as shown in the overlaying bar diagram in Fig. 4.11(a) indicates that the proposed scheme is competitive providing near unity power factor during duty cycle variations except at  $D = 0.9$  where performance of proposed schemes is not good.

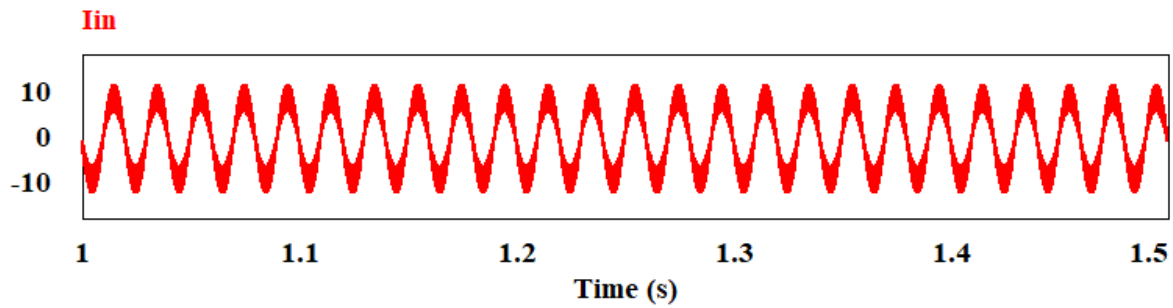


Figure 4.12 Input Current Waveform of Proposed Ćuk Converter.

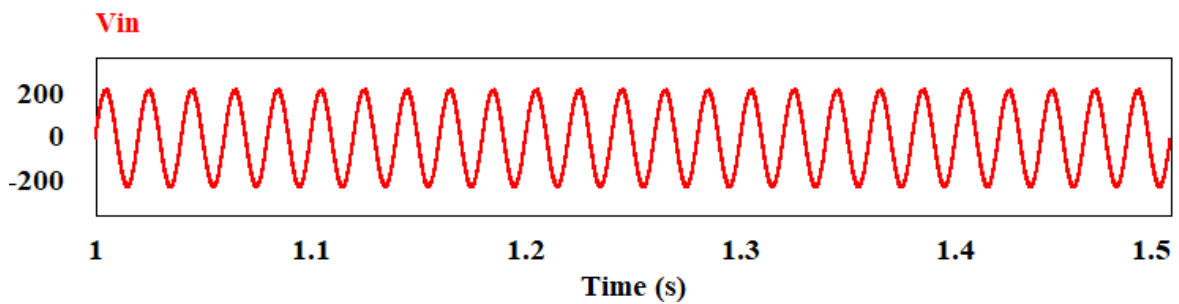


Figure 4.13 Input Voltage Waveform of Proposed Ćuk Converter.

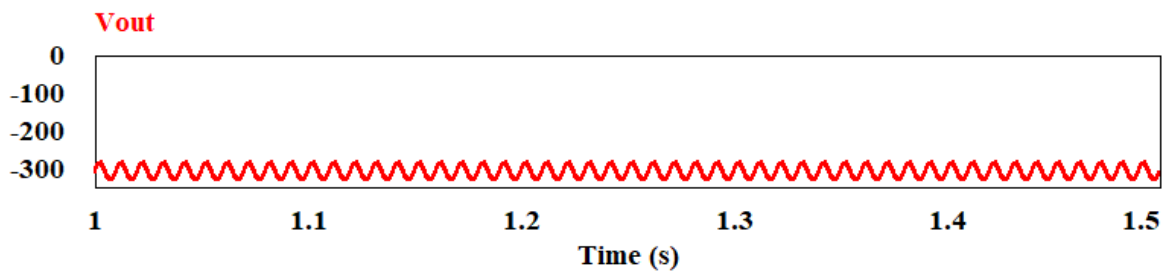


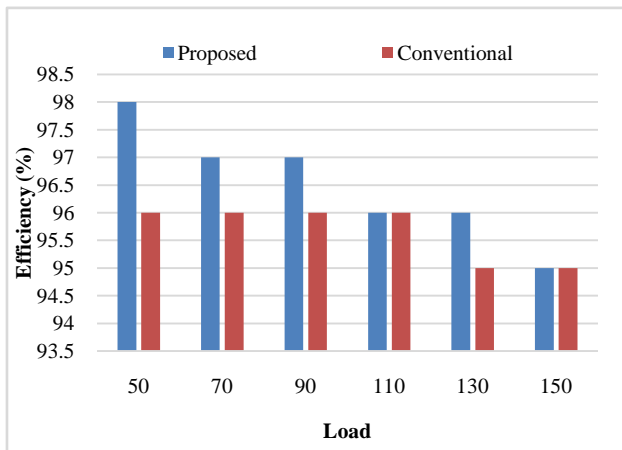
Figure 4.14 Output Voltage Waveform of Proposed Ćuk Converter.

### 4.3.2 Performance Analysis of Proposed Ćuk Converter under Load Variation

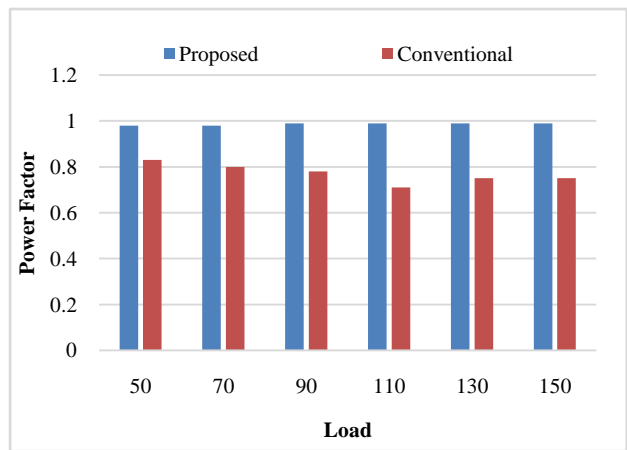
In Table 4.3 the circuit performance under load variation is justified for both conventional and proposed converter for the switching frequency 8 KHz and duty cycle of 0.5. Fig.4.11 graphically shows the performance of conventional to proposed Boost converter with respect to efficiency, input current THD and power factor for duty cycle variation.

Table 4.3 Performance Comparison under Load Variation of Proposed Ćuk Converter

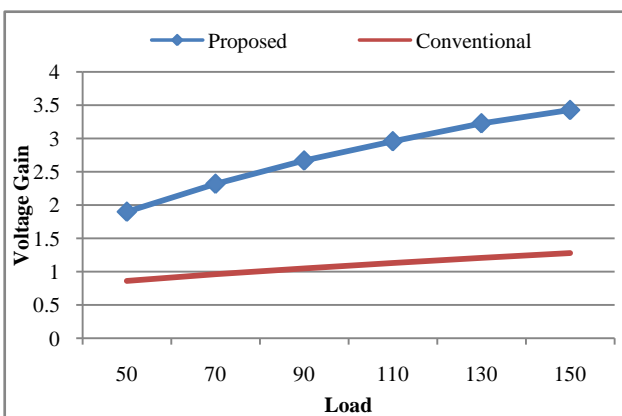
Load	Proposed Circuit				Conventional Circuit			
	Efficiency (%)	THD (%)	Power Factor	Voltage Gain	Efficiency (%)	THD (%)	Power Factor	Voltage Gain
50	98	21	0.98	1.90	96	65	0.83	0.86
70	97	20	0.98	2.32	96	73	0.80	0.96
90	97	18	0.98	2.67	96	78	0.78	1.05
110	96	18	0.98	2.96	96	82	0.71	1.13
130	96	19	0.98	3.23	95	85	0.75	1.21
150	95	20	0.98	3.43	95	87	0.75	1.28



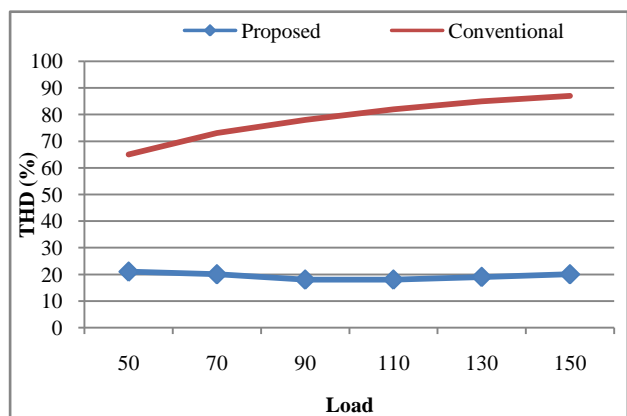
(a)



(b)



(c)



(d)

Figure 4.15 Graphical Representation of Efficiency (a), Power Factor (b), Voltage Gain (c) and Input Current THD (d) for the Proposed AC-DC Ćuk Converter with Conventional Ćuk Converter under Load Variation.

Fig.4.15 shows the performance for load variation of the proposed circuit and the conventional circuit. It is evident from the table that the circuit performance in case of the proposed converter shows better performance than the conventional converter under load variation with respect to the same measured parameters.



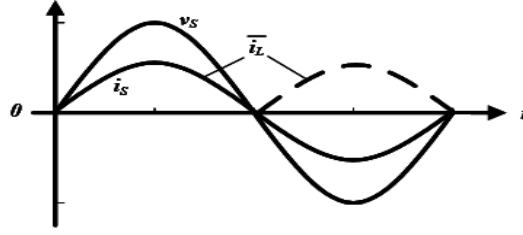


Figure 5.2 Waveform of PFC Circuit where Supply Voltage and Supply Current are in The Same Phase [4].

The DC transformer model of the circuit of Figure 5.1 is shown in Figure 5.3, where  $|v_s|$  is the absolute value of the supply voltage. In the Boost converter, it is essential that the output voltage  $V_o$  of the proposed converter be greater than the peak of the supply voltage  $\hat{V}_s$ .

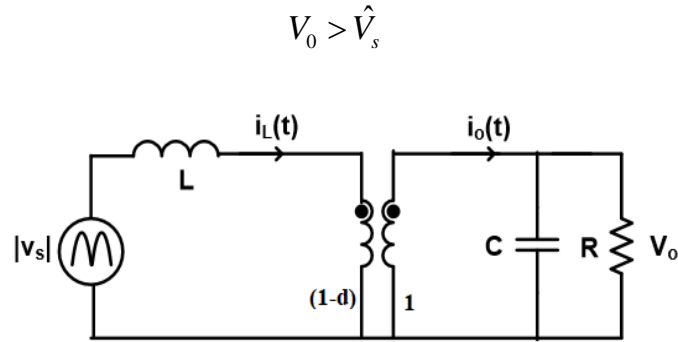


Figure 5.3 DC Transformer Model of Proposed AC-DC Boost Converter.

Figure 5.3 shows the average model of the Boost converter in the continuous conduction mode (CCM) with  $i_{L1} > 0$  at all times. Neglecting a small voltage drop across the inductor and assuming the voltage across the capacitor to be a pure DC, in a Boost converter, the voltage gain of the converter is given below.

$$\begin{aligned} \frac{V_o}{V_s} &= \frac{1}{1-d(t)} \\ \text{or, } 1-d(t) &= \frac{\hat{V}_s |\sin \omega t|}{V_o} \\ \text{or, } d(t) &= 1 - \frac{\hat{V}_s |\sin \omega t|}{V_o} \end{aligned} \quad (5.1)$$

According to Equation (5.1), a variable duty cycle is needed for keeping the input current in-phase with the supply voltage.

## 5.2 Control of PFC

The PFC power circuit for the proposed Boost converter along with its control circuit has been shown in Fig. 5.4 in block diagram form. The main objective of PFC circuit is to draw a sinusoidal current, in-phase with the utility voltage. The reference inductor current  $i_L^*$  is of the full-wave rectified form, similar to that in Fig. 5.2. The requirements on the form and the amplitude of the inductor current lead to two control loops, as shown in Fig. 5.4, to pulse-width modulate the switch of the proposed boost converter.

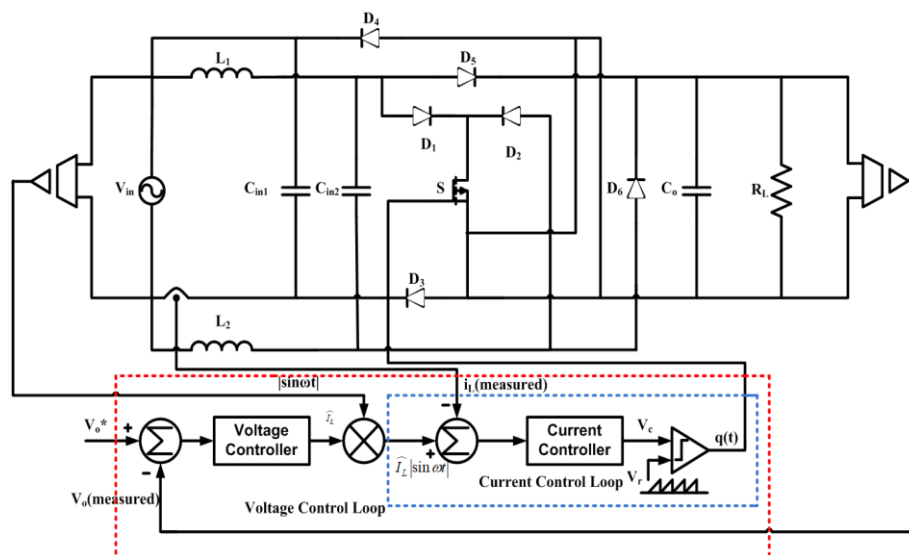


Figure 5.4 Block Diagram of PFC.

The average inner current control loop ensures the form of  $i_L^*$  based on the template  $\sin|\omega t|$  provided by measuring the rectifier output voltage. The outer voltage control loop determines the amplitude  $\widehat{I}_L$  of  $i_L^*$  based on the output voltage feedback. If the inductor current is insufficient for a given load supplied by the PFC, the output voltage will drop below its preselected reference value  $V_o^*$ . By measuring the output voltage and using it as the feedback signal, the voltage control loop adjusts the inductor current amplitude to bring the output voltage to its reference value. In addition to determine the inductor current amplitude, this voltage feedback control acts to regulate the output voltage of the PFC to the pre-selected DC voltage.



### 5.3 Designing the Inner Average-Current Control Loop

The inner current control loop is shown within the inner dotted box in Fig. 5.4. In order to follow the reference with as little THD as possible, an average-current-mode control is used with a high bandwidth, where the error between the reference  $i_L^*(t)$  and the measured inductor current  $i_L(t)$  is amplified by a current controller to produce the control voltage  $v_c(t)$ . This control voltage is compared with a ramp signal  $V_r(t)$ , with a peak of  $\hat{V}_r$  at the switching frequency  $F_s$  in the PWM controller IC, to produce the switching signal  $q(t)$ .

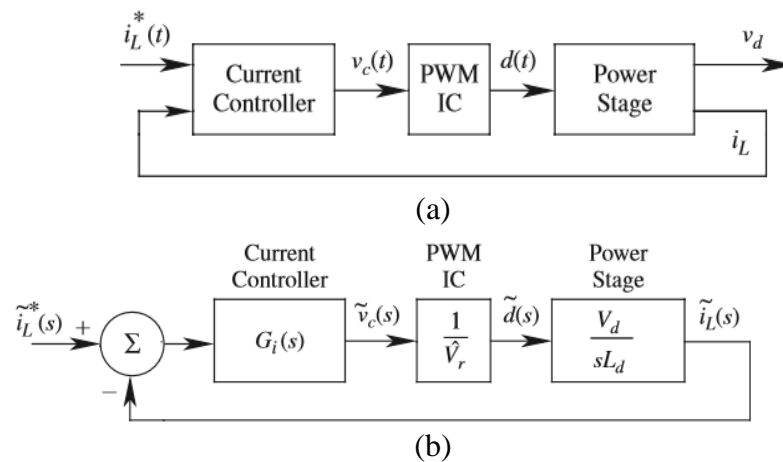
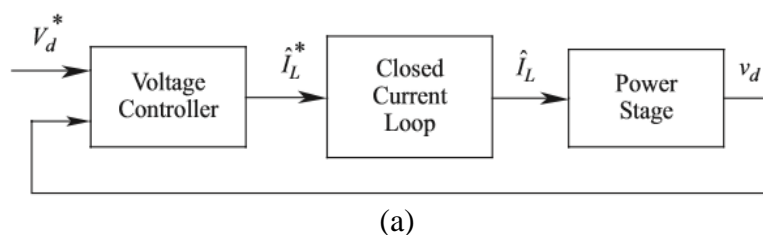


Figure 5.5 PFC Current Loop.

### 5.4 Designing the Outer Voltage-Control Loop

As mentioned earlier, the outer voltage-control loop is needed to determine the peak  $\hat{I}_{L1}$  of the inductor current. In this voltage loop, the bandwidth is limited to approximately 15 Hz. The reason has to do with the fact that the output voltage across the capacitor contains a component  $V_{oc}$  at twice the line-frequency (at 120Hz in 60-Hz line-frequency systems). This output voltage ripple must not be corrected by the voltage loop; otherwise it will lead to a third-harmonic distortion in the input current.



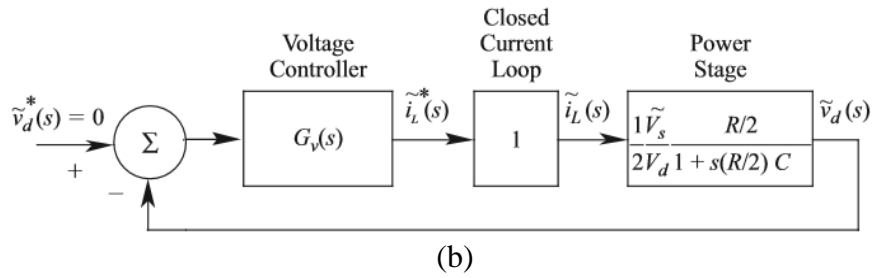


Figure 5.6 PFC Voltage Loop.

## 5.5 Simulation with Designed Controller

Simulation has been done for the proposed converter with feedback controller which has been shown in Fig. 5.7. The parameters of circuit are given in Table 5.1. The PFC controller is designed to obtain an average output voltage of 404 V<sub>dc</sub>. The simulation of the designed controller is given in Table 5.2. Typical input-output waveform of the proposed controller is shown in Fig. 5.6.

Table 5.1 Parameter Table for Close Loop Controller of Fig. 5.7

Parameters	Value
Nominal Input AC Source Voltage ( $V_1$ )	200V
Line Frequency (f)	60Hz
Switching Frequency ( $f_s$ )	30kHz
Inductors ( $L_1, L_2$ )	2.5m
Capacitor ( $C_o$ )	220 $\mu$ F
Resistor ( $R_L$ )	100 $\Omega$
Gain of Voltage Sensor ( $V_{SEN1}, V_{SEN2}$ )	0.015, -0.025
Gain of Current Sensor ( $I_{SEN1}$ )	1

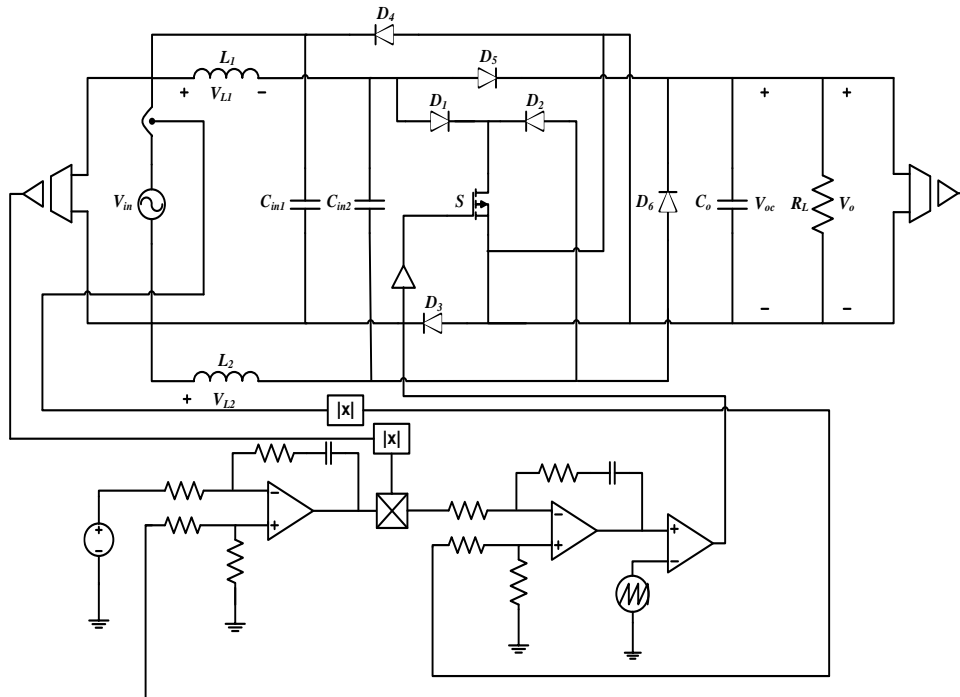
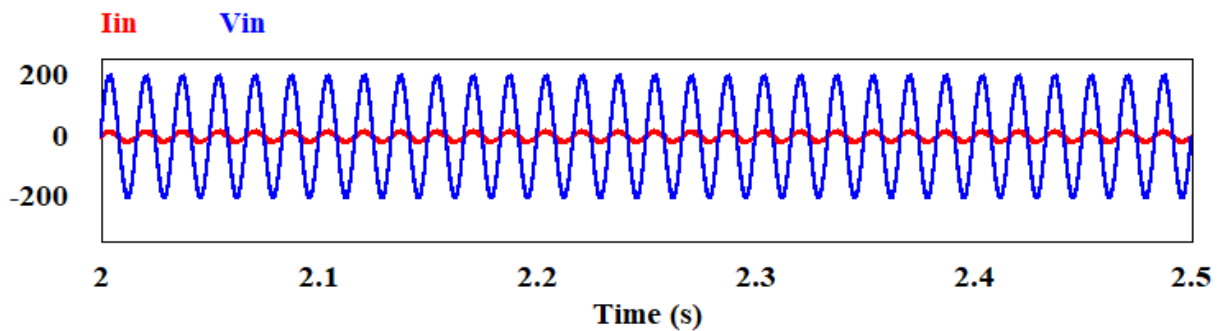


Figure 5.7 Proposed AC-DC Boost Converter with PFC Controller.

Table 5.2 Results of the Simulation of the Converter with Feedback Controller

Performance Parameters	Conventional Boost	Proposed Boost Without Feedback	Proposed Boost With Feedback
Efficiency	97%	98%	99%
Input Current THD	0.64	0.38	0.06
Input Power Factor	0.78	0.84	0.99



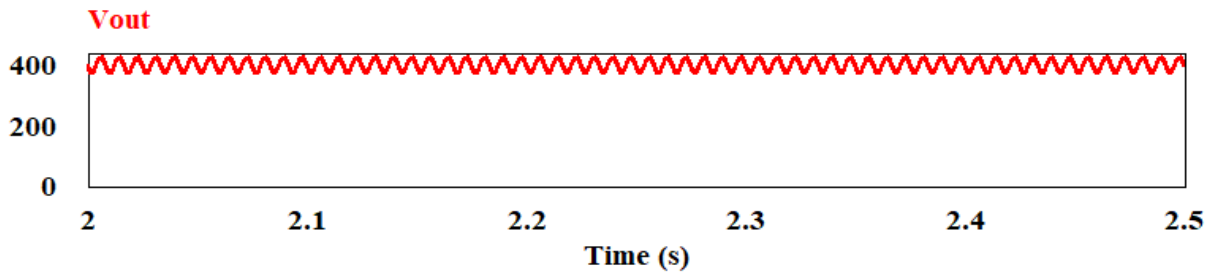


Figure 5.8 Input Voltage-Current and Output Voltage Waveforms of the PFC Controlled Converter of Fig. 5.7

## 5.6 Discussions

The design of controller with the proposed converter is focused to get the best possible outcome under ideal condition. After adding controller the input current THD is reduced to below 6%. The input power factor is almost unity (0.998). The proposed converter with feedback offered higher conversion efficiency compared to the conventional AC to DC boost converter. Controller does not decrease the efficiency of the proposed converter rather it has improved other performance parameters significantly. The proposed converter has offered 99% of conversion efficiency with PFC controller.

## Chapter 6 Conclusion and Future Work

### 6.1 Summary and Conclusion

The proposed converters with feedback offer higher conversion productivity contrasted with the conventional AC-DC Boost converter. There is no decrease in transformation proficiency because of the feedback controller and other performance parameters have enhanced sufficiently. The proposed converter with feedback has offered 99% of conversion efficiency. Conventional single phase AC-DC converters using switch mode topologies (e.g. Boost,Ćuk, SEPIC) suffers due to low conversion efficiency at extremely high and low duty cycle. This is because of the fact that, the gain and the attenuation property of the converter differs from ideal behavior due to the internal resistance of the inductor and non-linear behavior of the switch in achieving extreme high gain or attenuation. A short summary of the overall work which has been discussed in this thesis paper is given below.

Review of different types of converters with various control structures provide a clear concept associated with AC-DC converters. Conventional circuit investigation with single phase AC-DC converters is given with performance analysis. The working principle of the proposed and conventional single phase AC-DC Boost, SEPIC and Ćuk converters are discussed with necessary voltage gain relations. The proposed converters offered higher conversion efficiency at high voltage gains. The graphical analysis of the proposed input switched single phase AC-DC Boost, SEPIC and Ćuk converters are carried out to observe the performance in terms of THD, power factor, voltage gain and efficiency. The feedback controller was implemented for the proposed Boost converter along with performance analysis to obtain more precise result. After adding feedback controller the simulation results ensured high input power factor (0.99) and low input current THD (below 6%).

## 6.2 Future Works

With the present advance of the work, several future goals can be accomplished.

- Switching power loss at the switches and conduction power loss at the diodes and switches can be calculated theoretically in details. This will help to determine the output power to be delivered to load and thus the efficiency of the converters would have been evaluated.
  
- To make this research work more effective experimental study on the performance of the proposed converters can be done in collaboration with other research groups who have experimental facilities.

## References

- [1] R. W. Erickson, "Fundamentals of Power Electronics," New York: Chapman and Hall, 1997.
- [2] N. Mohan, Power Electronics: a first course. Hoboken, N.J.: Wiley, 2012.
- [3] Bimal K. Bose, "The Past, Present and Future of Power Electronics," IEEE Industrial Electronics Magazine, June 2009.
- [4] N. Mohan, T. Undeland, and W. Robbins, "Power Electronics: Converters, Applications, and Design," 2nd ed., New York: John Wiley & Sons, 1995.
- [5] N. Mohan, T. M. Undeland, and W. P. Robbins. (2003). Power electronics: converters, applications, and design (3rd ed.).
- [6] Reinaldo Perez., "A Comparative Assessment Between Linear and Switching Power Supplies in Portable Electronic Devices", Electromagnetic Compatibility, 2000. IEEE International Symposium on (Volume:2 ), August2000, pp. 839-843.
- [7] Alaoui, "Meeting IEEE 519-1992 with Zeta AC-to-DC Converter", International Journal of Engineering Science and Technology (IJEST),ISSN: 0975-5462, Vol. 3 No. 4 Apr 2011, pp. 3541-3548.
- [8] Ma Hao, Lang Yunping, "An improved algorithm for DSP implementation of boost PFC converter," Transactions of China Electrotechnical Society, 2006, Vol. 21, no. 2, pp. 83-87.
- [9] B. Axelrod, Y. Berkovich, and A. Ioinovici, "Switched-Capacitor/Switched Inductor Structures for Getting Transformer less Hybrid DC PWM Converters," Circuits and Systems I: Regular Papers, IEEE Transactions on, vol. 55, pp. 687-696, 2008.
- [10] M. Arias, Ferna, x, M. ndez Diaz, D. G. Lamar, D. Balocco, et al., "High Efficiency Asymmetrical Half-Bridge Converter Without Electrolytic Capacitor for Low-Output-Voltage;DC LED Drivers," Power Electronics, IEEE Transactions on, vol. 28, pp. 2539-2550, 2013.
- [11] G. Spiazzi, P.Mattavelli- "Design Criteria for Power Factor Pre regulators based on SEPIC and ĆUK converters in Continuous Conduction mode,"Industrial Society annual meeting,1994,conference record of 1994 IEEE.
- [12] M. Mahmood, C. Huang-Jen, L. Yu-Kang, N. Quang Trong, P. Phu Hieu, and I. Purnama, "Isolated dual boost bridgeless power factor correction AC-DC converter," in Future Energy Electronics Conference (IFEEC), 2013 1st International, 2013, pp. 465-470.
- [13] K. Jun-Ho, D.-Y. Cho, J.-P. Hong, and M. Gun-Woo, "Boost integrated flyback AC-DC converter with valley fill circuit for LED light bulb," in Power Electronics and

Motion Control Conference (IPEMC), 2012 7th International, 2012, pp. 457-462.

- [14] H.-S. Cho, J.-S. Yoo, J.-Y. Choi, M.-K. Yang, and W.-Y. Choi, "Bridgeless half-bridge AC-DC converter with series-connected two transformers," in Applied Power Electronics Conference and Exposition (APEC), 2013 Twenty Eighth Annual IEEE, 2013, pp. 3241-3245.
- [15] Mahshid Amirabadi; Jeihoon Baek; Hamid A. Toliyat; William C. Alexander, "Soft-Switching AC-Link Three-Phase AC-AC Buck-Boost Converter", IEEE Transactions on Industrial Electronics, Year: 2015, Volume: 62, Issue: 1, Pages: 3 – 14.
- [16] Abhishek Pratap Singh, V.K. Giri "Modeling and Simulation of Single Phase Cycloconverter" International Journal of Engineering Science and Technology, Vol. 2, Issue-2, March/April, 2012, pp. 346-351.
- [17] Sato, I., et al.: An Improvement Method of Matrix Converter Drives Under Input Voltage Disturbances. IEEE Trans. on Industrial Electronics. 22(1), 132–138 (2007).
- [18] C. Lai, C. Pan and Cheng, "High-Efficiency Modular High Step-Up Interleaved Boost Converter for DC-Microgrid Applications," IEEE Trans. Ind. Electron., vol. 48, no. 1, pp.161-171, Jan/Feb. 2012.
- [19] Vladimir Lazarov, Daniel Roye, Dimitar Spirov and Zahari Zarkov, "New Control Strategy for Variable Speed Wind Turbine with DC-DC converters," 14th International Power Electronics and Motion Control Conference, EPE-PEMC 2010.
- [20] Tarek Ahmed, Katsumi Nishida and Mutsuo Nakaoka, "Interleaved DC-DC Converter with Lead-acid Storage Batteries for Power Regulation of Gridconnected Variable-speed Wind Turbine," IEEE PEDS 2015, Sydney Australia, pp- 786-790, 9-12 June 2015.
- [21] Wuhua Li and Xiangning He, "Review of Nonisolated High-Step-Up DC/DC Converters in Photovoltaic Grid-Connected Applications," IEEE Trans. on Ind. Electron., vol. 58, no. 4, pp- 1239-1251, April 2011.
- [22] R.G Ganesan and M. Prabhakar, "Non-isolated high gain boost converter for photovoltaic applications," in Proc. IEEE ICPEC, pp.277-280, 2013.
- [23] B. Singh, B. N. Singh, A. Chandra, K. Al-Haddad, A. Pandey, and D. P. Kothari, "A review of single-phase improved power quality AC-DC converters", IEEE Transactions on Industrial Electronics, Vol. 50, No. 5, Oct. 2003, pp 962 – 981.
- [24] R. Martinez and P. N. Enjeti, "A high performance single phase rectifier with input power factor correction," IEEE Trans. Power Electronics., vol. 11, pp. 746-752, pp. 311-317, Mar. 1996.



- [25] Taufik, A. Hernadi, R. Rudianto, M. Anwari, “ Performance Study of Power Factor Correction Circuits”, Proceedings of the International Conference on Electrical Engineering and Informatics Institute Teknologi Bandung, Indonesia, June 17-19, 2007, Pg419-422.
- [26] M.R.T. Hossain, M. H. Rahaman, M. S.Arifin, M. A Choudhury. A.H.Abedin,M.N.Uddin,“Input Switched Single Phase High Performance Bridgeless AC-DC Zeta Converter”, IEEE International Conference on Power Electronics, Drives and Energy Systems, December16-19, 2012.
- [27] O. Gracia, J. A. Cobos, R. Prieto, and J. Uceda, “Single phase power factor correction: A survey,” IEEE Trans. Power Electron., vol. 18, no. 3,749–755, May 2003.
- [28] J. Sabzali, E. H. Ismail, M. A. Al-Saffar, and A. A. Fardoun, “New Bridgeless DCM SEPIC and Ćuk PFC Rectifiers With Low Conduction and Switching Losses”, IEEE Transactions on Industry Applications, Vol. 47, No. 2, March/April 2011, pp. 873-881.
- [29] M. Brkovic and S. Ćuk, “Input current shaper using Ćuk converter”, 14th International Telecommunications Energy Conference, INTELEC '92, Oct. 1992, pp. 532- 539.
- [30] Oscar García, , José A. Cobos, Roberto Prieto,Pedro Alou, and Javier Uceda, “Single Phase Power Factor Correction: A Survey”, IEEE Transactions on Power Electronics, Vol. 18, No. 3, May 2003, Pg:749-755.
- [31] Chongming Qiao and Keyue M. Smedley, “A Topology Survey of Single-Stage Power Factor Corrector with a Boost type Input Current-shaper”, 0-7803-5864-3/00/10.00 02 000 IEEE, Pg: 460-467.
- [32] Chan-Soo Lee; Young-Jin Oh; Kee-Yeol Na; Yeong-Seuk Kim; Nam-Soo Kim,“Integrated BiCMOS Control Circuits for High Performance DC–DC Boost Converter”, IEEE Transactions on Power Electronics,Year: 2013, Volume: 28, Issue: 5,Pages: 2596 – 2603.
- [33] S. Jeevitha; S. Edward Rajan; T. Rakesh, “Performance analysis of high gain DC-DC boost converter for thermoelectric power generation system”, Green Computing Communication and Electrical Engineering (ICGCCEE), 2014 International Conference on Year: 2014, Pages: 1 – 7.603.
- [34] H. Ismail, “Bridgeless SEPIC Rectifier with Unity Power Factor and Reduced Conduction Losses”, IEEE Transactions on Industrial Electronics, Vol. 56, No. 4, April 2009, pp. 1147-1157.

- [35] Abbas A. Fardoun, Esam H. Ismail, Ahmad J. Sabzali and Mustafa A. Al-Saffar, "New Efficient Bridgeless Ćuk Rectifiers for PFC Applications," IEEE transactions on power electronics, vol. 27, no. 7, July 2012.
- [36] L. Huber, Y. Jang, and M. M. Jovanovic, "Performance Evaluation of Bridgeless PFC Boost Rectifiers," IEEE Trans. Power Electron., vol. 23, pp. 1381-1390, May 2008.
- [37] Bing Lu, Ron Brown, Macro Soldnao, "Bridgeless PFC implementation using one cycle control technique," APEC, 2005, no. 2, pp. 812-817.
- [38] M. R. Sahid and A. H. M. Yatim, "An isolated bridgeless AC-DC converter with high power factor," in Power and Energy (PECon), 2010 IEEE International Conference on, 2010, pp. 791-796.
- [39] M. R. Sahid, A. H. M. Yatim, and T. Taufik, "A new AC-DC converter using bridgeless SEPIC," in IECON 2010 - 36th Annual Conference on IEEE Industrial Electronics Society, 2010, pp. 286-290.
- [40] Jongbok, S. Jongwon, P. Jang, and C. Bohyung, "A critical conduction mode bridgeless flyback converter," in Power Electronics and ECCE Asia (ICPE & ECCE), 2011 IEEE 8th International Conference on, 2011, pp. 487-492.
- [41] A. H. Abedin, M. H. Rahaman, M. M. S. Khan, M. A. Choudhury, M. Rubaiyat, T. Hossain, et al., "Input switched single phase high performance bridgeless C&#x00FB;K AC-DC converter," in Power Electronics, Drives and Energy Systems (PEDES), 2012 IEEE International Conference on, 2012, pp. 1-5.
- [42] M. M. U. Alam, W. Eberle, D. Gautom, and F. Musavi, "A soft-switching bridgeless AC-DC power factor correction converter for off-road and neighborhood electric vehicle battery charging," in Applied Power Electronics Conference and Exposition (APEC), 2014 Twenty-Ninth Annual IEEE, 2014, pp. 103-108.
- [43] B. Su and Z. Lu, "An interleaved totem-pole boost bridgeless rectifier with reduced reverse-recovery problems for power factor correction," IEEE Trans. Power Electron., vol. 25, no. 6, pp.769-780, June 2010.
- [44] A. K. Jha, B. G. Fernandes and A. Kishore, "Single Phase Single Stage AC-DC Converter with High Input Power Factor and Tight Output Voltage Regulation", Progress In Electromagnetics Research Symposium 2006, Cambridge, USA, March 26-29, Pg:322329.
- [45] B. Su and Z. Lu, "An interleaved totem-pole boost bridgeless rectifier with reduced reverse-recovery problems for power factor correction," IEEE Trans. Power Electron., vol. 25, no. 6, pp.769-780, June 2010.

- [46] A. A. Fardoun, E. H. Ismail, M. A. Al-Saffar, and A. J. Sabzali, "New bridgeless high efficiency AC-DC converter," in Applied Power Electronics Conference and Exposition (APEC), 2012 TwentySeventh Annual IEEE, 2012, pp. 317-323.
- [47] M. R. T. Hossain, M. H. Rahaman, M. S. Arifin, M. A. Choudhury, A. H. Abedin, and M. N. Uddin, "Input switched single phase high performance bridgeless AC-DC Zeta converter," in Power Electronics, Drives and Energy Systems (PEDES), 2012 IEEE International Conference on, 2012, pp. 1-5.
- [48] M. R. Sahid and A. H. M. Yatim, "An isolated bridgeless AC-DC converter with high power factor," in Power and Energy (PECon), 2010 IEEE International Conference on, 2010, pp. 791-796.
- [49] M. R. Sahid, A. H. M. Yatim, and T. Taufik, "A new AC-DC converter using bridgeless SEPIC," in IECON 2010 - 36th Annual Conference on IEEE Industrial Electronics Society, 2010, pp. 286-290.
- [50] C. Woo-Young, C. Jae-Yeon, and Y. Ju-Seung, "Single-stage bridgeless threelevel AC/DC converter with current doubler rectifier," in Power Electronics and ECCE Asia (ICPE & ECCE), 2011 IEEE 8th International Conference on, 2011, pp. 2704-2708.
- [51] T. Yichao and A. Khaligh, "A novel bridgeless high-frequency resonant ACDC converter," in Applied Power Electronics Conference and Exposition (APEC), 2014 Twenty-Ninth Annual IEEE, 2014, pp. 125-130.
- [52] M. Muntasir Ul Alam, W. Eberle, and F. Musavi, "A hybrid resonant bridgeless AC-DC power factor correction converter for off-road and neighborhood electric vehicle battery charging," in Applied Power Electronics Conference and Exposition (APEC), 2014 Twenty-Ninth Annual IEEE, 2014, pp. 1641-1647.
- [53] R. Baca Arroyo, G. R. Paredes, and R. Pena Sierra, "AC-DC Power-FactorCorrected Switching Converter Based on Air-Gap Transformer and Pulse Position Modulator for Lighting Applications," in Electronics, Robotics and Automotive Mechanics Conference (CERMA), 2011 IEEE, 2011, pp. 296-300.
- [54] S. Chenh, M. Sautreuil, D. Riu, Retie, x, and N. re, "Quasi-static decoupled load flow modelling of a power supply network with AC-DC converters applied to light rail system," in Power Electronics and Applications, 2007 European Conference on, 2007, pp. 1-10.
- [55] C. Chun-An, C. Hung-Liang, and C. Tsung-Yuan, "A novel single-stage highpower-factor LED street-lighting driver with coupled inductors," in Industry Applications Society Annual Meeting, 2013 IEEE, 2013, pp. 1-7.

- [56] C. Chun-An, C. Hung-Liang, and C. Tsung-Yuan, "A Novel Single-Stage HighPower-Factor LED Street-Lighting Driver With Coupled Inductors," *Industry Applications, IEEE Transactions on*, vol. 50, pp. 3037-3045, 2014.
- [57] C. Park, K. Jang, S. Woo, H. Yu, J. Lee, and J. Choi, "AC-DC converter using -multiplier circuit for LED lighting applications," *Electronics Letters*, vol. 49, pp. 984-985, 2013.
- [58] B. Singh and A. Shrivastava, "Buck converter-based power supply design for low power light emitting diode lamp lighting," *Power Electronics, IET*, vol. 7, pp. 946-956, 2014.
- [59] M. S. Patil, and S. P. Patil, "Single-Phase Buck-Type Power Factor Corrector with Lower Harmonic Contents in Compliance with IEC 61000-3-2" *International Journal of Engineering Science andTechnology*, Vol. 2(11), 2010, pp. 6122-6130.
- [60] W. Shu, R. Xinbo, Y. Kai, and Y. Zhihong, "A flicker-free electrolytic capacitor-less ac-dc LED driver," in *Energy Conversion Congress and Exposition (ECCE)*, 2011 IEEE, 2011, pp. 2318-2325.
- [61] Suman Dwari, and Leila Parsa, "An Efficient AC–DC Step-Up Converter for Low-Voltage Energy Harvesting," *IEEE transactions on power electronics*, vol. 25, no. 8, august 2010.
- [62] S. Dwari, R. Dayal, and L. Parsa, "A novel direct AC-DC converter for efficient low voltage energy harvesting," in *Proc. IEEE Ind. Electron. Soc. Annu. Conf.*, Nov. 2008, pp. 484–488.

## List of publications

### No.of Published Paper

- [1] K. Akter, G. Sarowar, and A. Hoque, "Open Access An Approach of Improving Performance of the Single Phase AC- DC Sepic Converter," American Journal of Engineering Research, no. 3, pp. 3–7, 2017

### No. of Accepted Papers

- [1] K. Akter, G. Sarowar, and A. Hoque ,S.F.B. Ahmed "Modeling and Simulation of Input Switched AC-DC SEPIC Converter with PFC Control for Optimized Operation",IEEE Conference,2018.
- [2] K. Akter, G. Sarowar, and A.M. Oninda, "A New Topology of Input Switched High Performance Single Phase AC-DC Boost Converter,"13<sup>th</sup> International Globalization Conference.
- [3] K. Akter, G. Sarowar, and S.F.B. Ahmed,"Closed Loop Analysis of a Novel Single Phase AC-DC ĆUK Converter with Low Input Current THD and Improved Power Factor," IEEE Conference, 2018.

### No. of Submitted Papers

- [1] K. Akter, G. Sarowar, A. Hoque, F. Faisal and A.M. Oninda, "Input Switched Single Phase AC-DCPFC Boost Converter to Improve Overall Power Quality for High Performance,"IEEE Conference, 2018.